Mechanisms of brain infection by the human fungal pathogen *Cryptococcus neoformans*

by

Wilber Sabiiti
Dip. Educ. BSc. MSc.

A thesis submitted to the University of Birmingham for the award of
degree of DOCTOR OF PHILOSOPHY

Institute of Microbiology and Infection
School of Biosciences
August 2012

UNIVERSITY OF BIRMINGHAM

University of Birmingham Research Archive

e-theses repository

Abstract

Known for over a hundred years, the human fungal pathogen, *Cryptococcus neoformans* causes cryptococcosis, a life threatening disease. Infection is acquired through inhalation of spores or dried yeast cells into the lungs from which the fungus can potentially transmit to all body parts; however, the brain is the most affected organ. Once in the brain, the yeast *C. neoformans* causes meningoencephalitis, a fatal condition even with optimal treatment. The mechanism by which *C. neoformans* penetrates the normally impermeable blood brain barrier in not understood. Using both in vivo and in vitro models, research in the past decade has demonstrated that the pathogen may penetrate the blood-brain barrier through either the Trojan horse pathway, hiding inside monocytes and or macrophages, or transcellularly through adherence to – and uptake by - brain microvascular endothelial cells. In the first part of this thesis, we make the first attempts to quantify the rate of binding and internalization of cryptococci by brain-microvascular endothelial cells. By combining dual colour microscopy and culture techniques, we have shown that adherence and internalization of cryptococci by brain microvascular endothelial cells is a rare event characterized by a small number of cryptococci. The rate of association (binding and uptake) with brain endothelial cells increases with time of incubation at 37°C, although neither presence of capsule nor opsonisation enhances this association within isogenic strains of *C. neoformans*.

In the second part of this thesis we provide the first exploration of the association between macrophage - *Cryptococcus* interaction and clinical outcome of HIV-associated cryptococcal meningitis. The ability of *C. neoformans* to parasitize

monocytes and macrophages has long been known, a phenomenon by which it is believed that these phagocytes systemically disseminate the pathogen from lungs to the brain. A panel of 47 isolates from cerebral spinal fluid (CSF) of HIV- associated cryptococcal meningitis patients was characterized for a number of traits, including rate of uptake by macrophages, intracellular proliferation rate in macrophages, melanisation and capsule expression. Association between macrophage – isolate interaction phenotype and patient clinical parameters were determined using linear and logistic regression models. We show that high rate of cryptococci uptake by macrophages is associated with patient fungal burden whilst the intracellular proliferation rate is inversely associated with TNF-α levels in the patient CSF. Interestingly, the high uptake – high fungal burden isolates were less encapsulated but more rapid melanin formers, traits known to modulate phagocytosis and protection from host-induced oxidative stress respectively. We therefore hypothesize that highly phagocytosed *C. neoformans* strains disseminate faster to the brain, resulting in high fungal burden by proliferating in the brain tissue and CSF.

Dedication

This thesis is dedicated to my Mum, step-Mum and Dad: Peace, Hope and Charles Ntungwamasha. Dad, you believed in me and worked hard to support my schooling; you did not live to see this but Mum represents you. Hope, I did not know my PhD would be on the disease, cryptococcal meningitis that cut your life short, you're the reason I will continue the fight against this disease.

Acknowledgement

The journey to a PhD is like a race, which cannot be won by curiosity alone. As an undergraduate Biochemistry student, it was simply exciting to learn new concepts and recite all the catabolic and anabolic cycles of metabolism. When I reflect on the three years of doctoral study I see a time of not only testing hypotheses in the laboratory but of assessing what I do and why, and whether it will contribute to the improvement of human health. One morning as I cycled to the laboratory, it dawned as I realized that despite all human civilization and modern technology, the battle against diseases is nowhere near the end and thus, the challenges it brings are the motivation to keep me researching.

In Rukiga we say, "Nyenga nyenka akenga mabi" which literally means that teamwork is essential for generating good and fully baked products. On this note I would like to express my sincere thanks to my Supervisor, Dr. Robin Charles May, whose guidance, support, insight and enthusiasm has made my doctoral journey meaningful and enjoyable. In such an uphill task, someone who focuses on the "gold" not the "sand" is what you need to succeed, and indeed Dr. May has been that person to me. Furthermore, as student parent, I could not have wished for a more supportive and understanding supervisor. Not only was Robin enthusing as a Supervisor but also

the whole May Lab group was very supportive and great team to be part of. A big thank you to all colleagues in the May Lab who either trained me in some experimental aspects or gave a hand in some of my PhD projects. Pursuing a PhD at the University of Birmingham has not only been about the laboratory and experiments but an environment for holistic professional development. Great thanks to the University Graduate School, ADEPT and Talent pool programmes, which gave me avenues to enhance my professional skill set.

With teamwork comes collaboration and I wish to acknowledge people whose collaboration makes part of this thesis: Dr. Mark Gambleton (Cardiff School of Pharmacy, UK) and Prof. Jane McKeating (Institute of Biomedical research, University of Birmingham) for providing us with the murine and human brain endothelial cell lines respectively, Prof. Joe Heitman's group (Duke University, USA) for providing the acapsular strain, cap59 and Prof. Arturo Casadevall (Albert Einstein college of Medicine, USA) whose anti-capsule antibody was a great resource in my research projects. Great appreciation and thanks to Dr. Tihana Bicanic (Prof. Tom Harrison's research group, St. George's University of London) for providing the clinical isolates for the macrophage – *Cryptococcus* interaction study and being instrumental in increasing my understanding and appreciation of the clinical aspects of cryptococcosis. In the same spirit, I am grateful to Prof. James Kronstad (Micheal Smith Laboratories, University of British Columbia, Vancouver, Canada) for inviting and hosting me as well as coordinating our gene expression study and training me in *Cryptococcus* – iron growth assays. Thanks to the Kronstad Lab members who made my stay in Vancouver very exciting and memorable. I am grateful to the British

and have been a great source of joy and fan and from him I have learnt to play and enjoy life in its simplicity. Hokmah, you came at the beginning of my PhD programme and with great expectation, your sister, Kristina comes at the end of the same programme, what a joy! As a family, our life in Belgium and the UK would not have been enjoyable without friends. Thank you Stuart and Judith Sanson for being our guardian angels in Belgium and for standing with us as we fought for the permission of leave to study in the UK; Denis and Deborah, you made us feel at home in Antwerp. I am indebted to Philip and Anne Simpson who have not only been friends but family to us in the UK. I gratefully appreciate your love and support as we moved home from Antwerp to Birmingham and being there for us during our stay in the UK.

Last but not least, I am grateful to the love and support from my Mum and siblings in Uganda. You introduced me to life, gave the first medium of socialization and indeed your presence gives me a great sense of belonging and pride in who I am. Great thanks to the almighty creator to whom all the glory be accorded.

Thesis overview

This thesis is made of five chapters, the conclusion, future perspectives and the appendix. Chapter I covers the Introduction in which the author expounds on the importance of cryptococcosis and the literature regarding the mechanism (s) by which *Cryptococcus neoformans* infects the human brain. To reach the brain, the inhaled cryptococci must overcome the host's physical and chemical barriers in the lungs and the circulatory system. This implies that *C. neoformans* may never reach the brain if encounters a strong and effective immune response in the lungs. Nevertheless, the pathogen is also endowed with protective gears (virulence traits) to enable it survive the hostile host defence response and take advantage of host phagocytes as vectors for its transmission to the brain. It is important to note that contents of this chapter have been submitted for publication as a review in the journal of future medicine.

Chapter II details the methods and materials used, which are divided into two sections. First section covers methods and materials for the study of *C. neoformans* interaction with brain microvascular endothelial cells (BMEC). The role of the capsule, effects opsonisation, IFN-γ, and viability in *Cryptococcus* – BMEC interaction are examined. In the second section, the author details methods used to study macrophage – clinical *Cryptococcus* interaction. Clinical isolates from HIV-associated cryptococcal meningitis are characterised for the rate of uptake by macrophages, intracellular proliferation inside macrophages, melanisation and capsule expression. The section further examines a selection of highly and less internalised isolates for their growth in low iron conditions and survival in whole blood from

healthy donors as well as rate of association with phagocytes in this blood. Linear and logistic regression model is used to determine the association the macrophage – isolate interaction phenotype with patient clinical parameters.

Chapter III gives the results from the *Cryptococcus* – BMEC study. Results in this chapter show the percentage association and internalisation of cryptococci by both murine and human BMEC at different time points. The effects of opsonisation, IFN-ɣ induction of BMEC, and viability on the rate of cryptococci – BMEC interaction are shown. As a control to verify that cryptococci binding and uptake observed is to non other than BMEC, we show that killing the BMEC monolayer using a fixative completely abrogates association and internalization of cryptococci by BMEC. These results, methods and discussion thereof have been published (Sabiiti, et. al., 2012).

Chapter IV comprises the results of the macrophage – clinical isolates interaction study. Rates of uptake and Intracellular proliferation for all isolates are given. The linear regression analysis results showing association between rate of cryptococci uptake and intracellular proliferation rate (IPR) as well as patient CSF fungal burden, Cryptococcal antigen, White cell and lymphocyte counts and also cytokine, TNF-α are given. Association between rate of macrophage cryptococci uptake, IPR and melanisation as well capsule expression are also given. The results also show the rates at which the high and low uptake isolates grow in different iron conditions, survival in whole blood and association with blood phagocytes. The chapter ends with a summary of all the determined phenotypic (uptake, IPR, melanisation, capsule expression) and the known genetic characteristics of the isolates.

Chapter V is the discussion of results from Chapters III and IV. First section discusses Chapter III results on *Cryptococcus* – BMEC interaction and concludes that cryptococci association and internalization by BMEC is a rare event characterised by small number of cryptococci binding to the endothelium and that this association is capsule independent. Second section discusses Chapter IV results and points out the rate of cryptococci uptake by macrophages as an important factor in *C. neoformans'* pathogenicity. Rate uptake is most likely crucial in the lungs when cryptococci first encounter alveolar macrophages and the outcome of this interaction sets the pace of systemic dissemination of which the high uptake strains disseminate faster to the brain.

The thesis ends with conclusion and future perspectives. The conclusion highlights that brain infection by *C. neoformans* is a result of successful manouver of the pathogen through the host's pulmonary and haematogenous defence barriers and that the fungus uses multiple means of dissemination and crossing the blood brain barrier. Based on the current understanding, the author forecasts and points out the areas that are likely to form the basis of *Cryptococcus* and cryptococcosis research in the coming years.

Table of Contents

List of abbreviations

AIDS	Acquired Immunodeficiency syndrom
AppI	Antiphagocytic protein one
ART	Anti-retroviral treatment
ATG3	Autophagy gene three
ATG9	Autophagy gene nine
BBB	Blood-brain barrier
bEnd3	Mouse brain endothelial cells three
BMEC	Brain microvascular endothelial cells
Cap	Capsule
Cap.Diam	Capsule diameter
CD4	Cluster differentiation four
CD44	Cluster differentiation fourty-four
Cfo1	Cryptococcus ferroxidase one
Cft1	Cleavage factor two protein one (permease)
CFU	Colony forming units
CM	Cryptococcal meningoencephalitis/meningitis
CNS	Central nervous system
CR2	Complement receptor two
CR3	Complement receptor three
CSF	Cerebral spinal fluid
CrAg	Cryptococcal antigen
Ctr2	Copper transporter protwin two
CTR4	Copper transporter gene four
Cuf1	Copper transcription factor 1
DE	Differentially expressed genes
DMEM	Dulbecco's Modified Eagle medium
DMSO	Dimethyl Sulfoxide
DNA	Deoxyribonucleic acid
DYPK3	Tyrosine phosphorylation-regulated kinase three
EDTA	Ethylenediaminetetraacetic acid
ELISA	Enzyme linked immunosorbent assay
FBS	Foetal bovine serum
FITC	Fluorescin isothiocyanate
Fre	Ferroxidase
GalXM	Galactoxylomannan
Gat201	Guanine adenine thymine two hundred one deletion mutant
GAT201	Guanine adenine thymine two hundred one transcrption factor
GDP	Guanine diphosphate
GM-CSF	Granulocyte macrophage - colony stimulating factor
GMI	Ganglioside one (Lipin raft marker)
gp-41	glycoprotein fourty-one (HIV)
GTP	Guanine triphosphate
GXM	Glucoronoxylomannan
hCMEC/D3	human brain Capillary microvascular endothelial cells or D three

HIV	Human Immunodeficiency virus
IFN-γ	Interferon-gamma
IL-17	Interleukin-seventeen
IL-6	Interleukin-six
IPR	Intracellular proliferation rate
L-DOPA	L-3,4-dihydroxyphenylalanine
Lim	Low iron medium
LPS	Lipopolysacchride
Mel	Melanin
Mel.Rate	Melanisation rate
MLST	Multilocus sequence type
MR	Melnisation rate
MR-Extra.	Extracellular Melanisation rate
MR-Intra.	Intracellular Melanisation rate
NCTC	National collection of Type culture
NK	Natural killer cell
OP	Opening pressure (Intracranial)
PBMC	Perpheral blood mononuclear cells
PGE	Prostanglandin E
PKA-α	Protein kinase alpha
PLB	Phospholipase B
PLB1	Phospholipase B one
PMA	Phorbol myristate acetate
RacI	Ras-related C3 botulinum toxin substrate one
rhIFN-γ	recombinant human Inteferon gamma
RNA	Riboxynucleic acid
RNAi	Riboxynucleic acid interference
RNAseq	RNA sequencing
RPMI	Rosewell park memorial institute medium
SP-D	Sarfactant protein-D
Sre1Δ	Sterol regulatory element one mutant
STAT3	Signal transducer and activator of transcription protein three
Tat	Trans-activator of transcription (HIV)
Tg26	T-Natural killer cell deficient mouse twenty-six
Th1	Type I T helper cell response
Th17	Type 17 T helper cell response
Th2	Type II T helper cell response
TJ	Tight junction
TJd	Damaged tight junction
TNF-α	Tumour necrosis factor-alpha
URE1	Urease gene 1
Ure1	Urease gene 1 mutant
UV	Ultraviolet light
VGI	*Variant Cryptococcus gattii one*
VGII	*Variant Cryptococcus gattii two*
VGIII	*Variant Cryptococcus gattii three*

VGIV	*Variant Cryptococcus gattii four*
VNB	*Variant Cryptococcus neoformans B*
VNI	*Variant Cryptococcus neoformans one*
VNII	*Variant Cryptococcus neoformans two*
VNIII	*Variant Cryptococcus neoformans three*
VNIV	*Variant Cryptococcus neoformans four*
YPD	Yeast peptone dextrose medium

List of figures

List of tables

CHAPTER I: INTRODUCTION

1.1 Importance of cryptococcosis

Cryptococcosis is a life threatening disease causing a significant global burden of disease. The central nervous system form of the disease, cryptococcal meningoencephalitis (or meningitis) is the most severe and accounts for most mortality arising from cryptococcosis. One million cases of cryptococcal meningoencephalitis (CM) are estimated to occur globally per year, with >60% mortality within 3 months of infection. HIV-associated CM accounts for the majority of these cases, 80% of which occur in Sub-Saharan Africa (Park et al., 2009). Despite increasing access to antiretroviral therapy, the incidence and mortality of cryptococcal meningitis remain high, the diagnosis of HIV frequently being coincident with the diagnosis of meningitis (Jarvis et al., 2009; Kambugu et al., 2008; Meya et al., 2010). Even when optimal treatment with amphotericin B and flucytosine is available, mortality is between 15-30% in both low and high-income settings (Lortholary, 2007; Saag et al., 2000), and much higher in low-income countries where such antifungal regimens are not readily accessible. In addition, the incidence of non-HIV associated CM is increasing in the Pacific North-Western America and Far East Asia caused by hypervirulent strains of *C. gattii* and *C. neoformans* respectively (Byrnes and Heitman, 2009; Chau et al., 2010; Zhu et al., 2010). Lastly, cryptococcosis is the third leading fungal infection in solid organ transplant patients (Singh et al., 2008; Singh et al., 2009) and thus advancements in organ transplant application and wide use of immunosuppressives is prospectively expected to account for increased incidence of cryptococcosis in the medically developed world (McQuiston and Williamson, 2012; Singh et al., 2008; Singh et al., 2009).

1.2 Historical overview

The genus *Cryptococcus* has been known for over 100 years (Springer and Chaturvedi, 2010). First isolated from fruit juice in 1894 by an Italian scientist, Sanfelice, the fungus *Cryptococcus neoformans* was later isolated from milk, humans, pigeon droppings and roosting places (Knoke and Schwesinger, 1994; Springer and Chaturvedi, 2010). The nomenclature of *Cryptococcus neoformans* evolved through the names *Saccharomyces neoformans*, *Blastomyces neoformans*, *Cryptococcus hominis*, and *Torula histolytica* until the 1950s when the current name was settled on (Mitchell and Perfect, 1995). *C. neoformans* is an encapsulated yeast and, based on the immunological reaction to the polysaccharide capsule, the yeast was classified into four serotypes: A, B, C and D. Serotypes A and D are characterized as *C. neoformans var. grubii* and C. *neoformans var. neoformans* while serotypes B and C were associated with *C. neoformans var. gattii* (Franzot et al., 1999; Springer and Chaturvedi, 2010). Molecular based typing has led to the recognition of *C. neoformans var. gattii* as a distinct species, *Cryptococcus gattii* (Boekhout et al., 1997; Kyung J. Kwon-Chung, Teun Boekhout, Jack W. Fell and Mara Diaz, 2002) restricting *C. neoformans var. neoformans* and *C. neoformans var. grubii* to serotypes D and A respectively (Franzot et al., 1998; Ngamskulrungroj et al., 2009; Springer and Chaturvedi, 2010).

The varieties are further divided into molecular types VNI, VNII and VNB of *C. neoformans var. grubii*; VNIV of *C. neoformans* var. *neoformans*; VNIII (hybrid, serotype AD); and VGI, VGII, VGIII and VGIV corresponding to *C. gattii* (Ngamskulrungroj et al., 2009). The serotype A *C. neoformans grubii* molecular types VNI and VNII have a global occurrence (Litvintseva et al., 2006; Simwami et al.,

2011) but VNI accounts for majority of infections in both immunocompitent and immunocompromised patients (Heitman Joseph, Kozel Thomas R, Kwon-Chung Kyung J, Perfect John R, Casadevall Arturo, 2010). The VNB lineage is geographically restricted to Southern Africa (Litvintseva et al., 2006). Recent population and phylogenetic studies suggest that *C. neoformans var grubii* VNI originated in Africa (Litvintseva et al., 2011; Simwami et al., 2011). This finding follows on the previous phylogenetic study, which suggested an African origin of the AD hybrid serotype (Litvintseva et al., 2007).

The first account of human cryptococcosis is attributed to two German Scientists, Busse and Buschke who, in 1895, described a 31-year-old woman with a lesion on her tibia (Casadevall and Perfect, 1998). Although many clinical cases of cryptococcosis were reported in the 1900s, the prevalence remained generally low until 1947 – 1968 when high numbers of cases were reported from Africa. The increase in cases is presumed to have been due to the emergence of AIDS in the Congo River basin in that period (Casadevall and Perfect, 1998; Molez, 1998; Springer and Chaturvedi, 2010). The global HIV/AIDS epidemic of the 1980s to present has seen a parallel rise in cases of human cryptococcosis, mainly due to the immunosuppressive nature of the HIV/AIDS disease (Casadevall et al., 1998; Lin et al., 2009; Mitchell and Perfect, 1995; Severo et al., 2009). Cryptococcal infection can potentially occur in any part of the human body, with cases involving organs such as skin, bone, prostate gland, or urinary tract, liver, spleen, lymph nodes, lungs and brain being reported (Hernandez, 1989; Lin et al., 2009; Liu et al., 2009; Severo et al., 2009). Of all the cryptococcal sites of infection, pulmonary and central nervous system (CNS) are the mainly

affected sites with most mortality arising from CNS cryptococcosis (Park et al., 2009).

1.3 Ecology and epidemiology

The genus *Cryptococcus* is composed largely of free-living environmental fungi, which belong to phylum Basdiomycota (Casadevall and Perfect, 1998). Reports have consistently associated *C. neoformans* with ecological niches such as soil, pigeon droppings while *C. gattii* is mostly associated with trees (Casadevall and Perfect, 1998; Sorrell, 2001; Springer and Chaturvedi, 2010). Historically*, C. neoformans var. grubii* and *var. neoformans* are known to have a global distribution while *C. gattii* was said to exist in the tropical and sub-tropical regions (Kwon-Chung and Bennett, 1984a; Kwon-Chung and Bennett, 1984b; Springer and Chaturvedi, 2010). However, the recent Vancouver outbreak of *C. gattii* cryptococcosis and further cases identified in the US and Europe confirms the presence of *C. gattii* in temperate regions (Bovers et al., 2008; Byrnes and Heitman, 2009; Datta et al., 2009; Kidd et al., 2004). The two species grow well at environmental temperatures ($25^{o}C - 30^{o}C$) (Schop, 2007); but their ability to grow at physiological temperature ($37^{o}C$) is fundamental to their ability to act as human pathogens (Casadevall and Perfect, 1998).

Cryptococcosis occurs in both animals and humans. Apart from rare examples of iatrogenic (Lin et al., 2006), zoonotic (Lagrou et al., 2005), and mother-to-child transmission (Sirinavin et al., 2004), no categorical animal-to-human or human-to-human transmission has been documented. The ability to cause infection in both animals and humans shows that the *C. neoformans* species complex is not an obligate human pathogen. The major environmental sources of *C. neoformans* are either soil

contaminated with pigeon guano for *C. neoformans* var. *neoformans* and var. *grubii* or trees (mainly eucalyptus) and decaying wood for *C. gatti* (Abraham et al., 1997; Balankura, 1974; Callejas et al., 1998; Chakrabarti et al., 1997; Fortes et al., 2001; Khosravi, 1997; Mahmoud, 1999; Montenegro and Paula, 2000; Pfeiffer and Ellis, 1992; Sethna et al., 1973; Yamamoto et al., 1995). *C. neoformans* is largely an opportunistic pathogen whilst *C. gattii* is a primary pathogen and is responsible for the least amount of cryptococcal infections globally (Mitchell and Perfect, 1995). *C. neoformans var. grubii* accounts for 95% of cryptococcal infections and 99% of HIV-associated cryptococcosis (Casadevall and Perfect, 1998; Mitchell and Perfect, 1995). Apparently cryptococcosis is neither a zoonosis nor contagious disease and therefore infection most likely occurs when humans are exposed to the environment infested with cryptococcal spores or dried yeast cells (Figure 1).
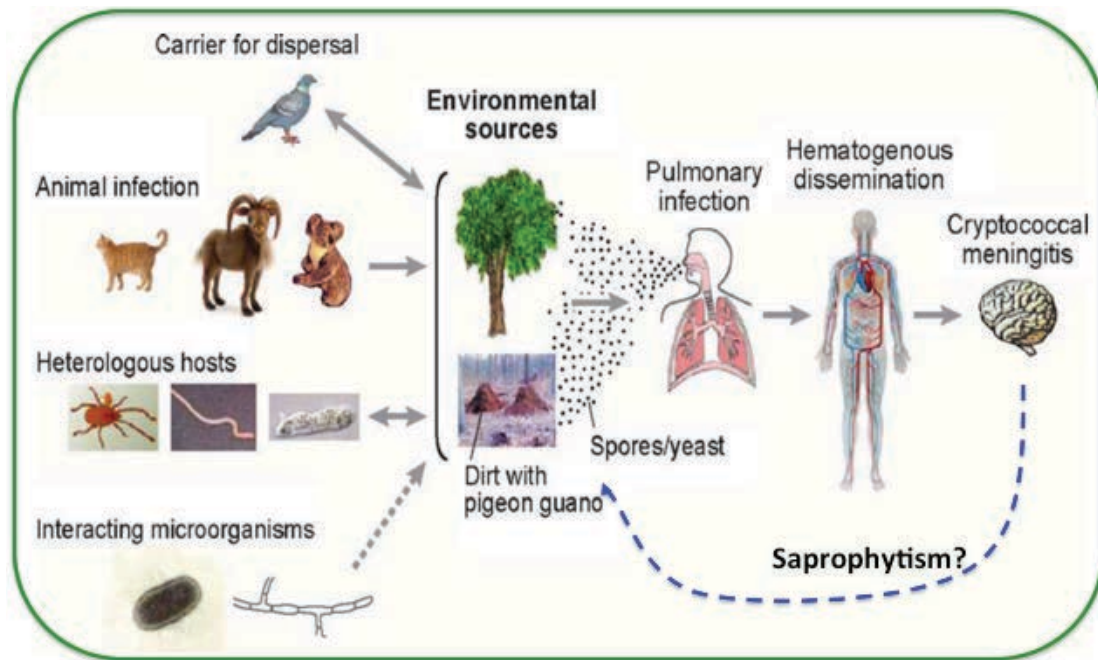
Figure 1: The transmission cycle of cryptococcal spores or desiccated yeast cells from environmental sources to the human body

Environmental niches such as soil contaminated with bird guano or trees are important in the infection cycle. Birds, especially pigeons, are a reservoir and could have been responsible for the worldwide transmission. The fungus infects various animals such as cats, goats and koalas; can survive environmental predators such as insects, worms and amoeba and may interact with other microorganisms such as bacteria and fungi. Through inhalation, the fungus establishes pulmonary infection where it may stay latent or disseminate to organs, particularly the CNS, depending on the immune status of the individual (Adapted from Lin and Heitman, 2006). Whether human infection (both pulmonary and brain) is a dead end in the transmission cycle of *C. neoformans* remains unanswered. However, given the fact that the fungus can live saprophytically in the environment there is no reason why it should not survive in decomposing human matter (blue broken arrow).

1.4 Reproduction

The *C. neoformans* species complex is capable of both asexual and sexual means of propagation. In most clinical and environmental isolates, *C. neoformans* is mostly found as yeast, which is the asexual form of the fungus (Casadevall and Perfect, 1998; Lin et al., 2005; Lin and Heitman, 2006). Under culture, the yeast population will undergo budding with an average doubling time of $5-7$hrs (Miller et al., 1990)In the perfect state (i.e the teleomorphic, bacidiomycetous, *Filobasidiella neoformans*) (Franzot et al., 1999; Staib, 1981; Sukroongreung et al., 1998). *C. neoformans* and *C. gattii* are able to reproduce sexually resulting in production of basidiospores (Casadevall and Perfect, 1998; Lin et al., 2005; Lin and Heitman, 2006). Basidiospore production can result from either haploid (monokaryotic) fruiting or diploid filamentation. Mating involves fusion of haploid cells of opposite mating types, a and α to produce dikaryotic filaments, which eventually lead to the formation of a basidium. In the basidium, meiosis occurs generating four chains of readily aerosolized basidiospores (Kwon-Chung, 1976a; Kwon-Chung, 1976b; Sia et al., 2000; Wickes et al., 1996)(Figure 2).
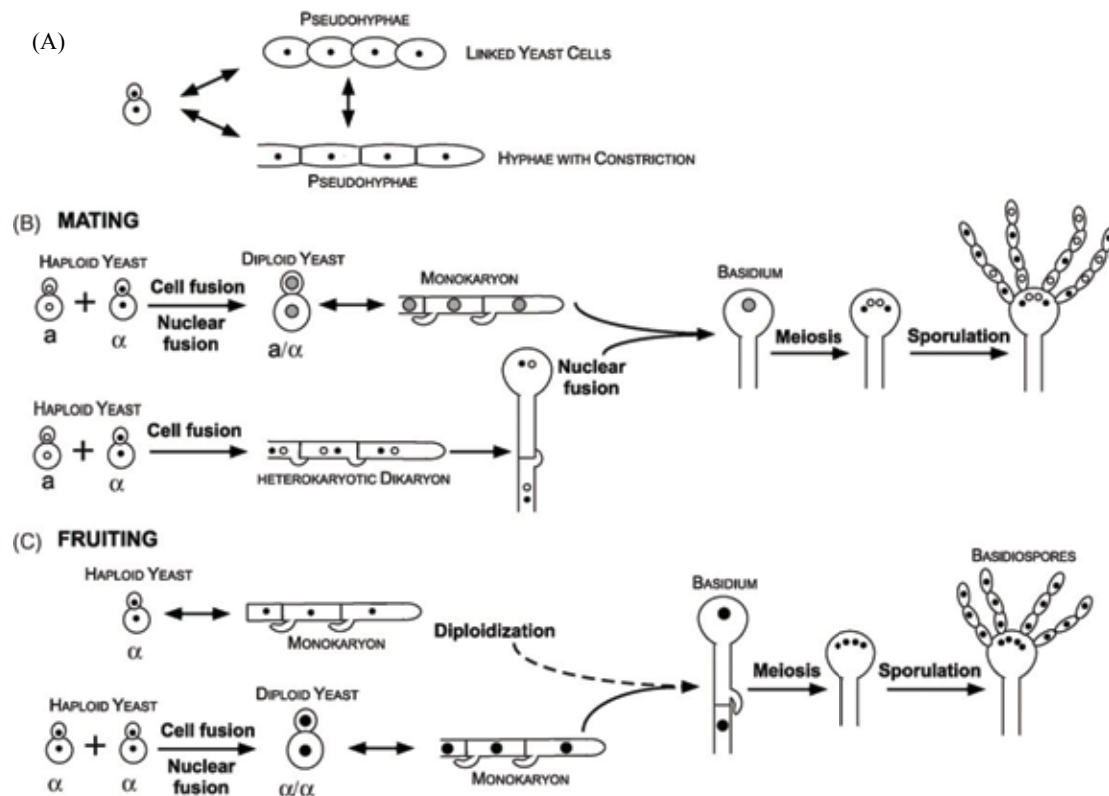
Figure 2: Morphological differentiation in *C. neoformans*

(A) Pseudohyphal differentiation. (B) Mating of alpha and a yeast cells secrete peptide pheromones that trigger cell–cell fusion under nutrient limiting conditions. The resulting dikaryon initiates filamentous growth, and the two parental nuclei migrate coordinately in the hyphae. A septum forms to separate the cells, and one nucleus is transferred to the penultimate hyphal cell via a clamp connection and clamp cell and hyphal cell fusion. During this hyphal growth, blastospores (yeast like cells), can bud from the hyphae and divide mitotically in the yeast form. Some hyphal cells can enlarge and form chlamydospores. At the stage of basidium development, the two nuclei fuse and undergo meiosis to produce four meiotic products that form chains of basidiospores by mitosis, and budding from the surfaceof the basidium. (C) Monokaryotic fruiting. During monokaryotic fruiting, cells of one mating type, e.g. a cells become diploid a/a cells, either by endoduplication or by nuclear fusion following cell fusion between two a cells. The diploid monokaryotic hyphae forms rudimentary clamp connections, but these are not fused to the preceding cell. Blastospores and chlamydospores also form during fruiting as in mating. At the stage of basidium development, meiosis occurs and haploid basidiospores are produced in four chains (Adapted from Lin et al., 2009).

Cryptococcus can undergo intervarietal (serotype A x serotype D) and interspecies (BxD, CxD) matings, but the viability of the basidiospores is reduced and many diploid and aneuploid progeny are generated from these matings, indicating that genomic divergence impairs meiosis (Lengeler et al., 2000).

1.5 Pathogenenesis and dissemination to the brain

Human infection is believed to occur through inhalation of airborne propagules from an environmental source to the lungs. These propagules are either spores (basidiospores) resulting from sexual reproduaction or dried yeast cell. A typical cryptococcal yeast cell ranges between $4 – 10\mu m$ (Okagaki et al., 2010; Rodrigues et al., 1999) but can be as small as $3\mu m$ and as large as $100\mu m$ (titan or giant cells) (Okagaki et al., 2010; Zaragoza et al., 2010) Studies have shown that cell and capsule size increases during infection (Okagaki et al., 2010; Zaragoza et al., 2008; Zaragoza et al., 2010). A polysaccharide capsule linked to the cell wall on the inner side coats the yeast cell but can be shade into the medium as a soluble compound (Okagaki et al., 2010; Zaragoza et al., 2008; Zaragoza et al., 2010). Associated with the cell wall is the enzyme Laccase, which acts on polyphenolic compounds to produce melanin (Zhu and Williamson, 2004) (Figure 3). The capsule and melanin are key factors in the pathogenicity of *C. neoformans.* On the other hand spores are much smaller than yeast cells with a size range of $1.8 - 2\mu m$ diameter (Rodrigues et al., 1999).
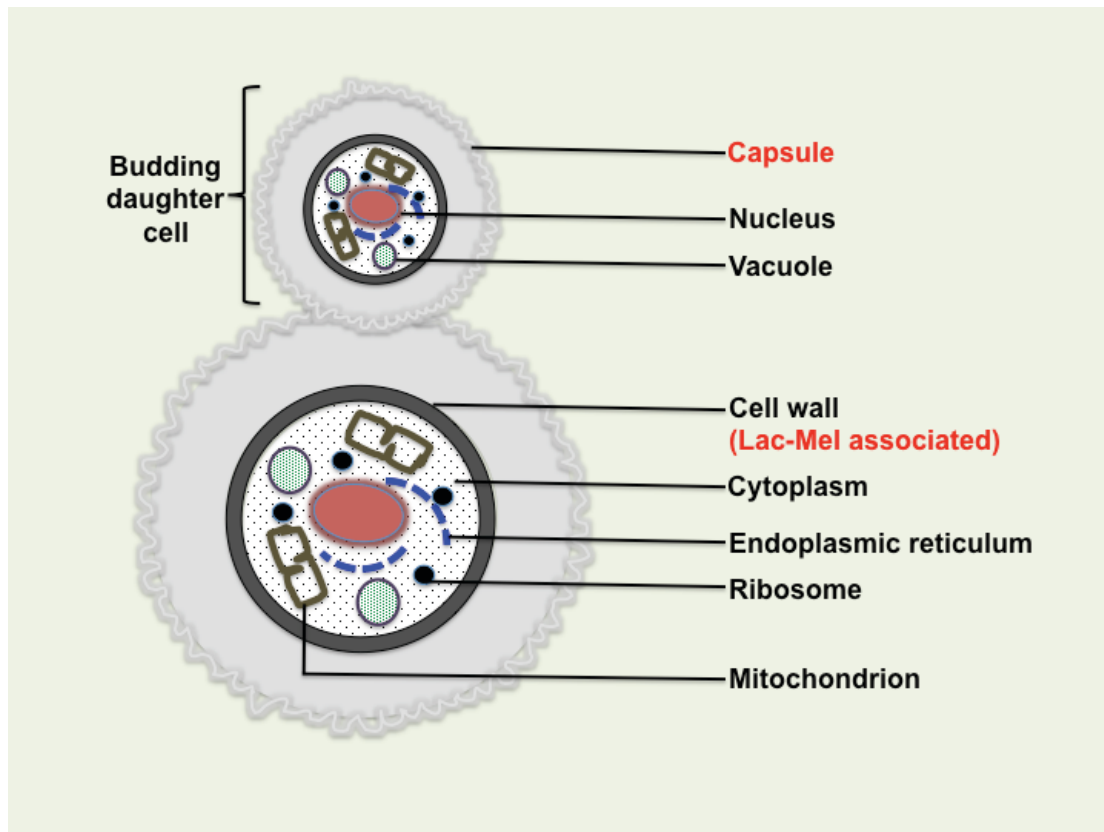
Figure 3: A diagrammatic representation of *C. neoformans* cell
The capsule forms the largest exterior layer of the yeast and appears white shiny when viewed microscopically with India ink staining. Inside the capsule is the cell wall, which is associated with enzyme laccase (Lac) and melanin (Mel). The polysaccharide capsule is both structural (coats the cell) and soluble (shade into medium e.g body fluids like blood, CSF etc) whilst melanin is a byproduct of the yeast's laccase enzyme action on polyphenolic compounds such as L-dihydroxyphenyl alinine (L-DOPA). The capsule and melanin are major virulence factors of *C. neoformans* (See pages 34, 36 & 37). As eukaryotic organism, *C. neoformans* possesses intracellular organelles such as nucleus, endoplasmic reticulum, ribosomes, mitochondria and vacuoles.

Colonization of the host can result in: 1) no disease - the fungus is cleared by the host immune response; 2), asymptomatic infection in which the fungus enters latency and may be reactivated when the host becomes immunocompromised; 3) pulmonary disease characterized by pulmonary nodules and inflammation of the lungs (Kishi et al., 2006; Wu et al., 2009) and 4) disseminated disease, which can potentially occur in all systemic organs with the brain being the most preferred destination (Dromer et al., 1992; Garcia-Hermoso et al., 1999; Goldman et al., 2001a; Lin and Heitman, 2006; Lin et al., 2009). Interestingly, Ngamskulrungroj et al. recently demonstrated that, unlike *C. gattii*, *C. neoformans* prefers the brain to the lung as a site of infection (Ngamskulrungroj et al., 2012). Cryptococcal infection of the brain will depend on the successful manoeuvre by the fungus through the barriers involved in the early phase of infection.

1.5.1 Host colonization and pulmonary infection

More than 50 basidiomycetous yeast *Cryptococcus* species live ubiquitously in the environment, but only *C. neoformans* and *C. gattii* are significant pathogens of humans. The infectious cryptococcal propagules are widely spread in the environment and, through inhalation, the spores or dried yeast cells gain access into the respiratory tract. Colonization and establishment of infection in the lungs is a process involving successful transmission of infectious propagules into the lungs as well as a complex interplay of pathogen virulence factors and host immune response.

1.5.1.1 Transmission into the alveolar space

Cryptococcal spores and or dried yeast cells are very small in size and can deposit deep in the respiratory tract following inhalation (Velagapudi et al., 2009). The kinetic action of host cilia and mucus may serve to drive the infectious particles down into the alveolar space (Velagapudi et al., 2009). While spores are largely known to mediate transmission from environment into the host by pathogenic fungi such as *Blastomyces dermatitidis*, *Histoplasma capsulatum*, *Coccidioides* spp., *Aspergillus fumigatus*, and *Paracoccidioides brasiliensis* (Giles et al., 2009; Levitz et al., 1986), the extent to which cryptococcal spores rather than desiccated yeast cells are infectious propagules is still debatable. Recent advances in isolating and characterising *Cryptococcus neoformans* spores has opened up opportunities to model infection using spores as infectious particles in order to determine their ability to infect and cause disease in the host (Botts et al., 2009; Velagapudi et al., 2009). Spores of serotype A *C. neoformans var. grubii* caused 100% lethal infection in a a murine inhalation model of infection and in the invertebrate host *Galleria mellonella* (Velagapudi et al., 2009). Both spores and yeast cells could be aerosolized by a stream of air, although there were more aerosolized spores than yeast cells (Botts et al., 2009; Velagapudi et al., 2009), suggesting a higher chance of spores being involved in environmental dispersal and host exposure. However, spores are more susceptible to killing by activated host alveolar macrophages and are thus speculated to depend on rapid germination into mature yeast cells in the host in order to establish infection (Botts et al., 2009; Velagapudi et al., 2009). Isolation of *C. neoformans* spores from the environment and characterization of wide range of spores from both clinical and environmental strains is needed to further substantiate the potency of spores as *C. neoformans* infectious propagules.

The lung alveolar space is lined by a tension reducing fluid, surfactant, which promotes adherence of cryptococcal cells to lung epithelial cells (Ganendren et al., 2006). Surfactant protein-D (SP-D) binds to and promotes phagocytosis of both encapsulated and acapsular *C. neoformans* by macrophages (Geunes-Boyer et al., 2012), an indication that cryptococcal opsonisation with host surfactant is most likely one of the first innate factors mediating transition of cryptococci from extracellular to intracellular life. Mannoprotein 1 (MP1) and glucoronoxylomannan (GXM) were shown to mediate the binding of cryptococcal cells to SP-D (van et al., 2004). Interestingly, SP-D-/- mice were partially protected from cryptococcal infection and had reduced lung fungal burden (Geunes-Boyer et al., 2012). The presence of alveolar macrophages that scavenge microbes in the respiratory tract (Gordon and Read, 2002) is also likely to drive cryptococci into deeper areas of the respiratory tract and lung tissue, since each alveolus contains at least one alveolar macrophage (Gordon and Read, 2002).

1.5.1.2 Pulmonary infection, barrier or stopover for disseminated cryptococcosis

Once in the alveolar space, cryptococcal yeast cells may survive extracellularly and/or transit into lung tissue by either direct internalization by lung epithelial cells or by resident alveolar macrophages (Goldman et al., 2001a; Goldman et al., 2000). At this stage, depending on the nature of host immune response, pulmonary colonization in which cryptococci are either cleared or develop into a localized latent asymptomatic infection. Alternatively, pulmonary involvement can serve as a temporary stopover in which cryptococci go on to establish symptomatic infection with subsequent dissemination to other parts of the body.

Alveolar macrophages comprise 95% of the broncho-alveolar cell population, which makes them the predominant first line phagocytes in the lungs (Gordon and Read, 2002). The interaction of cryptococci with alveolar macrophages most likely determines establishment and fate of pulmonary infection and subsequent systemic dissemination. Increased fungal burden and extrapulmonary dissemination were evident in alveolar macrophage-depleted rats (Shao et al., 2005). Absence of activated alveolar macrophages in T – NK cell deficient mice (Tg26) resulted in no granuloma formation, conditions under which the attenuated *C. neoformans* glucosylceramide mutants (*ΔgcS1*) become able to proliferate and disseminate to the brain (Kechichian et al., 2007). Cryptococcal phagocytosis and antigen presentation by alveolar macrophages induces a Th1 response, which in turn augments alveolar macrophages to kill intracellular cryptococci. Furthermore, immunocompetent individuals mount a strong Th1 inflammatory response, resulting in the formation of granulomas, which contain cryptococci and prevent extrapulmonary dissemination (McQuiston and Williamson, 2012). *Cryptococcus neoformans'* ability to survive and proliferate inside macrophages and reside inside protective granulomas might thus explain latent cryptococcosis in immunocompetent hosts.

Studies using the rat model of cryptococcosis have shown that rats mount a strong immune response, mimicking that of immunocompetent humans. In this model, cryptococcal infection is characterized by granuloma formation and pulmonary containment of infection (Goldman et al., 2000). This response is reversed by treating rats with an immunosuppressive dose of dexamethasone, resulting in the loss of granuloma formation and increased lung fungal burden (Goldman et al., 2000). This

mirrors the weak immune response and susceptibility to cryptococcal infection in immunocompromised patients. For example, CD4+ lymphocyte deficiency in HIV/AIDS patients renders them more susceptible to cryptococcal infection and, once infected, the likelihood of disseminated cryptococcosis and involvement of the central nervous system is high. Localized pulmonary cryptococcosis is seen in HIV/AIDS patients with higher CD4 counts (Meyohas et al., 1995), which further confirms the notion that the degree of brain involvement depends on the state of the pulmonary immune response.

1.5.2 Survival and dissemination in the host

Host antimicrobial molecules are designed to destroy both extracellular and internalised microbes. *Cryptococcus neoformans* has, however, evolved mechanisms to evade host antimicrobial agents and manipulate the immune response in a manner that promotes its survival, replication and persistence in the host.

1.5.2.1 Antiphagocytic factors

Capsule expression is a major virulence determinant for *C. neoformans,* involved in both phagocytosis resistance and immune modulation. The *Cryptococcus* polysaccharide capsule is antiphagocytic and consequently highly encapsulated strains are less phagocytosed by macrophages (Syme et al., 1999; Zaragoza et al., 2009). Reduced phagocytosis translates into reduced T-cell proliferation (Syme et al., 1999) and reduced antigen processing and presentation by macrophages, all resulting in an interference with the T-cell response (Vecchiarelli et al., 1994). Large sized and highly encapsulated cryptococci were found significantly more frequently in the lungs than brain in histopathological sections of a heart transplant patient who died of

cryptococcal meningitis (Xie et al., 2012), implying that encapsulated cryptococci resist phagocytosis, hence reducing their rate of systemic dissemination. Recent studies have demonstrated *C. neoformans* can deploy multiple antiphagocytic strategies, some of which are capsule independent and involve expression of antiphagocytic protein, App1 (Stano et al., 2009), and GATA family transcription factor, Gat201 (Chun et al., 2011). App1 inhibits phagocytosis through binding complement receptors, CR2 and CR3 whereas deletion of Gat201 generates hypocapsulated crypotococci that are highly phagocytosed (Chun et al., 2011; Garcia-Rodas and Zaragoza, 2012).

Phagocytosis avoidance may result in complex effects on dissemination. For instance, mating type α (MATα) strains of *C. neoformans* var.*grubii* are more likely to disseminate to the CNS during coinfection with congenic mating type a (MATa) strains via the pulmonary route of inoculation (Nielsen et al., 2005). Interestingly, MATa and MATα cells form giant cells during pulmonary infection, which are resistant to phagocytosis by macrophages (Okagaki et al., 2010; Zaragoza et al., 2010). However, in coinfection with both mating types, the proportion of giant MATa in the lungs was higher than the MATα cells, one reason why they had a reduced chance to disseminate to the brain (Nielsen et al., 2005). Okagaki and Nielsen have further confirmed the role of these giant (titan) cells in resisting phagocytosis, but they note that titan cell size alone is not enough to induce antiphagocytosis (Okagaki and Nielsen, 2012).

Despite the elaborate ability of *C. neoformans* to resist internalization, the host overcomes this evasion through antibody (Casadevall et al., 1992; Dromer et al.,

1987; Eckert and Kozel, 1987; Kozel et al., 1988; Pirofski et al., 1995; Todaro-Luck et al., 1989) and complement (Kozel and Pfrommer, 1986; Kozel et al., 1989). However, once inside the phagocyte, *C. neoformans* shows a remarkable ability to survive and proliferate inside mature, acidic phagosomes (Alvarez and Casadevall, 2006; Ma et al., 2006; Ma et al., 2009). Furthermore the fungus is able to escape from macrophages through a non-lytic mechanism and spreads from cell-to-cell (Alvarez and Casadevall, 2007; Johnston and May, 2010; Ma et al., 2007), an indication that cryptococci can potentially disseminate to the brain by hitchhiking inside phagocytes. Research into cryptococcal intracellular life has shown that survival in this hostile environment stems from orchestrated expression of both protective and nutrient acquisition factors.

1.5.2.2 Intracellular survival factors

Capsule: *C. neoformans* produces a complex polysaccharide made of two sugars, glucuronoxylomannan (GXM) and galactoxylomannan (GalXM). The capsule both forms a structural coating around the yeast cell surface and is secreted into the medium (Zaragoza et al., 2009). As well as reducing phagocytic uptake, capsule expression protects the fungus from oxidative stress when inside the host cell (Naslund et al., 1995; Zaragoza et al., 2008). Capsular material accumulates in the phagolysosome and renders it leaky (Lee et al., 1995; Tucker and Casadevall, 2002), a process that may allow cryptococci to release factors to inactivate intracellular antimicrobial elements or allow for inflow of nutrients, as well as diluting lysosomal contents (Garcia-Rodas and Zaragoza, 2012).

Melanin: Further protection to the fungus is afforded by production of melanin. Melanin is a negatively charged hydrophobic pigment of high molecular weight

produced by the oxidative polymerization of phenolic compounds (Casadevall et al., 2000). Melanin production is catalysed by the copper-dependent enzyme laccase, produced by *C. neoformans* when growing on substrates containing polyphenolic or polyaminobenzene compounds (Williamson, 1997). Melanin has antioxidant properties and protects *C. neoformans* from oxidative killing by phagocytes. Melanised cells have been shown to be resistant to killing both by oxidants (Emery et al., 1994) and by antifungal drugs such as amphotericin B and caspofungin (van Duin et al., 2002), although recent in vitro susceptibility study shows that *C. neoformans* is generally not susceptible to caspofungin (Messer et al., 2009), implying that the observed antifungal resistance may not be melanin dependent but most likely due to low potency of the drug. High melanin production has been associated with chromosome copy number, in that *C. neoformans* strains with chromosome 13 monosomy produced more melanin and were more virulent than their non-melanised chromosome 13 disomic counterparts in a murine model of cryptococcosis (Hu et al., 2011).

Metabolic machinery: As a natural environmental inhabitant, the fungus grows optimally under conditions of good oxygen supply. In addition to the ability to grow at the host body temperature of $37^{o}C$, cryptococci must adapt to growing under hypoxic conditions, particularly when in an intracellular environment. For instance, *sre1Δ* mutant strains, which are impaired in sterol biosynthesis, were unable to grow under low oxygen conditions and caused no disease in mouse model of cryptococcosis (Chang et al., 2007). A steady supply of energy is crucial for cryptococcal intracellular survival and thus glucose utilization mutants (lacking pyruvate kinase and or hexokinase I and II) are less virulent in a murine inhalation model of cryptococcosis and show decreased persistence in rabbit cerebral spinal fluid

(Price et al., 2011). On the other hand, genes involved in peroxosomal lipid metabolism were upregulated in macrophage internalized cryptococci and cryptococci from mice in the pulmonary phase of infection (Fan et al., 2005; Hu et al., 2008). A recent characterization of *C. neoformans* mitochondrial and peroxisomal β-oxidation mutants has shown that such mutants are unable to grow on fatty acids and have attenuated virulence in mice (Kretschmer et al., 2012), indicating that, like glucose, the metabolism of lipids is essential to *C. neoformans* survival and dissemination in the host.

1.5.2.3 Nutrient acquisition

Nutrient supply is crucial for both intracellular and extracellular cryptococci in the host. Biosynthesis of major virulence factors, melanin and capsule by *Cryptococcus species* require mineral ions such as copper and iron. These minerals are equally important to the host physiology, implying that the pathogen competes with the host for the precious nutrients. An ability to acquire these minerals under conditions of limited availability is essential for cryptococcal survival and pathogenicity. Copper is a cofactor for the cryptococcal enzyme laccase, responsible for melanin synthesis (Williamson, 1994), and is also involved in capsule biosynthesis through the copper transporter-encoding gene, *CTR2* (Chun and Madhani, 2010). Acquisition of Cu by *C. neoformans* is believed to be through the copper sensing/transport (*CFU1/CTR4*) system, which, when genetically disrupted, reduces viability and virulence factor expression by the fungus. High expression of the copper transporter protein Ctr4 was observed in both macrophage-internalized and brain isolated cryptococci, implying that copper acquisition is essential for *C. neoformans* intracellular survival and dissemination to the brain (Waterman et al., 2007). Denying *C. neoformans* access to

copper by the copper chelator microplusin reduces growth and completely inhibits melanisation in vitro (Silva et al., 2011).

In addition to copper, iron is an essential micronutrient required by many microbial organisms. However, high affinity molecules such as haemoglobin, transferrin and ferritin tightly bind iron and make availability of free iron very low in the human host (Schaible and Kaufmann, 2004). For example circulating transferrin binds ferric (Fe^{3+}) iron with a stability constant of 10^{-20}M (Philpott, 2006). To acquire this iron, *C. neoformans* deploys multiple strategies including the high affinity iron transporters Cft1 (permease) / Cfo1 (ferroxidase), the siderophore transporter Sit1 and low affinity uptake (heme utilization) systems (Jung et al., 2009). The high affinity uptake system can acquire ferric iron from transferrin and is able to reduce ferrous (Fe^{2+}) iron to the preferred Fe^{3+} for uptake using the metalloreductase (Fre) system (Jung and Kronstad, 2008; Jung et al., 2009). Although *C. neoformans* cannot produce siderophores, it has the ability to use sidephores expressed by other microbes in its vicinity, an indication that coinfection may exacerbate cryptococcosis by making more iron available to the fungus (Jung et al., 2009). The high affinity iron permease *cft1* mutants were unable to use transferrin as an iron source and showed less virulence and limited dissemination in the brains of infected mice (Jung et al., 2009). Additionally, it has been shown that *C. neoformans* can utilize heme as an iron source, (Jung and Kronstad, 2008), although the mechanism by which heme iron is accessed is still not clear.

Intracellular *C. neoformans* can also acquire and or recycle nutrients using its own or the host's autophagy system. *C. neoformans* autophagy genes *ATG3* and *ATG9* are

upregulated within 2hr and 24hr of intracellular life in J774 macrophages respectively and autophagy mutants are easily killed by macrophages and cause no disease in mouse model of infection (Reviewed in (McQuiston and Williamson, 2012)). Equally, *C. neoformans* can exploit host autophagy mediators to maintain its intracellular survival. Using RNA interference (RNAi), Qin et al have demonstrated that depletion of macrophage autophagy (Atg) proteins significantly reduces intracellular proliferation as well as escape from macrophages (Qin et al., 2011). However, a recent study suggests that macrophage autophagy is a complex process, which can promote or restrict pathogen growth as well as modulate the immune response depending on the host cell type (Nicola et al., 2012).

1.5.2.4 Immune modulation

The host immune response is a key determinant of cryptococcal pathogenesis. A strong Th1 response results in clearance or containment of pulmonary cryptococcal infection, but during early stage infection the fungus is thought to polarize the immune response towards Th2 to promote its survival and dissemination (Zhang et al., 2009). Cryptococcal Urease1 promotes accumulation of immature dendritic cells and biases immunity towards Th2 in the lungs, resulting in increased extrapulmonary dissemination of the fungus (Osterholzer et al., 2009). Through capsule expression, intracellular cryptococci ensure their survival by inhibiting lethal reactive nitrogen species, inducing production of anti-inflammatory cytokines and dampening adaptive immune responses through blocking antigen presentation (Vecchiarelli and Monari, 2012). Furthermore, the capsule inhibits IL-6 production by peripheral monuclear cells, a process thought to subvert the protective immune response against *C. neoformans* (Siddiqui et al., 2006). On the other hand, a recent study has shown that

the *C. neoformans* prostaglandin E (PGE) inhibits the production of IL-17 by differentiating Th17 cells (Valdez et al., 2012). The *C. neoformans* enzyme laccase is responsible for PGE production and consequently laccase mutant (*Δlac1*) strains were less virulent in a murine of infection (Pukkila-Worley and Alspaugh, 2004; Salas et al., 1996; Valdez et al., 2012).

1.5.2.5 Host Cell disruption and barrier penetration

C. neoformans produces degradative enzymes such as phospholipase, proteinase and urease and increasing evidence shows that these enzymes act to degrade membranes, which subsequently compromises host intracellular and intercellular integrity and paves the way for dissemination of the fungus to the brain..

***Phospholipase*:** Phospholipases are a heterogeneous group of enzymes that are able to hydrolyse one or more ester linkages in glycerophospholipids. The *Cryptococcus neoformans* phospholipase enzyme demonstrates phospholipase B (PLB), lysophospholipase hydrolase and lysophospholipase transacetylase activities (Wright et al., 2004). The action of phospholipases can result in the destabilization of membranes, cell lysis, and release of lipid second messengers, promoting interstitial lung infection and the dissemination of cryptococci in lymph and blood (Ghannoum, 2000; Santangelo et al., 2004). Phospholipase B cleaves dipalmitoyl phosphatidylcholine, one of the main components of lung surfactant, enhancing adherence to lung epithelial cells and thus assisting fungal spread (Ganendren et al., 2006; Santangelo et al., 2004; Steenbergen and Casadevall, 2003). Furthermore PLB enhances both cryptococcal phagocytosis by macrophages and intracellular survival (Noverr et al., 2003; Wright et al., 2007). Through Phospholipase B1 action,

cryptococci take up macrophage arachidonic acid, which is subsequently used to generate eicosanoids (Noverr et al., 2003; Wright et al., 2007). The generated eicosanoids can be used to suppress the host immune response and hence promote intracellular survival and dissemination of the fungus (Djordjevic, 2010; Noverr et al., 2003; Wright et al., 2007). Interestingly, there is a correlation between phospholipase expression and virulence in a dose dependent manner among strains used to infect mice (Chen et al., 1997; Ghannoum, 2000), and hence disruption of the PLB1 gene leads to reduced virulence *in vivo* and growth inhibition in a macrophage-like cell line (Cox et al., 2001). PLB1 has also been shown to enhance penetration of the blood-barrier through activation of host cell Rac1 (the small GTP- binding Rho family of proteins) and its association with STAT3 (Maruvada et al., 2012).

Proteinase: Possession of proteinase by both environmental and clinical isolates has been demonstrated to confer the ability to degrade host proteins including collagen, elastin, fibrinogen, immunoglobulins and complement factors (Chen et al., 1996). It was further proposed that these proteinases, together with phospholipases, enable replication of *C. neoformans* inside the host macrophages by damaging phagosomal membranes and thus escaping killing by phagocytic enzymes (Tucker and Casadevall, 2002). Despite these advances a decade ago, no more work has been done to elucidate the mechanism by which proteinases enhance virulence of *C. neoformans* in the host.

Urease: Urease catalyses the hydrolysis of urea to ammonia and carbamate and is an important pathogenesis factor in certain bacteria (Steenbergen and Casadevall, 2003). The cryptococcal urease Ure1 is an important virulent factor. Mice infected with *Ure1Δ* mutants live longer than mice infected with the wild type strain H99 (Cox et al., 2000). Although urease was not required for growth in the brain, the

dissemination patterns to the brain, spleen, and other organs after intravenous inoculation differed from the wild type strain, leading to the proposal that Ure1 is important for CNS invasion by enhancing yeast sequestration within microcapillary beds (such as within the brain) during hematogenous spread, thereby facilitating blood-to-brain transmission (Olszewski et al., 2004). This sequestration affected cryptococcal adherence and or toxicity to the brain endothelial cells, a view supported by Charlier and colleagues' observation of brain lesions as early as 6hrs after intravenous inoculation of *C. neoformans* (Charlier et al., 2005a). Indeed Shi and colleagues, using intravital microscopy for real time imaging of *C. neoformans* transmigration in a murine model, recently demonstrated that cryptococcal Ure1 was responsible for increased transmigration sites at the blood-brain barrier (Shi et al., 2010).

1.5.3 Dissemination mechanisms: how does the fungus get into the brain?

The blood-brain barrier (BBB) ensures that the brain is highly protected, with little access by circulating macromolecules and microorganisms. The human BBB is made of microvascular endothelial cells supported by astrocytes, pericytes and neuronal feet (Correale and Villa, 2009; Weksler et al., 2005). Unlike the peripheral endothelial cells, the brain endothelial cells are joined together by tight junctions making the BBB a formidable barrier to many pathogens (Weksler et al., 2005). For *C. neoformans* to infect the brain, cryptococci must penetrate the normally impermeable blood-brain barrier (BBB). The current understanding is that, once in the body, cryptococcal yeast cells may use multiple ways to enter the brain (Figure 1: Dissemination model of *C. neoformans* from the environment to the brain).
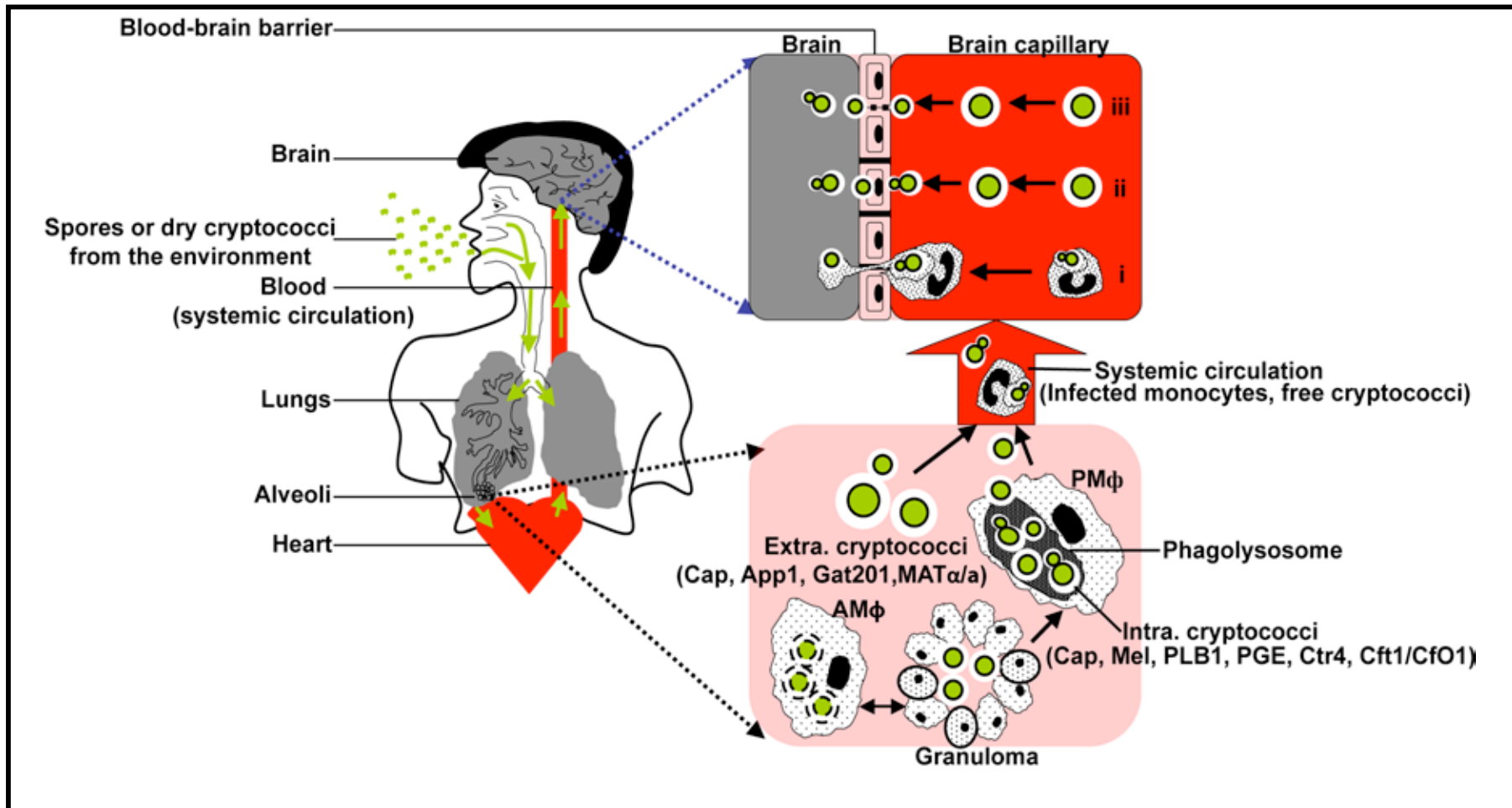
Figure 4: The dissemination model of *C. neoformans* from the environment to the human brain
Through inhalation and with the help of mucocilliary movement, spores or dry cryptococci colonize the alveolar space in the lungs (Velagapudi et al., 2009) In immunocompetent individuals, activated alveolar macrophages (AMФ) phagocytose and kill cryptococci and surround

cryptococci to form granulomas. Cryptococci in granulomas may stay latent or be reactivated and cause infection once the immune status of an individual changes. In immunodeficient individuals, parasitized alveolar macrophages (PMΦ) with intracellular cryptococci act as Trojan horses within the lungs, triggering dissemination into systemic circulation (McQuiston and Williamson, 2012). In order to survive in the hostile intracellular environment, *C. neoformans* secretes or enlarges its capsule (Cap), forms melanin (Mel) as an antioxidant against reactive oxygen and nitrogen species, prostaglandin E (PGE) to downregulate antimicrobial activity, upregulates nutrient acquisition genes, Ctr4 for Copper and Cft1/Cfo1 for Iron and secretes phospholipase (PLB1) which impairs intracellular antimicrobial responses (Emery et al., 1994; Garcia-Rodas and Zaragoza, 2012; Jung et al., 2008; Waterman et al., 2007; Wright et al., 2007). Alternatively, cryptococci may resist phagocytosis by growing to a very large size (Titan cells), generating a large capsule, expressing antiphagocytic protein (App1) or through the activity of the antiphagocytic transcriptional regulator GAT201 (Chun et al., 2011; Okagaki et al., 2010; Okagaki and Nielsen, 2012; Stano et al., 2009; Zaragoza et al., 2009; Zaragoza et al., 2010). Extracellular cryptococci may remain localized in the lungs or disseminate transcellularly into the blood circulation. In the systemic circulation, cryptococci associate with monocytes or are carried freely into the brain capillary bed. In the brain capillary, cryptococci may penetrate the blood-brain barrier by either i) riding inside infected monocytes/macrophages (Trojan horse) (Charlier et al., 2009), ii) transcytosis – binding to and being internalized by brain microvascular endothelial cells (Shi et al., 2010), iii) paracellular traversal between endothelial cells, most likely permitted by damaged or weakened tight junctions (Stie et al., 2009).

1.5.3.1 Trojan horse dissemination model

The Trojan horse form of dissemination involves parasitized phagocytes such as monocytes and/or macrophages smuggling pathogens across the BBB into the brain (Charlier et al., 2005b; Charlier et al., 2009; Kim, 2008). The intracellular parasitism of monocytes/macrophages has been demonstrated in both *in vitro* and *in vivo* models (Alvarez and Casadevall, 2006; Feldmesser et al., 2001a; Ma et al., 2006). A study of infected mouse lungs demonstrated an 8hr peak of intracellular cryptococci in phagocytes after infection and after day 7 of infection, intracellular cryptococci were more abundant than extracellular ones (McQuiston and Williamson, 2012). Following phagocytosis, cryptococci survive and proliferate inside macrophages (Alvarez and Casadevall, 2006; Ma et al., 2006). Furthermore, live cryptococci can be expelled in a novel non-lytic exocytosis (vomocytosis), leaving the host macrophage unharmed (Alvarez and Casadevall, 2006; Alvarez and Casadevall, 2007; Johnston and May, 2010; Ma et al., 2006; Ma et al., 2007). The exocytosed cryptococci then spread to other cells (Alvarez and Casadevall, 2006; Alvarez and Casadevall, 2007; Johnston and May, 2010; Ma et al., 2006; Ma et al., 2007). This direct cell-to-cell spread potentially explains how cryptococci can take advantage of phagocytes to penetrate the BBB in a 'Trojan horse' manner (Ma et al., 2007). By infecting mice with cryptococcal-laden monocytes, Charlier et al. demonstrated the occurrence of the Trojan horse traversal of *C. neoformans* across the BBB *in vivo,* since mice infected with cryptococcal-laden monocytes had high brain fungal burdens compared to mice infected with free cryptococci. The originally cryptococcal-laden monocytes (labelled) were found in the brain parenchyma indicating that they had penetrated the BBB (Charlier et al., 2009). Reduction of disseminated cryptococcosis was observed

in alveolar macrophage-depleted immunodeficient mice, which indirectly affirms the importance of the Trojan horse model in dissemination of cryptococci (Kechichian et al., 2007).

Exploitation of host leukocytes to gain entry into the brain has also been demonstrated in other intracellular pathogens such as *Listeria monocytogenes*, *Mycobacterium tuberculosis*, HIV and the protozoan parasite *Toxoplasma gondii* (Drevets, 1999; Drevets and Leenen, 2000; Drevets et al., 2004; Kanmogne et al., 2007; Lachenmaier et al., 2011). *T. gondii is* a life-long intracellular parasite that infiltrates the BBB by hiding in phagocytes and lymphocytes, a process mediated by proinflammatory cytokines and involves high expression of endothelial cell adhesion proteins, ICAM and VCAM (Lachenmaier et al., 2011; Montoya and Liesenfeld, 2004). The non-specific lodging of cryptococci in brain capillaries observed by Shi et al, followed by transmigration (which is urease dependent) at 6hr might be causal to localized toxicity and inflammation (Shi et al., 2010). Inflammation can either result in breakdown of intercellular junctions or attract and promote infiltration of inflammatory phagocytes, which in the process phagocytose and traffic cryptococcal yeast cells into the brain.

1.5.3.2 Transcellular pathway

This pathway allows pathogens to cross the BBB by transcytosis through the brain microvascular endothelial cells (BMEC) by taking advantage of cellular endocytic processes (Chang et al., 2011; Charlier et al., 2005a; Jain et al., 2005). A number of bacterial pathogens such as *Escherichia coli,* Group B *Streptococcus*, *Listeria monocytogenes,* and the fungal pathogen *Candida albicans* are reported to use the

transcytosis pathway (Charlier et al., 2005a; Kim, 2008). Cryptococcal transcellular traversal of the BBB has been widely studied using *in vitro* models of the blood-brain barrier, which have demonstrated the ability of *C. neoformans* to adhere to, be internalised by, and traverse brain microvascular endothelial cells (Charlier et al., 2005a; Vu et al., 2009).

Occurrence of transcytosis across the BBB depends on adherence and internalization of cryptococcal yeast cells by BMEC. Chen et al. showed that binding but not internalization could occur when cryptococci were incubated with human BMEC at 37°C and that binding induced cytoskeletal changes (Chen et al., 2003). However, using transwell apparatus and electron microscopy, studies by Chang et al and Vu et al. have shown that coincubation of brain microvascular endothelial cells with encapsulated and acapsular strains of *C. neoformans* results in both adherence and internalization of crypotococci with subsequent penetration of the BBB (Chang et al., 2004b; Vu et al., 2009). Crossing at the endothelial surface was further demonstrated in a murine model of cryptococcosis which showed that cryptococcal yeast cells were mostly localized in the brain parenchyma close to brain capillaries and no association was observed with the choroid plexus at both early and late stages of infection (Chang et al., 2004a; Charlier et al., 2005a). Recent study using real time intravital imaging has further elucidated the process of cryptococcal transcytosis across the brain endothelium. Six hours after intravenous inoculation cryptococci were seen transmigrating across BBB in a manner that involved transcytosis through brain endothelial cells (Shi et al., 2010).

The nature of interaction between *Cryptococcus* and brain microvascular endothelial cells (BMEC) remains poorly understood. While most bacterial pathogens are reported to use receptor-mediated endocytosis to traverse BMEC, no receptor has been identified for adherence of *C. neoformans* to brain endothelial cells (Charlier et al., 2005b; Vu et al., 2009). The non-tethered movement and eventual trapping of cryptococci in the brain capillaries of similar diameter, described by Shi et al, implies that brain endothelium lacks specific surface molecules or receptors to capture cryptococci (Shi et al., 2010). However, an independent *in vitro* study previously demonstrated the involvement of glycoprotein CD44 expressed by human brain microvascular endothelial cells in enhancing the binding of *C. neoformans* (Jong et al., 2008). Binding of CD44 by cryptococcal hyaluronic acid induces downstream signaling mediated by protein kinase alpha (PKA-α), which results in cytoskeleton reorganisation and phagocytosis of cryptococci by BMECs (Jong et al., 2008). In line with CD44 involvement, Sheng-He et al recently demonstrated that CD44 is exposed in lipid rafts, through which it interacts with *C. neoformans* hyaluronic acid, and that antibody blocking of CD44 inhibits cryptococcal adherence and uptake by human brain endothelial cells (Huang et al., 2011) (Figure 2). The glycoprotein CD44 is a widely expressed protein by many cell types (Goodison et al., 1999; Ponta et al., 2003) and thus *Cryptococcus*-CD44 interaction may not be specific to the brain endothelium alone. However, alternative splicing and post-translational modification make the multi-exon CD44 gene functionally diversified in different cell types (Goodison et al., 1999; Ponta et al., 2003), and hence investigating the nature of BMEC CD44 expression when exposed to cryptococci is needed to determine if the interaction is specific to brain endothelium. Apart from hyaluronic acid, a recent study has demonstrated that *C. neoformans* Phospholipase B1 interacts with lipid

mediators in the brain endothelial cell membrane thereby activating GDPrac1 to GTPrac1 which then associates with STAT3. The GTPrac1/STAT3 association induces cytoskeletal rearrangements resulting in phagocytosis of cryptococci (Maruvada et al., 2012)(Figure 2). Other studies have indicated capsule to be important in *Cryptococcus*-brain endothelial cell interaction (Chang et al., 2004a; Charlier et al., 2005a; Fries et al., 2001; Guerrero et al., 2006; Ibrahim et al., 1995; Jain et al., 2006a). However, these studies demonstrated varying contributions of the capsule and/or its absence, leaving the role of capsule in *C. neoformans* transmission across the BBB unclear. By exposing both murine and human BMEC to encapsulated *C. neoformans* serotype A or D and their acapsular mutant derivatives, we have recently shown that the binding and uptake of cryptococci by BMEC is capsule independent (Sabiiti and May, 2012).

1.5.3.3 Paracellular pathway

The paracellular pathway involves pathogens traversing the BBB through the intercellular spaces (Chang et al., 2004a; Kim, 2008). This mechanism involves the pathogen damaging and weakening tight junctions, which join the brain endothelial cells together, in order to gain entry. *Trypanosoma* species are thought to use the paracellular pathway (Kim, 2008). Severe damage of the endothelium characterized by neuropil edema (neuro-accumulation of fluid) and sequestration of yeast in the brain microvessels were observed following cryptococcal penetration of the BBB (Charlier et al., 2005b; Olszewski et al., 2004). Furthermore, Chen et al showed that cryptococcal binding of the microvascular endothelium induced tight junction alteration (Chen et al., 2003). In addition, a recent study has shown that cryptococcal mannoproteins bind host plasminogen, which is activated to the effector form,

plasmin. Plasmin binds and breaks down extracellular matrix and membrane, thereby increasing the chance for paracellular penetration of the blood-brain barrier to occur (Stie et al., 2009). Taken together, these data indicate the possibility of cryptococci using a paracellular entry by inducing damage or exploiting host mechanisms that weaken the brain endothelial cell tight junctions (Figure 2).
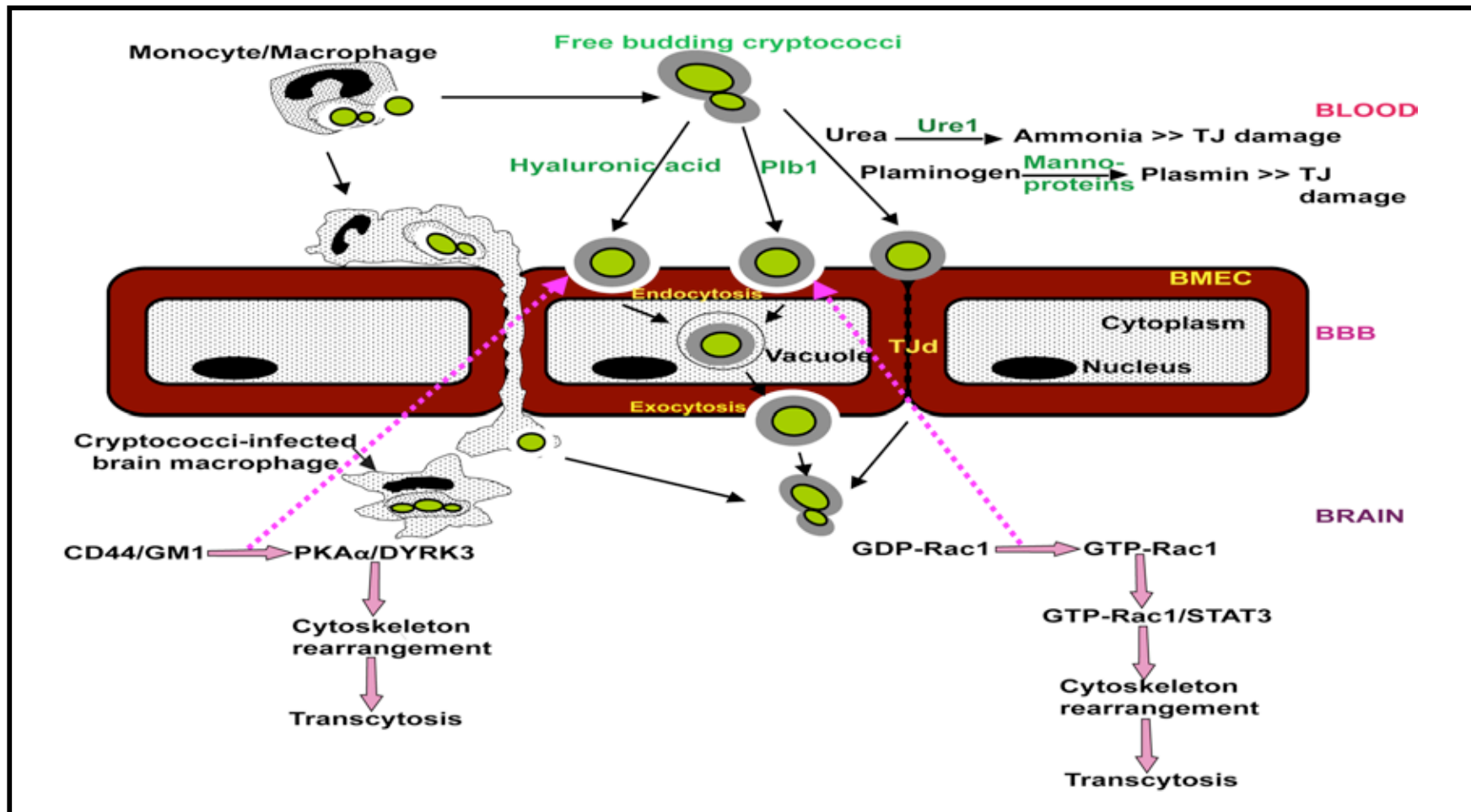
Figure 5: Cryptococcal interaction of with brain microvascular endothelial cells and subsequent penetration the blood-brain barrier

Cryptococcal yeast cells bind to – and are encircled by - microvilli-like protrusions on endothelial cells, resulting in internalization into intracellular vacuoles (endosomes) (Chang et al., 2004a). *C. neoformans* interaction with BMEC induces lipid rafts (GM1) to expose cell

adhesion glycoprotein CD44, which binds cryptococcal hyaluronic acid (Huang et al., 2011; Jong et al., 2001). Hyaluronic acid-coated cryptococci bind to CD44 in lipid rafts (GM1) and the interaction induces cytoskeleton rearrangement mediated by protein kinase A-alpha α (PKAα) or dual specificity tyrosine phosphorylation-regulated kinase-three (DYRK3) resulting in phagocytosis by – and transcytosis across BMEC (Huang et al., 2011; Jong et al., 2001). Alternatively internalisation/transcytosis may occur through GTP-Rac signalling induced by secreted *C. neoformans* Phospholipase B1 (Plb1) (Maruvada et al., 2012). Cryptococcal - Urease (Ure1) can convert urea to Ammonia (Shi et al., 2010) whereas mannoproteins bind and activate plasminogen to plasmin (Stie et al., 2009). Both Ammonia and Plasmin have damaging effects on the extracellular cell matrix and may promote paracellular penetration of the BBB by cryptococci through damaged tight junctions (TJd). While it is known that circulating monocytes are attracted to regions of inflammation through which they infiltrate into tissue, factors involved in the attraction of cryptococci-laden monocytes to brain endothelium and subsequent penetration of the blood-brain barrier are still unknown.

The fact that >95% of cryptococcal meningitis cases are HIV/AIDS patients, often in the AIDS state, in which the blood-brain barrier is most likely inflamed and thus more permeable, makes the paracellular invasion of the brain quite plausible. During HIV, virus-infected monocytes are reported to infiltrate the blood brain barrier in the early stages of infection resulting in inflammatory disease and damage to the BBB (Boven et al., 2000; Nottet et al., 1997). Moreover, the HIV-1 Tat (*trans-activator* of viral replication) protein has been implicated in damaging the blood-brain barrier by inducing apoptosis of brain microvascular endothelial cells with subsequent increased permeability (Avraham et al., 2004; Kim et al., 2003). Whether HIV infected monocytes or the HIV-1 Tat protein mediate damage of the BBB to promote cryptococcal penetration of the BBB remains unknown. Despite the occurrence of both diseases among HIV/AIDS patients, there are so far no clinical reports associating HIV induced neuroinflammatory disorders (HIV associated encephalitis and or dementia) with the occurrence of cryptococcal meningitis, implying that the two conditions might occur independently. Interestingly, however, the HIV protein gp-41 has been shown to enhance cryptococcal binding to human brain endothelia (Jong et al., 2007).

1.6 Cryptococcal meningoencephalitis

Once in the brain, the fungus causes meningoencephalitis, a severe form of the disease, which is uniformly fatal if untreated (Casadevall and Perfect, 1998). Even with treatment, mortality can be as high as 30 – 100% in HIV/AIDS cohorts (Bicanic and Harrison, 2005; Boulware et al., 2010; Kambugu et al., 2008; Mwaba P. et al. , 2001; Nussbaum et al., 2010). Patients present with headache, fever, malaise and altered mental status and less often with signs such as meningism, papilloedema,

cranial nerve palsies, focal neurological deficit and depressed level of consciousness (Bicanic and Harrison, 2005). Raised intracranial pressure is the most common complication, which results in visual and hearing loss (Bicanic and Harrison, 2005). Pathologically, non-HIV CM victims are found with more inflammation of the brain tissue and lower numbers of extracellular cryptococci than HIV-associated CM (Lee et al., 1996). Postmortems of HIV-associated CM victims showed large number of cryptococci in the arachnoid area and this number was associated with raised intracranial pressure, suggesting that the accumulation of cryptococci in the arachnoid and subsequent obstruction of CSF outflow underlies a raised intracranial pressure (Loyse et al., 2010). Cerebral spinal fluid fungal burden has been demonstrated to be associated with mortality in HIV-associated cryptococcal meningitis (Bicanic et al., 2009a).

C. neoformans accounts for 99% of the cryptococcal meningitis cases and is the main cause of disease in immunocompromised people, while *C. gatti* is responsible for the remaining 1% of the cases and primarily infects immunocompetent people. Although the underlying complications and clinical outcome can be different, the form and severity of CM disease does not vary between the two aetiological agents (Mora et al., 2012; Steele et al., 2010). Treatment guidelines have been designed with consideration of the patient's other underlying conditions such as HIV status or the presence of an organ transplant (Perfect et al., 2010). For example intravenous (IV) Amphotericin B (AmB) deoxycholate (Ambd) 0.7 - 1.0mg/kg plus flucytosine (100 mg/ kg) for 4 days followed by 2 weeks of fluconazole 6mg/kg is recommended as primary induction and consolidation therapy for HIV infected patients (Perfect et al., 2010). Despite the different regimens to manage the disease, new antifungal drug

development is highly neglected, with the 2002 introduction of Voriconazole being the most recent new antifungal to come to market. The current most effective antifungal is amphotericin, which is unfortunately toxic and requires sophisticated administration procedures that are not easily accessible in resource poor settings where cryptococcal meningitis is most prevalent.

1.7 Project Aims

Transmission of *C. neoforms* across the normally impermeable blood-brain barrier (BBB) is a pertinent question in cryptococcosis research. Understanding the mechanism(s) by which *Cryptococcus* infects the brain is crucial for developing effective therapies to treat the fatal cryptococcal meningoencephalitis. Transcytosis, one of the mechanisms put forward to explain the transmigration of the fungus across the BBB, occurs through cryptococci adherence and uptake by brain microvascular endothelial cells (BMEC) (Chang YC 2004, Vu et al 2009). BMEC are not professional phagocytes and we were therefore interested in dissecting how cryptococci adhere and traffic across this barrier. The first part of this thesis thus focuses on our attempts to quantify cryptococcal uptake by both murine and human brain endothelia and to address a potential role for the fungal capsule in this process.

In the second part of this thesis, we report a systematic study of macrophage-cryptococci interaction using clinical isolates from cerebral spinal fluid of HIV-associated crytptococcal meningitis patients and the association between this interaction and patient clinical parameters. Extensive previous work by our group and others has indicated roles for intracellular survival and growth in driving cryptococcal virulence in a hypervirulent outbreak of cryptococcosis (Ma et al 2009). However, no similar study had ever been undertaken for HIV-associated cryptococcosis. Thus we undertook an extensive characterisation of 47 clinical isolates obtained (in collaboration with Dr. Tihana Bicanic, St. Georges University of London) in order to establish the relative importance of different phenotypic parameters in determining clinical progression.

CHAPTER II: MATERIALS AND METHODS

2.1 BMEC – Cryptococcus interaction study

2.1.1 Strains and culture

Laboratory *C. neoformans* strains consisting of two isogenic pairs: 1) Serotype A H99 and its isogenic acapsular strain cap59 and 2) Serotype D B3501 with its isogenic acapsular strain B4131 were used. For phagosome acidification studies, a GFP-expressing derivative of H99 (Voelz et al., 2010) was used. Strains were propagated on YPD agar (1% yeast extract, 1% peptone, 2% dextrose and 1% agar) at 25°C. Prior to experimentation, cultures of both strains were grown in YPD broth (1% yeast extract, 1% peptone and 2% glucose) at 25°C with rotation at 20rpm overnight. The yeast cells were washed with sterile phosphate buffered saline (PBS) and counted with a haemocytometer to the required inoculum, 1×10^6 and 2×10^6 yeast cells for macrophages and endothelial cells respectively. For some assays, yeast cells were opsonised with 5μg/ml mouse IgG anti-capsule antibody 18B7 (kind gift from Prof. Arturo Casadevall) for 45 – 60 min or stained with 0.5mg/ml FITC (save for the GFP expressing H99 strain) for 30min with rotation (Labrolller, Labnet Inc.) at room temperature prior to use.

2.1.2 BMEC tissue culture

2.1.2.1 Murine brain endothelial cell-line, bEnd3

Immortalized mouse brain derived endothelial (bEnd3) cells were obtained from the European Cell Collection Centre, London, and a comparative batch was a kind gift from Dr. Mark Gumbleton, Cardiff School of Pharmacy. Cells were grown to monolayer confluence in T75 flasks (Greiner, UK) for sub-culturing and or 24 well tissue culture plates (Greiner, UK) for binding/uptake assays. Cells were maintained in Dulbecco's modified Eagle's medium (DMEM, Sigma Aldrich) supplemented with

10% foetal bovine serum (FBS), 1% streptomycin/penicillin and 2mM L-glutamine, 1% non-essential aminoacids, 1% Sodium pyruvate and 5µM 2-Mercaptoethanol and incubated at $37^{\circ}C$ with $5\%CO_2$ for 4-6 days when they formed complete monolayer. Cells were lifted off plastic using 1X Trypsin EDTA for 5-10min at $37^{\circ}C$ and passaged 1/10 a number of times until the usable passage or frozen for later use. Passages 20 – 35 were used in assays. Freezing was done by suspending cell freezing medium (50% DMEM, 40% FBS and 10% DMSO) followed by slowdown freezing at $-20^{\circ}C$ for 1hr, overnight at $-80^{\circ}C$ and finally long-term storage under liquid Nitrogen.

2.1.2.2 Human brain endothelial cell-line, hCMEC/D3

HCMEC/D3 cells (a gift from Prof. Jane McKeating, Institute of Biomedical Research, University of Birmingham) were grown in endothelial growth medium 2 (EGM-2, Lonza, UK) in T75 flasks for passaging and or 24 well tissue culture plates precoated with Calf Skin collagen (Sigma Alderich, UK). Passages 24 – 29 were used in assays. Like bEnd3 cells, hCMEC/D3 cells were detached using Trypsin EDTA, passaged 1/10 and or frozen in 90% FBS and 10% DMSO for later use. The tissue culture was maintained at $37^{\circ}C$ with $5\%CO_2$ for 4-6 days to obtain a fully matured cell monolayer.

2.1.3 Seeding endothelial cells for infection assay

To ensure even growth of cell monolayers, 24-well plates were seeded with 10^5 endothelial cells per well and grown at $37^{\circ}C$ with $5\%CO_2$ for 4-6 days with media change every 2 – 3 days. For microscopic examination, 13mm sterile glass coverslips (collagen coated for hCMEC/D3 cells) were inserted into the 24 well plates before seeding with endothelial cells, allowing the monolayer to grow on the coverslip,

which could then be easily transferred for microscopy. Prior to infection, tissue culture growth medium was replaced with serum free medium and incubated for 1hr at 37°C. The cultures were then inoculated with $2x10^{6}$ yeast cells per well, producing an approximate infection ratio of 1:3 (target: effector). Infections were allowed to proceed for either 2hr or 4hr, as described, at 37°C with 5% CO_2. To ensure that the infection media did not have negative effect on cryptococcal growth, cryptococci (10^{5} yeast cells/ml) were directly inoculated into bEnd3 and or hCMEC/D3 infection medium and growth recorded over 24hr.

2.1.4 Cryptococci binding and uptake by BMEC cells

The rate of cryptococcal yeast cell association with BMEC (bEnd3 and hCMEC/D3) cells was determined both microscopically and using viable cell (CFU) counts. In the former, dual colour fluorescence microscopy (Nikon Eclipse T*i* - S, Japan) was used to determine associated (adherent and internalized) yeast cells. After infection (1:3 infection ratio), the non-adherent yeast cells were removed by washing four times with sterile PBS and the extracellular adherent yeast cells stained for 10 - 15min with 20µg/ml calcoflour white at room temperature (adapted from Jong et al., 2001). Since mammalian cells are impermeable to calcofluor white, internalized yeast retained the green FITC signal while adherent cells stain blue. Nine random fields per coverslip were viewed and the internalized and non-internalized yeasts therein counted. Association (total number of yeast cells attached or internalized by BMEC) internalization were determined and compared to the original inoculum. Since this microscopic approach did not distinguish between live and dead cryptococci, we exploited colony forming unit (CFU) assays to determine the viability of cryptococci that had been internalised by cells of the BBB. After removal of non-adherent

cryptococci by extensive washing, endothelial cells were lysed with 200μl sterile water for 15min at 37°C to release internalized cryptococci and the lysate plated on YPD agar for colony counts (CFU assay). The associated cryptococci were determined as the ratio of cryptococcal yeast cells (CFU/ml) to the original inoculum. Thus, by comparing data derived both from microscopy (which distinguishes internalised from attached cryptococci, but not live from dead cells) and from CFU counts (which have the opposite profile) we were able to accurately estimate both uptake and survival of cryptococci. The results were recorded as endothelial cell associated cryptococci per well, which is equivalent to cryptococci per coverslip for microscopy and CFU/ml for colony counts.

2.1.5 Opsonisation and cryptococci – BMEC interaction

Antibodies to *Cryptococcus* have been reported to exist in circulation as early as childhood (Goldman et al., 2001b). Furthermore, phagocytosis studies using macrophages have shown that internalization of cryptococcal yeast cells is enhanced by antibody and or complement mediated opsonisation (Bolanos and Mitchell, 1989a; Mukherjee et al., 1995a; Vecchiarelli et al., 2002). However, no studies have investigated whether adherence and uptake of cryptococci by BMEC requires opsonisation. To address this, opsonised and non-oposonized live and heat killed H99 cryptococci were incubated with BMEC for 2hr and 4hr at 37°C. The rate of association and internalization was determined as described in section 2.1.4.

2.1.6 Effect of viability on Cryptococcus – BMEC association and internalization

We tested whether dead cryptococci adhere and are internalized by BMEC at the same rate as live cells. 1ml aliquots of both encapsulated and non-capsulated cryptococci were heated at $65^{o}C$ for 15min prior to infection. Adherent and internalized yeasts were determined microscopically. To determine if the yeast culture was completely killed, 20μl aliquots were plated on YPD agar and no growth was observed.

2.1.7 Effect of IFN -γ induction bEnd3 cell – cryptococci association

IFN-γ and other inflammatory cytokines such as TNF-α are reported to increase expression of cell adhesion molecules by brain-microvascular endothelial cells (Dietrich, 2002; Lachenmaier et al., 2011). To investigate whether exposure of bEnd3 cells to IFN-γ increases the binding and phagocytosis of encapsulated or acapsular cryptococci, mature bEnd3 cell monolayers were treated with 100U and 500U of mouse IFN-γ in serum free medium 12 prior to the infection assay. Untreated bEnd3 cells (IFN-γ NIL) were used as negative controls. After 2hr and 4hr of infection, the cells were washed four times to remove non-adherent cryptococci and lysed with 200μl of sterile water for 15min at $37^{o}C$. The lysate was diluted to ½ and ¼ and plated on YPD agar for colony counts.

2.1.8 Tracking phagosome acidification in BMEC

To test whether cryptococci that have been internalised into BMEC undergo 'normal' phagosome maturation, we made use of LysoTracker, (Molecular Probes, UK), an acidotropic probe with a fluorophore linked to a weak base, which labels acidic organelles in different cell types including endothelial cells (Schroder et al., 2006). Mature bEnd3 and hCMEC/D3 cell monolayers were infected with the GFP-labelled H99 strain for 2hr and 4hr at 37^oC with $5\%CO_2$. After infection, non-adherent yeast cells were removed by washing four times with sterile PBS. The cells were then treated with 50nM/ml Lysotracker for 30min at 37^oC, washed and counter labelled with 20μg/ml calcofluor white to stain extracellular adherent yeast. Cells were fixed with PFA 4% in PBS and viewed with fluorescence microscopy to determine lysotracker positive yeast cells. Percentage acidification was determined as the proportion of endothelial cells with lysotracker positive (red signal) intracellular yeast cells to the total endothelial cell population in the viewed fields.

2.2 Macrophage – clinical *Cryptococcus* interaction study
2.2.1 Patients and clinical isolates

Fourty-seven HIV-associated cryptococcal meningitis patients, a fraction of >500 patients in the four completed clinical trials in Africa and Asia were the source of the 47 *Cryptococcus neoformans* isolates we studied. Patients were ART naïve under the clinical trials for a combination of antifungal regimens. Baseline patient clinical parameters including fungal burden, fungal clearance, mental status, 2 and 10 weeks mortality were determined. From patient CSF cultures the isolates were obtained and preserved (Dr. T Bicanic and group, St. Georges University of London) (Table 1).

| Patient code | CD4 count | CSF Parameters | | | | | | | | | | | | | Mental Status | 2 Wk M | 10 Wk M | Isolate |
		Neuts	Lymphs	WBC	Protein	Glc	CrAG (Log2)	Fungal load (Log10)	Slope	TNF (Log10)	IL6 (Log10)	IFN (Log10)	OP				
20	20	ND	ND	2	0.2	4.8	8	5.778151	-0.088	0	1.30792	0	8	0	0	1	CM20
24	97	18	202	220	0.34	3.2	6	4.633469	-0.269	0.83187	2.71451	1.2615	24	0	0	0	CM24
36	14	ND	ND	0	1	3.8	2	2.816241	-0.939	1.33886	2.81378	1.95804	ND	0	0	0	CM36
50	8	ND	ND	3	0.58	2.4	6	4.153815	-0.586	1.20412	3.13441	1.65456	20	0	0	0	CM50
52	8	ND	ND	5	0.94	2.7	11	5.322219	-0.264	1.27531	3.15122	1.67256	31	0	0	0	CM52
64	ND	ND	ND	1	0.33	2.7	9	6.389166	-0.647	1.00689	2.96881	1.4387	27	0	0	0	CM64
102	4	0	0	0	0.6	1.7	12	6.39794	ND	1.02646	1.69897	0	40	0	1	1	CCTP02
103	56	0	2	2	1.6	0.3	11	5.961421	-0.38	2.05567	2.06752	1.88066	76	0	0	0	CCTP03
110	18	0	15	15	0.86	1.3	9	6.612784	-0.398	1.9614	1.69897	1.78432	37	0	0	1	CCTP10
112	21	0	0	0	0.52	3.3	11	6.518514	-0.364	0	3.96827	0.37778	39	0	0	0	CCTP12
113	37	3	1212	1215	4.1	2.1	12	5.149219	-0.122	ND	2.62598	ND	9	0	0	0	CCTP13
125	19	31	72	103	0.9	1.1	10	6.290035	-0.472	2.09287	ND	1.92801	ND	0	0	ND	CCTP25
126	ND	0	0	0	1.2	1.9	11	6.118926	ND	1.0961	4.28071	0.55387	34	1	1	1	CCTP26
129	21	0	0	0	0.44	2.9	9	5.352182	-0.92	0	2.94644	0.71022	7	0	0	0	CCTP29
130	42	0	5	5	0.84	2.3	10	6.525045	-0.421	0.2982	3.81584	0	12	0	0	0	CCTP30
149	74	8	124	132	0.92	1.8	9	2.612784	-0.123	1.34598	4.39002	2.26801	53	1	0	0	CCTP49
152	41	0	25	25	1.06	0.3	13	6.332438	0.029	1.94804	3.72876	2.15834	ND	1	0	1	CTTP52
203	8	0	2	2	0.84	2.4	15	6.40654	-0.428	1.02213	0	1.51196	30	0	0	0	RCT03
206	14	1	13	14	0.6	1.0	12	5.361728	-0.553	1.88278	2.81257	2.19399	35	0	0	0	RCT06
207	12	0	1	1	0.3	2.4	11	5.961421	-0.262	0.58915	0.41996	0.73002	80	0	0	0	RCT07
221	7	0	0	0	0.49	2.2	15	5.76342799	ND	0.69973	0.87967	1.08473	32	1	1	1	RCT21
224	9	0	0	0	0.41	2.3	9	6.273001	-0.393	0.40738	1.54307	0.94263	20	0	0	0	RCT24

233	2	0	0	0	0.48	3.0	5	3.612784	-0.723	0.14617	0.78746	1.66345	10	1	0	1	RCT33
236	9	0	0	0	0.32	3.5	13	6.361728	-0.546	0.72643	0.5172	0.68171	15	0	0	0	RCT36
244	44	0	22	22	1.08	1.9	12	6.283301	-0.502	1.02213	2.11893	1.71844	19	0	0	0	RCT44
250	31	0	36	36	1.45	1.7	14	6.361728	-0.791	1.22573	1.97011	2.10544	38	0	0	0	RCT50
251	40	0	19	19	0.98	1.2	12	6.002166	-0.651	0.49786	2.41774	1.53762	6	1	0	1	RCT51
252	163	0	93	93	3.15	1.6	13	6.332438	-0.391	1.11316	2.15652	1.71844	5	0	0	0	RCT52
254	58	0	13	13	0.71	2.4	12	5.643453	-0.311	0.84335	1.13033	1.33776	10	0	0	0	RCT54
255	2	0	0	0	0.42	2.6	13	6.886491	-0.273	0.52301	1.3969	0.99533	18	0	0	0	RCT55
260	115	0	207	207	1.06	1.2	14	6.447158	-0.785	0.94969	1.81624	1.27734	32	1	1	1	RCT60
401	151	2	344	346	0.91	2.2	9	4.96614173	-0.575	0.90741	3.04302	1.75005	ND	0	1	1	IFN1
402	37	0	449	449	1.02	2.1	11	5.62324929	-0.418	1.27161	3.19192	2.13293	35	0	0	0	IFN2
404	13	0	0	0	0.55	0.7	12	5.80277373	-0.411	0.36922	1.82814	1.23603	26	0	0	0	IFN4
405	48	0	0	0	0.82	2.6	9	4.5797836	-0.42	0.43457	2.28176	0.93399	26	0	0	0	IFN5
406	58	40	100	140	3.08	0.4	11	6.44715803	-0.411	0.49415	3.13502	1.16077	31	0	0	1	IFN6
408	27	8	211	219	2.65	2.0	8	2.54406804	-0.287	0.85914	2.7102	1.63829	36	0	0	0	IFN8
409	86	0	57	57	1.54	2.4	10	5.38916608	-0.661	1.22737	4.0992	1.9429	34	0	0	0	IFN9
410	18	0	0	0	0.4	2.8	10	5.72835378	-0.29	0.85914	2.0404	0	41	0	0	0	IFN10
411	37	0	0	0	1.92	0.1	12	5.81291336	-0.485	1.33122	3.49171	1.93344	53	1	0	1	IFN11
412	99	8	33	41	1.15	2.7	11	6.35218252	-0.349	0.67486	3.93972	1.82223	18	1	1	1	IFN12
415	7	0	2	2	0.6	3.7	12	6.03342376	ND	0	2.33486	0	17	1	1	1	IFN15
416	12	0	0	0	0.66	2.0	13	6.63848926	-0.377	1.1784	2.80957	1.29798	10	0	0	0	IFN16
417	ND	0	132	132	1.93	1.1	12	6.06632593	ND	1.02776	3.74477	2.01047	ND	0	1	1	IFN17
418	25	0	65	65	2.61	1.6	8	4.92427929	-0.549	1.02776	3.86212	1.9429	27	1	0	0	IFN18
419	242	0	56	56	1.96	2.1	8	4.52504481	-0.506	0.54654	2.5737	0.93399	34	0	0	0	IFN19
424	19	0	5	5	0.37	2.2	10	5.8419848	ND	0.36922	2.45676	0	25	0	1	1	IFN24

Table 1: Patient charateristics from whom the isolates were taken

Baseline parameters: CD4 count at admission, mental status (0 = normal, 1 = altered), CSF - neutrophils (Neuts, mm^3/CSF), lymphocytes (Lymphs, mm^3/CSF), white blood cell count (WBC, mm^3/CSF), protein (g/L), glucose (Glc, g/L), Cryptococcal antigen titre (CrAG), fungal load (log CFU of quantitative cryptococcal cultures), pro-inflammatory cytokine (TNF, IFN, IL-6) levels (pg/mL), opening pressure (OP, cmH$_2$O),

and slope (rate of fungal clearance during antifungal treatment), 2 and 10 week mortality (0 = live, 1 = died) were determined. Patient – isolates CM20 – 64 were obtained from the Thailand study; CCTP02 – 30, RCT03 – 60, IFN1 – 24 were obtained from the South African study. ND = Not determined. Dr. Tihana Bicanic, St. Georges University of London, provided the patient data and the isolates.

Parameter	Statistic: Median (range) unless indicated
Baseline CSF fungal load (CFU/ml of quantitative cryptococcal culture)	9.15×10^5 ($3.5 \times 10^2 - 7.7 \times 10^6$)
CD4 count at admission	23 (2 - 242)
CSF Cryptococcal antigen (CrAG) titre	2.05×10^3 ($4 - 3.28 \times 10^4$)
CSF glucose (mg/dl)	2·2 (0·1 - 4·83)
CSF lymphocytes	13 (0 - 1212)
CSF neutrophils	0 (0 - 40)
CSF opening pressure (cm H_2O)	27 (5 - 80)
CSF protein	0.86 (0.2 – 4.1)
CSF white cell count	5 (0 - 1215)
Mental Status	11/47 (23% altered mental status)
2 week mortality	9/47 (19% mortality)
10 week mortality	14/47 (29.8% mortality)
Pro-inflammatory cytokine levels:	
IFN-γ	1.48 (0 – 2.28)
TNF-α	0.93 (0 – 2.09)
IL-6	2.59 (0 – 4.39)
SLOPE (rate of fungal clearance)	-0.42 (-0·94 – 0.03)

Table 2: Summary of the patient clinical parameters

2.2.1.1 Isolate characteristics

All isolates were isolated from CSF of HIV-associated cryptococcal meningitis and span a 7-year period of collection from 2002 - 2009. 6/47 (12.8%) came from the Thailand clinical study (Brouwer et al., 2004) while the rest (87.2%) are from the three clinical studies in South Africa (Bicanic et al., 2007; Bicanic et al., 2008; Bicanic et al., 2009b) Out of the 47 isolates, 30/47 (63.8%), 30/47 (63.8%) and 31/47 (65.9%) had their mating type, MLST and molecular type (VN) known. The 30 isolates were 100% α mating type but were very diverse in terms of MLST although the all the six Thailand isolates were MLST 6. All the 31 known molecular types were *C. neoformans var. grubii* represented by VNI (n = 28), VNII (n = 2) and VNB (n = 1). VNI makes 90.3% of the known molecular types in this set of isolates (Table 3).

Isolate	Site of isolation	Year of isolation	Region of origin	Mating type	MLST	VN type
CM20	CSF	2002	Thailand	α	6	VNI
CM24	CSF	2002	Thailand	α	6	VNI
CM36	CSF	2002	Thailand	α	6	VNI
CM50	CSF	2002	Thailand	α	6	VNI
CM52	CSF	2002	Thailand	α	6	VNI
CM64	CSF	2002	Thailand	α	6	VNI
CCTP2	CSF	2005	South Africa	α	37	VNI
CCTP3	CSF	2005	South Africa	α	5	VNI
CCTP10	CSF	2005	South Africa	α	57	VNI
CCTP12	CSF	2005	South Africa	α	58	VNI
CCTP13	CSF	2005	South Africa	α	5	VNI
CCTP25	CSF	2005	South Africa	α	51	VNI
CCTP26	CSF	2005	South Africa	α	51	VNI
CCTP29	CSF	2005	South Africa	α	51	VNI
CCTP30	CSF	2005	South Africa	α	5	VNI
CCTP49	CSF	2005	South Africa	α	66	VNII
CCTP52	CSF	2005	South Africa	α	52	VNII
RCT3	CSF	2005/2006	South Africa	α	51	VNI
RCT6	CSF	2005/2006	South Africa	α	6	VNI
RCT7	CSF	2005/2006	South Africa	α	51	VNI
RCT21	CSF	2005/2006	South Africa	α	56	VNB
RCT24	CSF	2005/2006	South Africa	α	1	VNI
RCT33	CSF	2005/2006	South Africa	α	51	VNI
RCT36	CSF	2005/2006	South Africa	ND	Diploid	VNI
RCT44	CSF	2005/2006	South Africa	α	54	VNI
RCT50	CSF	2005/2006	South Africa	α	74	VNI
RCT51	CSF	2005/2006	South Africa	α	23	VNI
RCT52	CSF	2005/2006	South Africa	α	32	VNI
RCT54	CSF	2005/2006	South Africa	α	75	VNI
RCT55	CSF	2005/2006	South Africa	α	51	VNI
RCT60	CSF	2005/2006	South Africa	α	76	VNI
IFN1	CSF	2007/2009	South Africa	ND	ND	ND
IFN2	CSF	2007/2009	South Africa	ND	ND	ND
IFN4	CSF	2007/2009	South Africa	ND	ND	ND
IFN5	CSF	2007/2009	South Africa	ND	ND	ND
IFN6	CSF	2007/2009	South Africa	ND	ND	ND
IFN8	CSF	2007/2009	South Africa	ND	ND	ND
IFN9	CSF	2007/2009	South Africa	ND	ND	ND
IFN10	CSF	2007/2009	South Africa	ND	ND	ND
IFN11	CSF	2007/2009	South Africa	ND	ND	ND
IFN12	CSF	2007/2009	South Africa	ND	ND	ND
IFN15	CSF	2007/2009	South Africa	ND	ND	ND
IFN16	CSF	2007/2009	South Africa	ND	ND	ND
IFN17	CSF	2007/2009	South Africa	ND	ND	ND
IFN18	CSF	2007/2009	South Africa	ND	ND	ND
IFN19	CSF	2007/2009	South Africa	ND	ND	ND
IFN24	CSF	2007/2009	South Africa	ND	ND	ND

Table 3: The characteristics of clinical isolates used in the study
Fourty-seven isolates, 6 from Thailand and 41 from South Africa were studied. All isolates were derived from CSF of HIV-associated CM. Molecular, mating and sequence types were known for 31, 30 and 30 isolates respectively. One isolate was diploid. VNI makes 90.3 % of the known molecular types. ND = Not done.

Like the BMEC – *Cryptococcus* interaction assays, isolates were propagated in YPD medium prior macrophage infection or phenotypic characterization.

2.2.2 Macrophage tissue culture

2.2.2.1 Murine macrophage-like cell-line, J774

Prior to use, 10^5 J774 macrophages were grown in 24 well tissue culture plates (Greiner) containing DMEM supplemented with 10% FBS, 1mM L-Glutamine and 1% Penicillin/Streptomycin for 24hr at 37^oC with 5% CO_2. Macrophage batches used were kept within the range of three passages to limit passage-to-passage variations. From frozen, J774 macrophages were propagated at 3/12 until passage 7 before they were used for assay.

2.2.2.2 Primary human macrophages

Primary human macrophages were obtained through differentiation of monocytes from buffy coat of health donors (Birmingham Blood Bank). Peripheral blood monoclear cells (PBMCs) were isolated by Ficoll gradient centrifugation. Briefly, buffy coat was dissolved 1:1 in sterile PBS. 25ml of the mixture was then carefully pipetted onto 20ml of Ficoll-Paque (GE Healthcare Life Sciences) and centrifuged for 40min, 3200g at 20^oC. Centrifugation divided the mixture into 4 layers from which the upper middle white layer containing peripheral blood mononuclear cells (PBMC) was drawn out into a new tube. The PBMC population was washed with sterile PBS x5 – 7 times with spinning, 1057g at 25^oC to remove platelets. Monocytes were isolated from the PBMC population through adherence to plastic following overnight culture in Tissue culture flasks (T75 Greiner) in RPMI 1640 medium with L-Glutamine (GIBCO) supplemented by either 10% AB male human serum (First Link,

UK) or 10% FBS (Sigma) plus 1% Penicillin/Streptomycin in presence or absence of 1000U/ml Granulocyte macrophage colony stimulating factor (GM-CSF). Monocytes were counted and propagated in 24 well Tissue culture plates with 10% FBS, 1% Penicillin/Streptomycin – RPMI 1640 medium for 14 days to differentiate into macrophages before use. Medium was changed every 3 days.

2.2.3 Phagocytosis and Intracellular proliferation assay

Clinical Cryptococcus isolates were tested for the rate at which they were phagocytosed by – and proliferated inside - murine J774 macrophages. Prior to infection, J774 macrophages were activated with 15µg/ml Phorbol myristate acetate (PMA) for 30-40min in serum free medium. Macrophages were infected with opsonized cryptococci at 1:10 ratio and incubated for 2hr (time point zero), 18hr (time point one), 24hr (time point 2) and 48hr (time point three) at 37°C with 5%CO_2. At 2hrs, the infection medium was aspirated off and macrophages extensively washed (4-5 times) with sterile PBS to remove extracellular adherent cryptococci. Part of the culture was lysed with 200µl of sterile water for 20min at 37°C to release intracellular cryptococci, which were counted using a haemocytometer. At time points one, two and three cultures were gently washed x2 to rinse off extracellular cryptococci, lysed and counted as at time point zero. Rate of phagocytosis (uptake) was determined as the number of cryptococci engulfed by macrophages by 2hr of incubation whereas intracellular proliferation rate (IPR) was determined as the ratio of number of intracellular cryptococci at 18hr to the number of intracellular cryptococci at 2hr.

Eleven high (n=5) and low (n=6) uptake isolates in murine J774 macrophages were selected and tested in primary human macrophages. Prior to infection, the human

monocyte-derived macrophages were stimulated with 1000U/ml rhIFN-γ (Immunotools, German) and 10μg/ml LPS (Sigma Aldrich) 24hr before the assay. Rate of cryptococci uptake and IPR were determined as with J774 macrophages.

2.2.4 Non-opsonisation and cryptococci – macrophage interaction

To evaluate opsonin influence on cryptococci uptake and IPR in macrophages, a no opsonisation assay was set. Cryptococci were harvested from 24hr YPD cultures, washed with PBS and counted to the required inoculum, 1×10^6 yeast cells and directly added to macrophages without opsonisation. Rate of uptake and IPR were determined as in section 2.2.3.

2.3 Determination of melaninisation and capsule expression
2.3.1 Melanisation

Through secretion of the phenoloxidase enzyme, *C. neoformans* can use host catecholamines to produce melanin (Polacheck et al., 1982; Polacheck et al., 1990). Melanin is resistant to reactive oxygen and nitrogen species generated by host phagocytes. The rate of melanization of each isolate was determined by plating 5μl of the fresh yeast culture on L-2, 3-dihydroxphenylalanine (L-DOPA) agar (0.7% L-DOPA, 0.9% Vitamin B1, 3.4% Glycine, 4.2% $MgSO_4$, 9.5% Glucose, 12.1% KH_2PO_4 and 69.3% Agar). Plates were incubated at 37^oC to determine melanin formation (colony browning) and scored daily for 15 day. The samples were also tested for melanisation at 25^oC and compared with rates at 37^oC. An arbitrary scale of 0 – 5 (0 = No browning; 5= Maximum browning) was used to determine the rate of melanization (Appendix 1: Melanisation scores). Melanization rate (MR) was thus calculated as the ratio of maximum browning to the number of days taken to attain

maximum browning. For clinical isolates, the rate of melanin was tested for a statistical association with rate of cryptococcal uptake by – and intracellular proliferation in - macrophages.

2.3.2 Capsule induction

To promote capsule induction *in vitro*, *C. neoformans* isolates were inoculated into SD broth and grown overnight at 37°C with shaking. The following day 20 μl of culture was inoculated into 5 ml capsule inducing media (DMEM with 1% NCTC 109 medium, 10% heat-inactivated foetal bovine serum, Sigma Aldrich) and incubated at 37°C with 10% CO_2 for 48 hr. Cells were subsequently harvested by centrifugation at 2000 rpm for 5 min and observed by counter-staining with India Ink, using a 40X brightfield objective, and measured using ImageJ v1·440 (National Institutes of Health, USA) (work done by Dr. Emma Robertson, St. Georges University of London). The rate of capsule expression was also analyzed for correlation with rate of uptake, IPR and patient fungal burden.

2.3.3 Iron utilization

Iron is important in virulence of *C. neoformans* because it influences the biosynthesis of major virulence factors, melanin and capsule (Jung and Kronstad, 2008). A set of selected high and low uptake clinical isolates were investigated for their ability to use different Iron sources (Work done as part of research visit to Prof. James Kronstad, University of British Columbia, Vancouver).

2.3.3.1 Iron media preparation

Low Iron water was prepared first by passing double distilled water (2L) through 5g Chelex 100 resin (BioLabs) in a flex column (Fisher Scientific) to remove all divalent metallic ions. To make 1L of Low iron medium (Lim), 5g Glucose, 5g L-Asparagine, 4.78g HEPES, 0.4g KH_2PO_4, 1.85g $NaHCO_3$ were added to low iron water and pH adjusted to 7.2 before adding 400µl 1M $MgSO_4$, 340µl 1M $CaCl_2$ and 400µl of 4mg/ml Thiamine and 1ml 1000X salt solution (5mg $CuSO_4.5H_2O$, 2g $ZnSO_4.7H_20$, 10mg $MnCl_3.4H_2O$, 0.460g Sodium Molybdate, 5.7mg Boric acid per in 1L of Low iron water). The mixture was filter sterilized or autoclaved before use. Transferrin and Hemin media were prepared by adding 1mg human Holo-transferrin (Sigma Aldrich) and 100mM Porcine Hemin (Sigma Aldrich) respectively to 100ml of Low iron medium.

2.3.3.2 Iron utilization assay

Iron utilization ability was measured as a function of rate of growth in different Low iron media. Prior to the growth curve determination, cryptococci were harvested at 4500g from overnight YPD culture, washed x3 with sterile low iron water and grown in Lim for 3 days to reduce their iron reserves. Following iron starvation, yeast cells were harvested and washed x2 in low iron water, counted by a haemocytometer to the inoculum size of 10^5 cells /ml. Four media: Lim, Lim-Transferrin, Lim-Hemin and YPD as a control were inoculated and incubated at 37^oC with shaking at 200rpm for 7 days. After every 24hr, 100µl aliquots were taken, 10-fold diluted to $1/10^5$ and plated on YPD agar for colony counts. Growth curve per isolate per medium was plotted exponentially as the number of CFUs versus time in days and the slope of each curve was calculated and used to determine rate of growth.

2.4 Whole blood characterization of high uptake and low uptake isolates

2.4.1 Whole blood survival assay

Whole blood from six (4 male and 2 female) healthy donors was obtained at different days and infected with a selection of high uptake, n = 5 isolates; and low uptake, n = 6 isolates. Each milliliter of blood was inoculated with 10^4 cryptococci per isolate and incubated for 8hr at 37°C with minimal rotation (Labroller). 100μl aliquots were taken at different time points (10min, 30min, 1-, 2-, 3-, 4-, and 8 hr) and plated in 4 replicates of 25μl on YPD agar. Colony forming units were counted after 48hr of incubation at 25°C and recorded as CFU/ml. To confirm the viable cryptococci present in the initial inoculum, an aliquot was suspended in sterile phosphate buffered saline (PBS) and plated on YPD agar for colony counts.

2.4.2 Blood phagocyte-cryptococci association assay

Cryptococci association with circulating neutrophils and monocytes/macrophages in whole blood was measured by flow cytometry (FACSCaliber and CellQuestPro software, BD Biosciences). Prior to inoculation, cryptococci were stained with 0.5mg/ml FITC (Invitrogen) for 30min at room temperature with rotation (Labroller), washed and counted with a haemocytometer to the required inoculum, 10^4 cryptococci per 1ml of blood. Two replicates of culture per isolate were made and incubated at 37°C with 5% CO_2 for two time points (30min and 60min). After incubation, erythrocytes were eliminated by lysis in 5ml of lysis buffer (12mM Na hydrogen carbonate, 0.25mM tetrasodium EDTA and 15mM ammonium chloride) followed by 5min spin at 1057g and the pellet resuspended in 0.5 ml sterile PBS for flow cytometry. Forward and side scatter was used to distinguish neutrophil and

macrophage/monocyte populations. By FITC fluorescence, cryptococci associated phagocyte cells were distinguished from free phagocytes.

2.5 Genetic characterization of high uptake and low uptake isolates

We hypothesized that there is differential expression of genes between high uptake and low uptake isolates than influence the rate of phagocytosis. Isolate RNA was extracted before the phagocytosis assay in order to detect which genes were expressed before cryptococci interact with macrophages (work done as part of the collaborative research visit to Prof. James Kronstad, Michael Smith Laboratories, University of British Columbia, Vancouver, Canada).

2.5.1 RNA extraction

Total RNA was extracted from a set of high uptake (n=4) and low uptake isolates (n=4) and the H99 *C. neoformans* serotype A strain as a reference. Prior to RNA extraction, strains were grown in a pre-phagocytosis medium (YPD broth) for 24hr. RNA was then extracted using the RNAeasy mini kit (Qiagen) according to manufacturer's guidelines. The quality and quantity of RNA were assessed using Nanodrop, agarose gel electrophoresis and Bioanalyzer (Appendix 2: Bioanlysis results of RNA extracts).

2.5.2 Sequencing and gene expression analysis

RNA sequencing was done using the Illumina RNAseq technology by Data2Bio, Iowa, USA. Eight pairwise comparisons were performed between clinical isolates and reference strain, H99. This was followed by sixteen binary sequence alignments

between the high and low uptake isolates to determine the differentially expressed genes. Geneontology analysis (Goanlysis) was performed to determine the functions of the differentially expressed genes.

2.6 Statistical analysis

2.6.1 Quantifying cryptococci – BMEC interaction

Non-parametric Mann-Whitney U Test and Wilcoxon Signed Ranks Test were used to measure the significance of adherence at different conditions and time points. Mann-Whitney U Test was applied to compare the means of test different setups, for instance comparing the mean association of encapsulated and acapsular strain to bEnd3 and or hCMEC/D3 cells. Wilcoxon Signed ranks test was applied to compare means of the same setup at different time points, for example comparing the mean association of encapsulated H99 strain or the acapsular mutant with endothelial cells after 2hrs and 4hrs of incubation at 37°C.

2.6.2 Determining association between macrophage-cryptococci and patient clinical parameters

Bivariate analysis was performed using Stata v11 (StataCorp, TX 77845 USA) to look for associations between Intracellular proliferation rate and uptake and clinical variables and outcome, using linear regression for continuous variables and logistic regression for categorical variables.

CHAPTER III: CRYPTOCOCCUS-BMEC INTERACTION

3.1 *C. neoformans* binding and internalization by BMEC

Cryptococcal transcellular traversal of the blood-brain barrier (BBB) occurs through adherence and uptake of cryptococci by brain microvascular endothelial cells (Chang et al 2004; Vu et al 2009), but the rate at which this occurs is unknown. In order to quantify the binding and uptake of cryptococci by BMEC, we established an *in vitro* blood-brain barrier model using murine and human brain microvascular endothelial cell lines. The brain endothelial cells were grown in suitable media (see Methods) until they formed a complete mosaic of cell monolayer (Figure 6) and then exposed to cryptococci. The cryptococcal capsule, a major virulence factor of *C. neoformans,* has been implicated by various studies as being important in interactions with BMEC (Chang et al., 2004a; Charlier et al., 2005a; Charlier et al., 2005b; Fries et al., 2001; Guerrero et al., 2006; Ibrahim et al., 1995; Jain et al., 2006b), we therefore investigated the effect of presence or absence of the capsule on the rate of cryptococcal binding and uptake by BMEC. A large part of the results presented in this chapter and the methods used (Chapter II section 2.1) have already been published (Sabiiti and May, 2012).
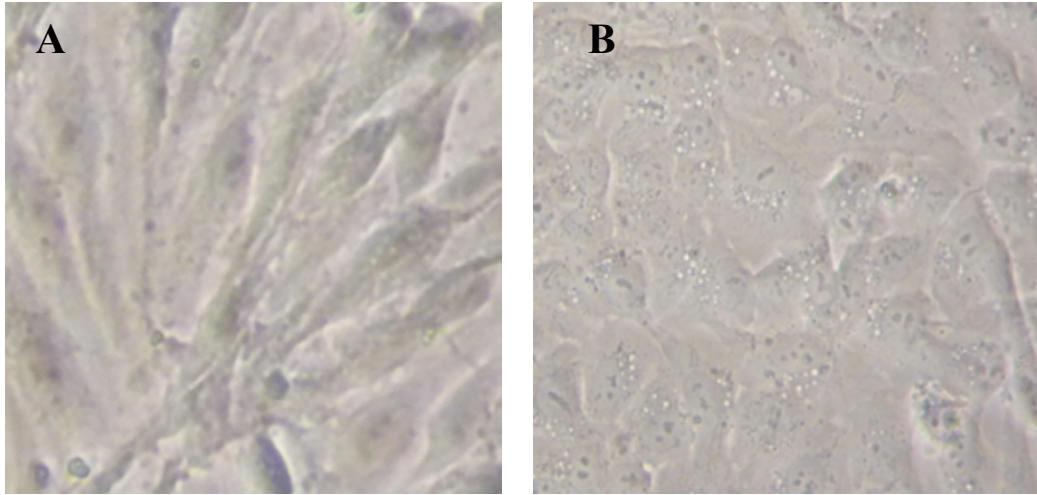
Figure 6: Both murine and human brain microvascular endothelial cells form confluent cell monolayers

A) The murine bEnd3 cell monolayer. B) The human hCMEC/D3 cell monolayer. Images taken with a phase contrast light microscope.

3.1.1 Association with and internalization by the murine brain endothelial cell line bEnd3

We exposed the mouse brain endothelial cell line bEnd3 to wildtype C. *neoformans* H99 and its isogenic acapsular derivative, cap59 (De Jesus et al., 2010). The two strains were tested for their rate of binding and internalization by BMEC and whether the presence or absence of capsule has an effect on this interaction. After two hours of exposure to bEnd3 cells at 37°C, 8.8×10^{3} (0.43%) of inoculated wild type (H99) cryptococci had adhered strongly to the endothelial layer, rising to 2.0×10^{4} (1.2%) after four hours, $P < 0.01$. Similarly, 1.6×10^{4} (0.8%) of the acapsular cryptococci had associated with bEnd3 cells at 2hr rising to 2.5×10^{4} (1.23%) after four hours of incubation at 37°C, $P < 0.01$. By using calcoflour staining to discriminate surface bound from internalised cryptococci, we determined that 3.1×10^{3} (35% of associated) and 4.4×10^{3} (28% of associated) wild type and acapsular cryptococci, respectively, had been internalised by 2 hours at 37°C, rising to 8.1×10^{3} (40%) and 8.6×10^{3} (35%) respectively by 4hrs, $P < 0.01$. The acapsular strain cap59 showed a slightly higher but not significant rate of association at 2hr, $P = 0.1$, which diminished by 4hr when both cap59 and H99 were equally associated with bEnd3 cells, $P = 0.5$. Importantly, for both strains, microscopic yeast cell counts and live CFU counts gave the same rate of association for both H99 and cap59, suggesting that there is no significant drop in cryptococcal viability upon adherence to or uptake by bEnd3 cells (Figure 7).
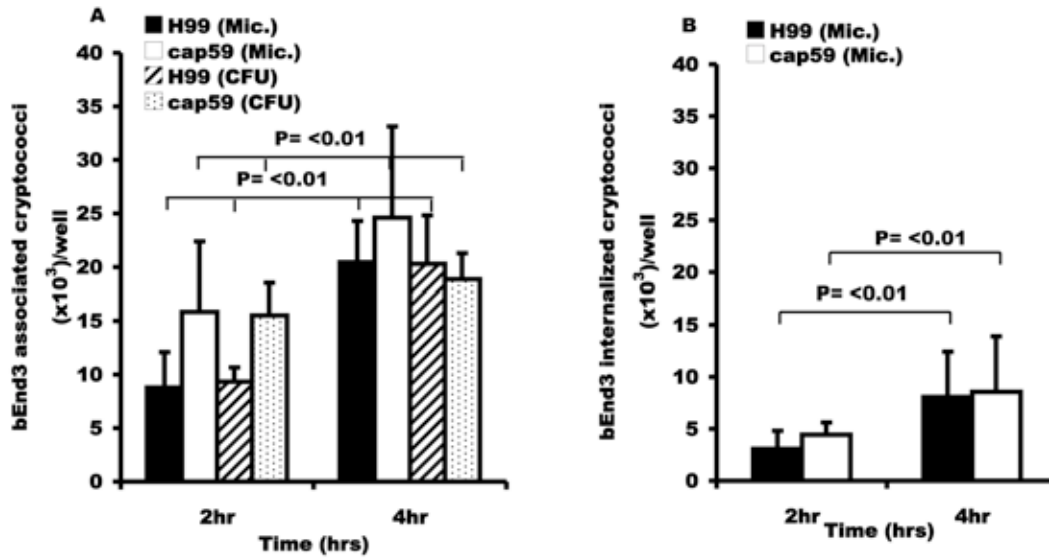
Figure 7: Binding and uptake of H99 and cap59 to the murine brain endothelial cells

BEnd3 cells were exposed to wild type H99 and its acapsular derivative cap59 for 2hr and 4hr at 37°C. (A) The rate of association (bound and internalized cryptococci) was determined both by microscopy and live CFU counts. The rate of association increased significantly in a time dependent manner, (P <0.01 for both strains). However, there was no difference in association of encapsulated H99 or acapsular cap59 cells (P = 0.1 and 0.5 at 2hr and 4hr respectively). (B) Internalization of the strains, H99 and cap59 by bEnd3 cells as determined by fluorescence microscopy. Internalized cryptococci (pre-stained with FITC) were distinguished from extracellular adherent ones by counter labelling with calcofluor white after infection. Intracellular cryptococci retained the FITC green signal while extracellular cells acquired the blue signal from calcofluor. The number of phagocytosed cryptococci increased significantly in a time dependent manner, (P < 0.01 for both strains). However, there was no difference in internalization of encapsulated H99 and acapsular cap59, (P = 0.5 and 0.8 at 2hr and 4hr respectively). Error bars are standard error of the mean, n = 5 repeats.

3.1.2 Association and internalization by human brain endothelial cells, hCMEC/D3

To test whether the rates of adherence and uptake that we had observed in bEnd3 cells were species specific, we repeated our analyses using the human brain endothelial derived cell-line, hCMEC/D3. As with bEnd3 cells, both microscopic and CFU counts showed that encapsulated H99 and its isogenic acapsular mutant cap59 associated and were engulfed at the same rate, $P > 0.05$ (Figure 8) at 2hr and 4hr of infection respectively. To determine whether the interaction varies from strain to strain, we tested a different pair of *C. neoformans* serotype D strains, encapsulated B3501 and its isogenic acapsular strain B4131. Like the H99/cap59 isogenic pair, both B3501 and B4131 strains associated and were internalized at the same rate with hCMEC/D3 cells $P > 0.05$ (Figure 9). However, unlike bEnd3 cells, we observed a significant decrease over time in cryptococcal CFU counts for both strains. Microscopic counts revealed that association and internalization for both strains increases with time of incubation, suggesting a loss of viability by cryptococci during association with hCMEC/D3 cells. One potential explanation for this result is that hCMEC/D3 cells may generate a more antimicrobial environment for cryptococci following uptake than that produced by bEnd3 cells. In support of this, microscopic examination of infected endothelial cells labelled with Lysotracker (a reporter for acidic, mature phagosomes) (Figure 10) demonstrated that 50% of intracellular cryptococci in hCMEC/D3, but <10% in bEnd3 cells, were Lysotracker positive at 4hr of incubation. Thus bEnd3 cells and hCMEC/D3 cells bind and engulf cryptococci at similar rates, but only hCMEC/D3 cells are able to significantly reduce cryptococcal viability following uptake.
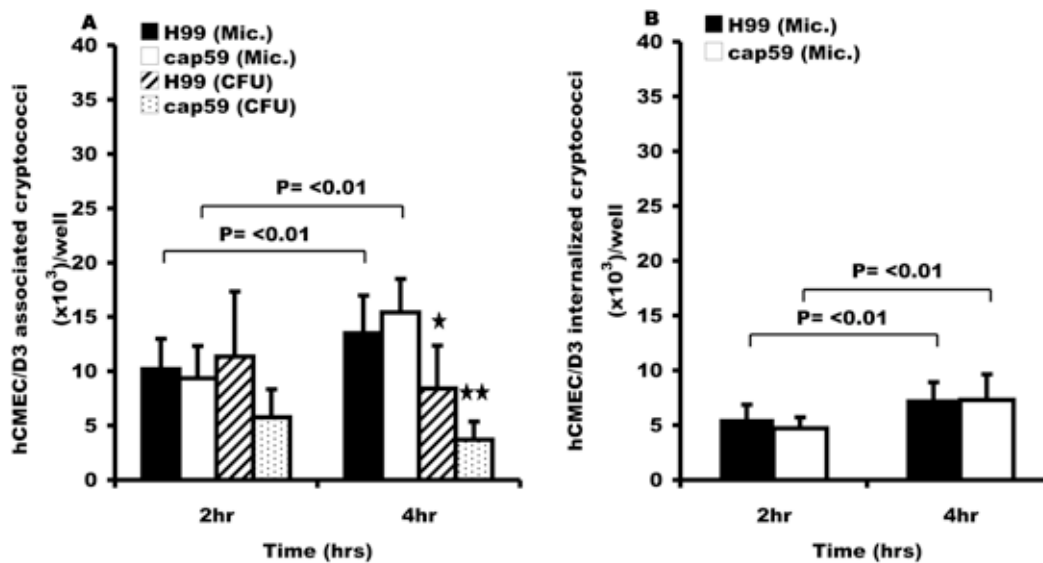
Figure 8: Binding and uptake of H99 and cap59 to the human brain endothelial cells

Like bEnd3 cells, hCMEC/D3 cells were exposed to the *C. neoformans* serotype A isogenic strains, wild type H99 and acapsular derivative cap59 for 2hr and 4hr at 37°C. Microscopic (Mic.) and live CFU counts were performed to determine the association and survival of cryptococci. (A) Association efficiency of H99 and cap59 cryptococci with hCMEC/D3 cells. As opposed to microscopic counts, live CFU counts showed a time dependent decrease in the number of associated cryptococci by 4hr of incubation, ★ = P < 0.05 and ★★ = P <0.01 for H99 and cap59 respectively, suggesting a drop in viability of the hCMEC/D3 associated H99 and cap59 cryptococci. There was no difference in association of encapsulated H99 and acapsular cap59, P = 0.7 and 0.6 at 2hr and 4hr respectively. (B) Internalization of encapsulated H99 and acapsular cap59 cryptococci by human brain endothelial cell line, hCMEC/D3 cells. The internalized cryptococci and extracellular adherent were determined as in Figure 7. As with association, the number of phagocytosed cryptococci increased significantly in a time dependent manner, P = 0.01 and <0.01 for H99 and cap59 respectively. However, there was no difference in internalization of H99 and acapsular cap59 cryptococci, P = 0.5 and 0.8 at 2hr and 4hr respectively. Error bars are standard error of the mean, n = 6 repeats.
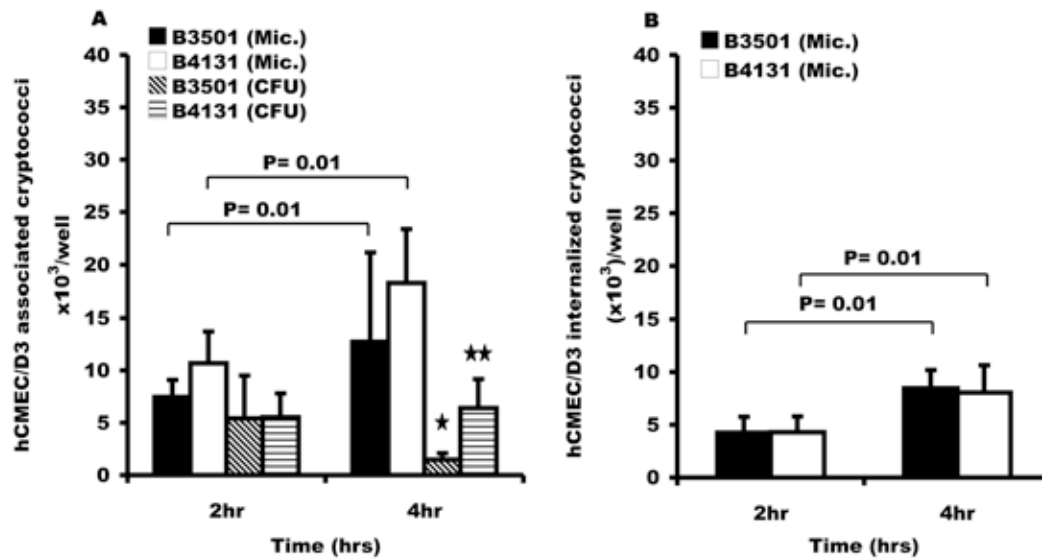
Figure 9: Binding and uptake of B3501 and B4131 to the human brain endothelial cells

HCMEC/D3 cells were exposed to *C. neoformans* serotype D wild type B3501 and its isogenic acapsular mutant B4131 for 2hr and 4hr at 37°C. Microscopic and live CFU counts were performed to determine the association and survival of cryptococci. (A) Association efficiency of B3501 and B4131 cryptococci with hCMEC/D3 cells. Like the H99-cap59 pair, live CFU counts showed a time dependent decrease in the number of associated cryptococci by 4hr of incubation, ★ = P < 0.05, ★★ = P < 0.01 for both B3501 and B4131. There was no difference in association by encapsulated B3501 and acapsular B4131, P > 0.05 at 2hr of incubation. However, B4131 was significantly more associated, P = 0.02 (Microscopy) and <0.01 (CFU) by 4hr of incubation. (B) Internalization of encapsulated B3501 and its acapsular mutant derivative B4131 by hCMEC/D3 cells determined by fluorescence microscopy (Mic). The number of phagocytosed cryptococci increased significantly in a time dependent manner, P = 0.01 for both strains. However, there was no difference in internalization of B3501 and B4131, P = 0.5 and 0.2 at 2hr and 4hr respectively. Error bars are standard error of the mean, n = 6 repeats.
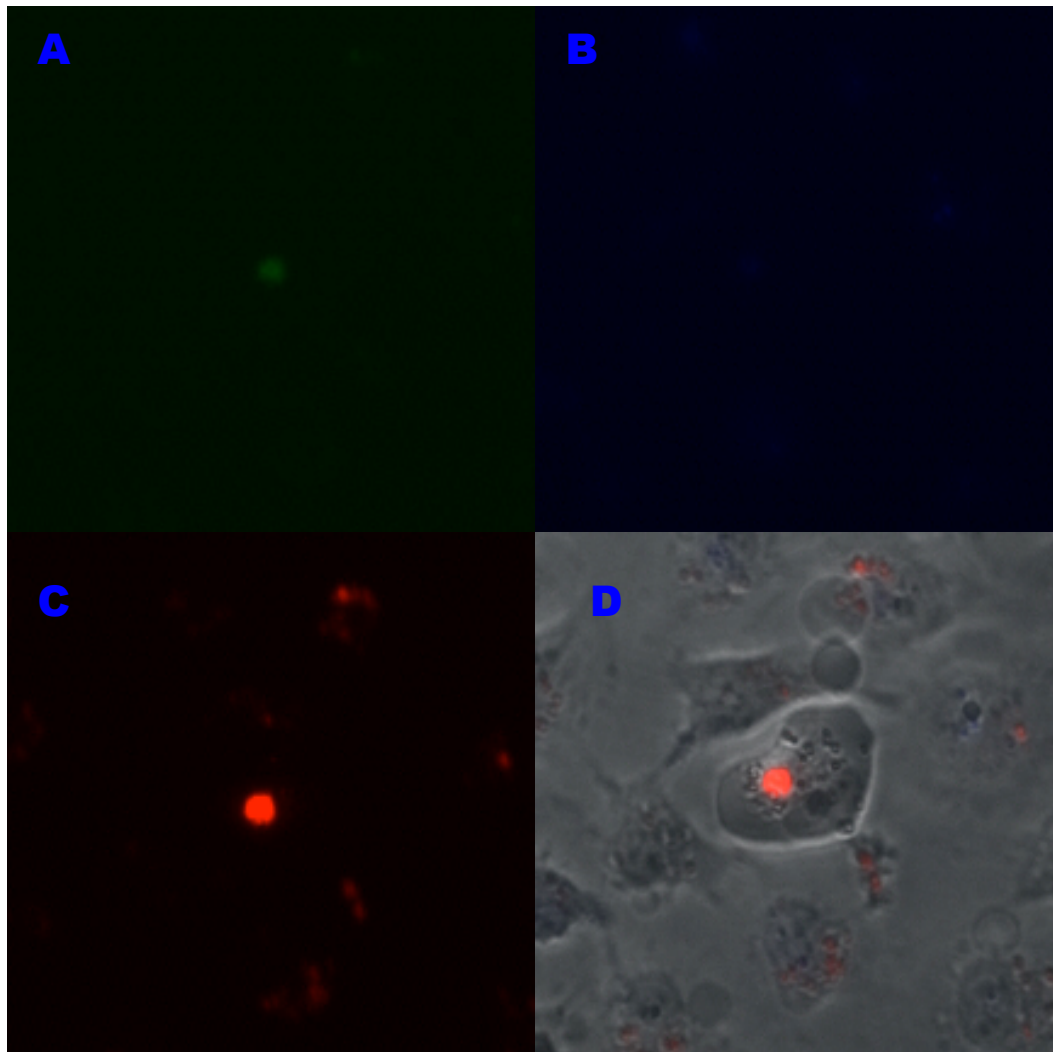
Figure 10: hCMED3/D3 internalized crytococci acquire the phagosomal marker, Lysotracter

HCMEC/D3 cells were exposed to *C. neoformans* serotype A H99 (GFP-expressing) strain for 2 – 4hr and thereafter treated with lysotracker dye for 30min at 37°C followed by 10min treatment with calcofluor white at room temperature to label extracellular cryptococci. Images were taken within 1hr after treatment using multicolour fluorescence microscopy and x40 phase objective. A) GFP signal (confirming that the observed particle is a cryptococcal cell). B) Absence of signal in the UV channel (calcoflour gives blue signal under UV light), indicating that the observed yeast cell is intracellular. C) The red channel showing that the observed internalized yeast cell has acquired lysotracker, which implies that is within acidified phagosome. D) The merged image showing the lysotracker-stained cryptococcus internalized by hCMEC/D3 cell.

3.1.3 Effect of opsonisation on *Cryptococcus* – BMEC association and internalization

Since most individuals produce circulating antibodies to cryptococci by late childhood (Goldman et al., 2001b), we investigated whether opsonisation of cryptococci with antibody increases the association and internalization with brain endothelial cells. However, there were no significant differences between opsonised and non-opsonised yeast in either adherence or uptake at either time point tested, $P > 0.05$ (Figure 11), suggesting binding and uptake by brain endothelial cells is opsonin independent.
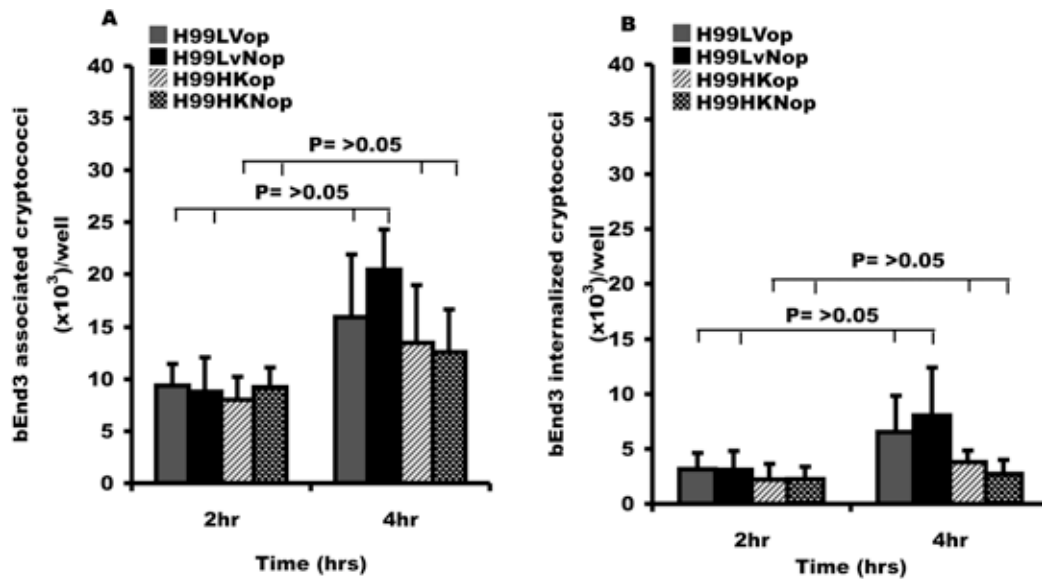
Figure 11: Effect of opsonisation on cryptococci binding and uptake by bEnd3 cells

Live (LV) and heat-killed (HK) H99 cryptococci were opsonised with mouse derived anti-capsule IgG antibody, 18B7 and the rate of adherence and internalization was determined by fluorescence microscopy. (A) Association of opsonised (op) and non-opsonised (Nop) cryptococci with bEnd3 cells. Rate of association of opsonised and non-opsonised H99LV cryptococci was similar, P = 0.8 and 0.4 at 2hr and 4hr respectively. Similarly, there was no difference between opsonised and non-opsonised heat-killed H99 cryptococci, P = 0.9 and 0.5 at 2hr and 4hr respectively. (B) Rate of internalization of opsonised and non-opsonised cryptococci internalized by bEnd3 cells. The number of internalized H99LV cryptococci was similar, regardless of opsonisation status (P = 0.9 at both 2hr and 4hr). Similarly, there was no difference between opsonised and non-opsonised heat-killed H99 cryptococci, P = 0.5 and 0.4 at 2hr and 4hr respectively. Error bars are standard error of the mean, n = 5 repeats.

3.1.4 Rate of association and internalization

The rate of association and internalization of cryptococci by both murine and human cell-lines was less than 2% of the inoculum, an indication that this interaction is not a frequent event (Table 4).

BMEC	Strain	% Assoc. at 2hr	% Intern. at 2hr	% Assoc. at 4hr	% Intern. at 4hr
bEnd3	H99LV	0.44	0.15	1.03	0.4
	H99HK	0.46	0.11	0.62	0.13
	cap59LV	0.79	0.22	1.23	0.43
	cap59HK	0.24	0.1	0.48	0.19
hCMEC/D3	H99LV	0.51	0.28	0.68	0.37
	H99HK	0.49	0.19	0.73	0.28
	cap59LV	0.47	0.23	0.77	0.37
	cap59HK	0.43	0.21	0.57	0.28
	B3501LV	0.37	0.21	0.64	0.42
	B4131LV	0.53	0.21	0.91	0.4

Table 4: A summary of the percentage association and internalization of cryptococci by BMEC at different time points as determined by microscopic counts

The percentages are calculated as ratio of the number of cryptococci associated with - and or internalized by – BMEC (bEnd3 or hCMEC/D3) to the original cryptococcal inoculum ($2x10^6$ yeast cells). Association (Assoc.) equals to the total number of cryptococci adhered to – and internalized by – BMEC whereas internalization (Intern.) is the number of cryptococci phagocytosed by BMEC. LV = Live and HK = Heat killed.

3.1.5 Effect of IFN-γ induction on Cryptococcus – BMEC association and internalization

The inflammatory cytokine IFN-γ has previously been shown to mediate changes in brain endothelial behaviour (Dietrich, 2002; Lachenmaier et al., 2011). Thus we considered whether IFN-γ mediated inflammation might increase cryptococcal uptake by BMEC. However, treatment of bEnd3 cells with either 100U or 500U of mouse IFN-γ 12hr prior to infection did not significantly alter uptake of either wild type or acapsular cryptococci at either time point tested (Figure 12).
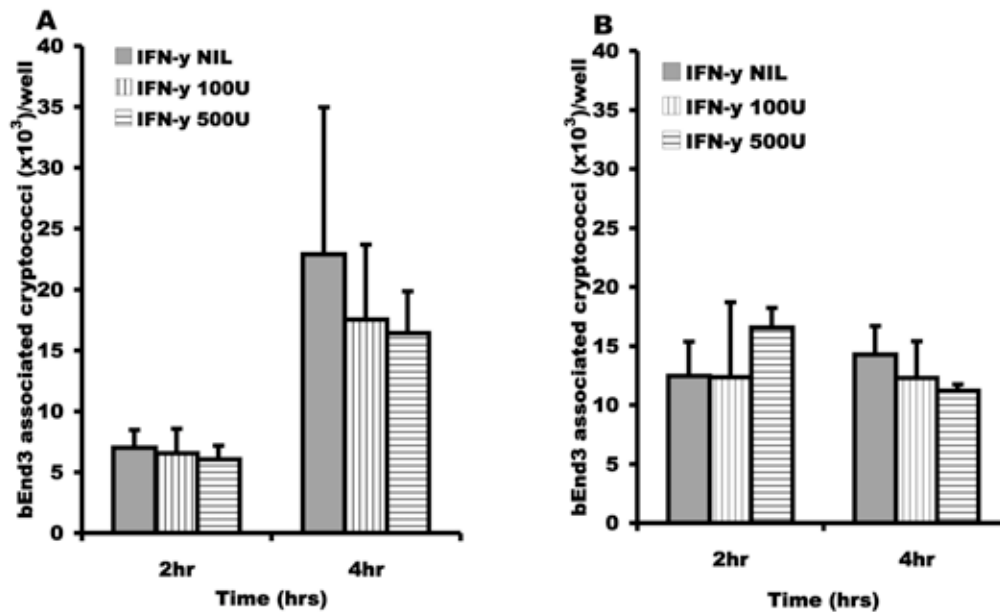
Figure 12: Effect of IFN-gamma induction on binding and uptake of cryptococci by BMEC

Murine brain endothelial cells (bEnd3) cells were induced with different concentrations (100U and 500U) of IFN-γ 24hr prior to exposure to encapsulated H99 (A) and acapsular mutant cap59 (B) cryptococci. Non-stimulated bEnd3 cells (IFN-γ NIL) were used as a negative control. IFN-γ did not have effect on the rate of association since both induced and non-induced (control) bEnd3 cells showed the same level of binding encapsulated and acapsular cryptococci. Error bars are standard error of the mean, n = 3 repeats.

3.1.6 Viability of cryptococci is not a prerequisite for association and internalization by BMEC

We next investigated whether the uptake of cryptococci into BMEC requires active signals from the pathogen. However, heat-killed H99 retained the ability to bind and enter both mouse bEnd3 and human hCMEC/D3 cells at a similar rate to live yeast. Although viable cryptococci showed higher association efficiency in bEnd3 cells, there was no significant difference between internalization of viable and heat-killed cryptococci in both bEnd3 and hCMEC/D3 cells. Thus BMEC invasion is most likely a passive process that occurs without active signals from the yeast cell (Figure 13).
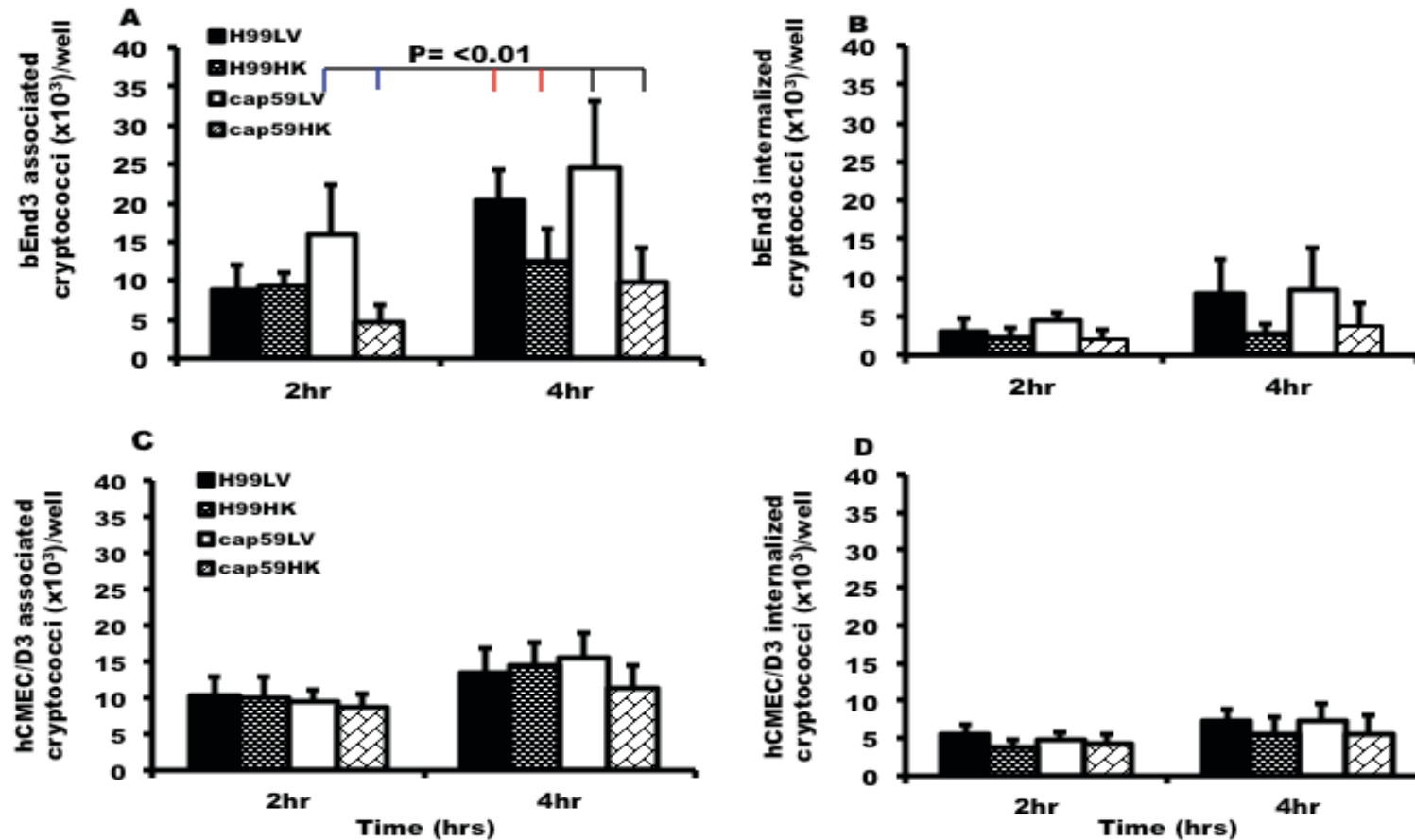
Figure 13: Effect of viability on binding and uptake of H99 and cap59 strains by BMEC
Heating for 15min at 65°C prior to infection killed H99 and cap59 cryptococci. Brain microvascular cells (BMEC), bEnd3 and or hCMEC/D3 cells were exposed in parallel to live (LV) and heat-killed (HK) cryptococci for 2hr and 4hr at 37°C and the number of bound and internalized

cryptococci was determined by fluorescence microscopy. (A and C): Association efficiency of live and heat-killed H99 or cap59 cryptococci by bEnd3 and hCMEC/D3 cells respectively. There was no difference in association of viable H99 and cap59 cryptococci with hCMEC/D3 cells at either time point, $P > 0.05$. However, viable cryptococci were more associated than non-viable ones both 2hr and 4hr (for cap59) and 4hr (for H99) of incubation with bEnd3 cells, $P < 0.01$. (B and D): Internalization efficiency of LV and HK H99 and cap59 cryptococci by bEnd3 and hCMEC/D3 cells. Both live and heat-killed cryptococci showed a time dependent increase in phagocytosis by both bEnd3 and hCMEC/D3 cells, however the rate of phagocytosis did not vary between the viable and non-viable cryptococci in both cell-lines, $P > 0.05$ at both 2hr and 4hr of incubation. Error bars are standard error of the mean, n = 5 repeats.

3.1.7 Viability of BMEC

To verify that the observed binding occurred in association with endothelial cells, and not due to indirect sequestration of yeast cells, bEnd3 and hCMEC/D3 monolayers were killed by paraformaldehyde fixation prior to cryptococci inoculation. For all conditions, cryptococcal binding was reduced by between one and two log orders, indicating that that viable endothelial cells were responsible for the observed cryptococcal association (Figure 14).
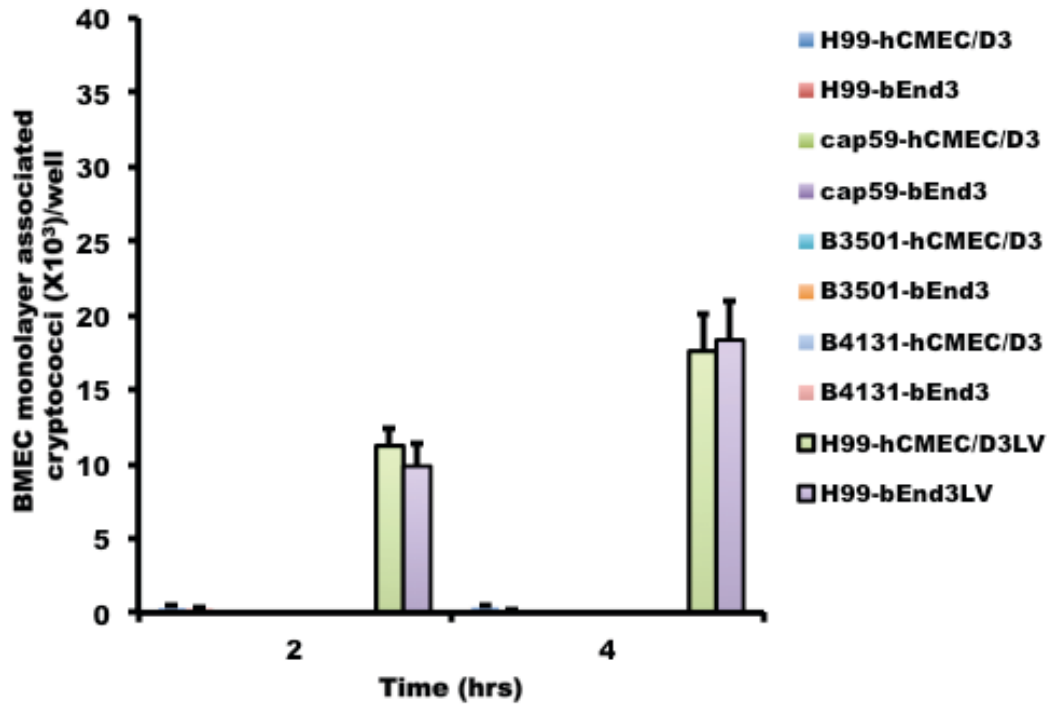
Figure 14: Binding to fixed brain endothelial cell monolayer (negative control)
To verify that the observed binding occurred in association with endothelial cells, and not due to indirect sequestration of yeast cells, bEnd3 and hCMEC/D3 monolayers were killed by paraformaldehyde fixation prior to cryptococci inoculation. For all conditions, cryptococcal binding was reduced to almost zero compared to the positive controls, H99 versus live hCMEC/D3 cells (green bars) and H99 versus live bEnd3 cells (pink bars), indicating that viable endothelial cells were responsible for the observed cryptococcal association. Error bars are standard deviation of the mean, n = 2 repeats.

3.2 Chapter III summary

To infect the brain, *C. neoformans* has to cross the normally impermeable blood-brain barrier (BBB). Transcytosis is one of the mechanisms put forward to explain cryptococcal traversal of the BBB. Brain microvascular endothelial cells (BMEC) are the major component of the blood-brain barrier and hence define the transport of substances into the brain. *C. neoformans* has been shown to take advantage of the cellular endocytosis transport apparatus by which cryptococci are phagocytosed by BMEC on the luminal side of the BBB and exocytose on the basal side into the brain tissue. We therefore asked, at what rate does the adherence and internalization of cryptococci by BMEC occur and does the capsule influence this rate? Using both murine (bEnd3) and human (hCMED/3) brain endothelial cells we have shown that the binding and uptake of cryptococci to BMEC is an infrequent event characterized by smaller number of cryptococci at a given time but one that increases with time as demonstrated by the significant rise of cryptococci associated with BMEC from 0.43-0.8% at 2hr to 1.2-1.23% at 4hr. To determine whether the capsule influences the rate of binding and uptake, we made use of 2 pairs of isogenic strains of encapsulated and acapsular *C. neoformans* strains, H99/cap59 and B3501/B4131. We have shown that there was no difference in binding and uptake by BMEC of encapsulated and acapsular cryptococci, suggesting that the binding and uptake of cryptococci by brain microvascular endothelial cells is independent of the capsule. Taken together, the low rate of cryptococcal association with BMEC and the capsule independent interaction suggests that *C. neoformans* most likely uses multiple means to associate with and penetrate the BBB mediated by non-capsule molcules such as hyaluronic acid. Heat killing cryptococci did not alter the rate of binding and uptake, which indicates that the molecules involved in BMEC-cryptococci interaction are heat resistant. Unlike

the pathogen, viability of the endothelium is preliquisite to cryptococcal adherence and internalization.

Unlike macrophages, antibody opsonisation does not enhance binding and uptake of cryptococci by BMEC, which suggest that BMEC do not possess FC receptor required for binding IgG opsonized molecules, the reason why opsonisation did not enhance binding and uptake. Alternatively, other opsonisation mechanisms such as compliment could be important for this intearction. Furthermore BMEC induction with IFN-γ, a known inducer of cell surface adhesion molecules (e.g Intercellular cell adhesion molecule, ICAM; Vescular cell adhesion molecule, VCAM), did not increase binding and uptake of cryptococci. Cell surface adhesion molecule expression by an induced endothelium is most likely important for cell-to-cell adhesion such as phagocyte to endothelim and hence would promote intracellular pathogen traversal of BBB rather than free extracellular cryptococci.

CHAPTER IV: MACROPHAGES AND CLINICAL *CRYPTOCOCCUS*

Cryptococcal parasitism of macrophages is well documented (Alvarez and Casadevall, 2007; Feldmesser et al., 2001b; Ma et al., 2007; Ma et al., 2009) and has been shown to mediate the dissemination of cryptococci into the brain in a murine model of cryptococcosis (Charlier et al., 2009). By studying the *C. gattii* isolates from the so-called 'Vancouver Island Outbreak', our laboratory has previously demonstrated that isolates with high intracellular proliferation rates in macrophages were hypervirulent in a mouse model of infection (Ma et al., 2009). These observations confirmed the importance of macrophage – *Cryptococcus* interactions in the pathogenesis of cryptococcosis. While the Vancouver outbreak was caused by *C. gattii* and mainly affected immunocompetent people (often presenting with pulmonary cryptococcosis), no such studies have been undertaken on cryptococcal isolates from HIV-associated cryptococcosis, which is mainly caused by *C. neoformans*. Thus we studied 47 *C. neoformans* clinical isolates from cerebral spinal fluid (CSF) of HIV-associated cryptococcal meningitis patients, analyzing the rate at which they are engulfed by macrophages and their subsequent rate of intracellular proliferation. Isolates were also characterized for melanin production, capsule expression and iron utilization, traits required for *C. neoformans* intracellular survival and dissemination in the host. Isolates were also investigated for their survival and association with phagocytes in fresh whole blood from healthy donors. Finally, by studying gene expression, we sought to decipher the genetic factors underlying the difference in cryptococci phagocytosis by macrophages.

4.1 Rate of uptake (phagocytosis) and intracellular proliferation rate (IPR)

Murine derived J774 macrophages were infected with cryptococci at an infection ratio of 1:10 and incubated for 2, 18, 24, and 48hrs at $37^{o}C$ with 5% CO_2. At each time point, macrophages were thoroughly washed to remove extracellular cryptococci and then lysed to release intracellular cryptococci, which were counted using a haemocytometer. The rate of uptake was calculated as the number of cryptococci phagocytosed by macrophages at two hours of incubation and intracellular proliferation rate was determined as the ratio of intracellular cryptococci at 18hr to intracellular cryptococci at 2hr. Isolates exhibited an array of uptake rates, Median (range) = 422 (93 – 1530) cryptococci/ 1μL lysate (Figure 15) or 4.22 (0.93 – 15.3) cryptococci per macrophage. Intracellular proliferation rates were similarly variable (Figure 16), Median (range) =2.77 (1.38 – 4) in murine macrophages.
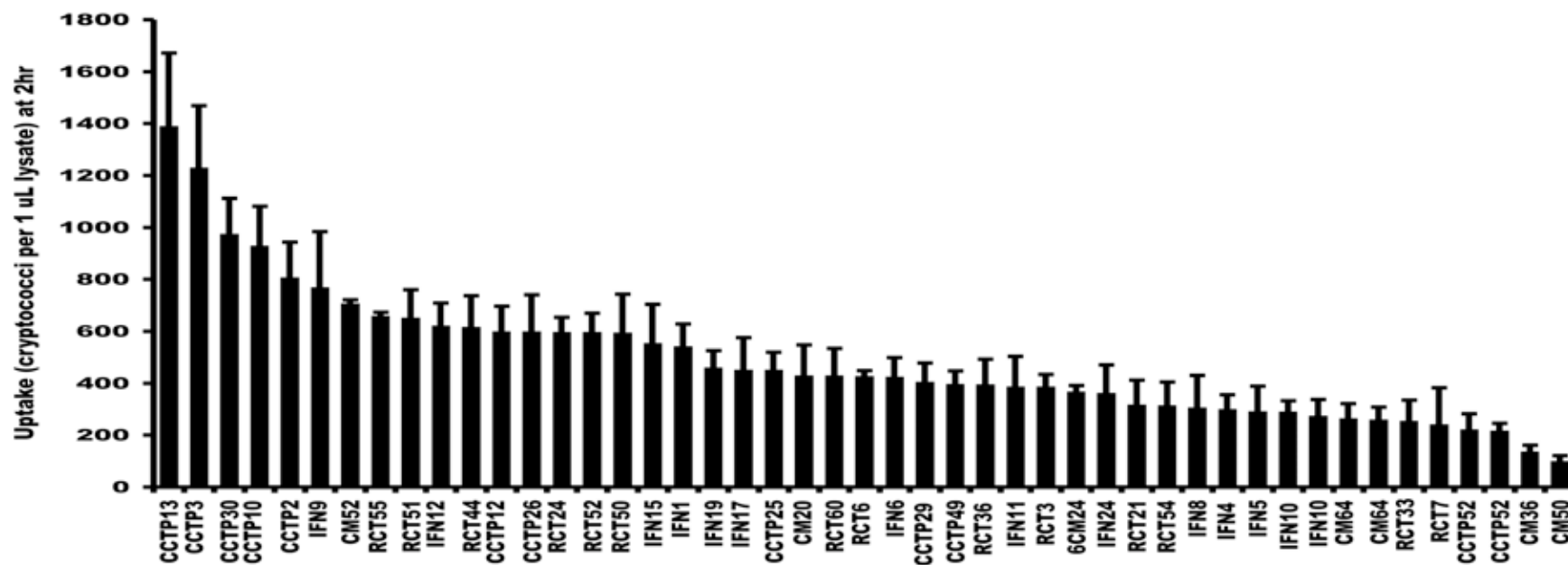
Figure 15: Cryptococci uptake rates by J774 macrophages
The murine macrophage-like cell-line, J774, were exposed to *C. neoformans* clinical isolates at an infection ratio of 1:10 in quadruplicates in 24 well tissue culture plates for two 2hr at 37°C with 5% CO_2. After the two-hour incubation, macrophages were extensively washed to remove extracellular cryptococci. Macrophages in one of the wells were then lysed to release intracellular cryptococci, which were counted by haemocytometer and recorded as number of cryptococci per 1 μL lysate. The remaining wells were further incubated to determine intracellular growth. Rate of uptake for each isolate was determined as the number of cryptococci internalized by macrophages within 2hr of incubation. Isolates were taken up at different rates ranging from the highest, CCTP13 = 1.383 x10^3 cryptococci per 1 μL lysate to the lowest, CM50 at 0.93x10^2 cryptococci per 1μL lysate. The error bars are standard error of the mean (n = 4 – 7 repeats).
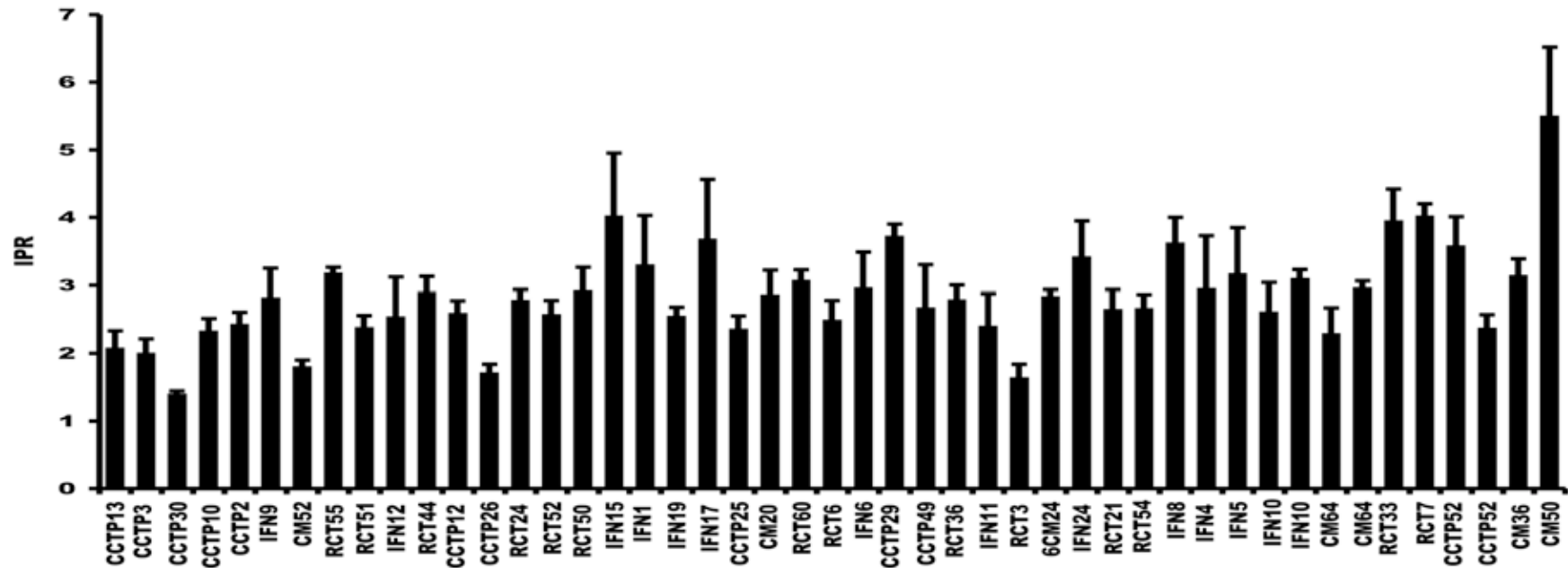
Figure 16: Intracellular proliferation rates of clinical isolates in J774 macrophages
Following the two 2hr exposure during which the rate of uptake was determined, remaining cultures were incubated at 37°C with 5% CO_2 for 18-, 24- and 48hr. At each time point, extracellular cells were removed by washing and macrophages lysed to release intracellular cryptococci for counting with haemocytometer. Intracellular proliferation rate (IPR) for each isolate was determined as ratio of crypotococci at 18hr to cryptococci at 2hr. All isolates had IPRs above 1, which affirms *C. neoformans'* ability to proliferate inside macrophages. Compared to high uptake isolates, the low uptake isolates generally had high IPR (highest uptake isolate CTTP13 IPR = 2.2 while lowest uptake isolate CM50 IPR = 5.83). Error bars are standard error of the mean (n = 4 – 7 repeats).

To test whether this variation was species specific, a selection of high and low uptake isolates were tested in human primary macrophages. This analysis showed a consistent pattern of uptake with J774 macrophages (Figure 17).
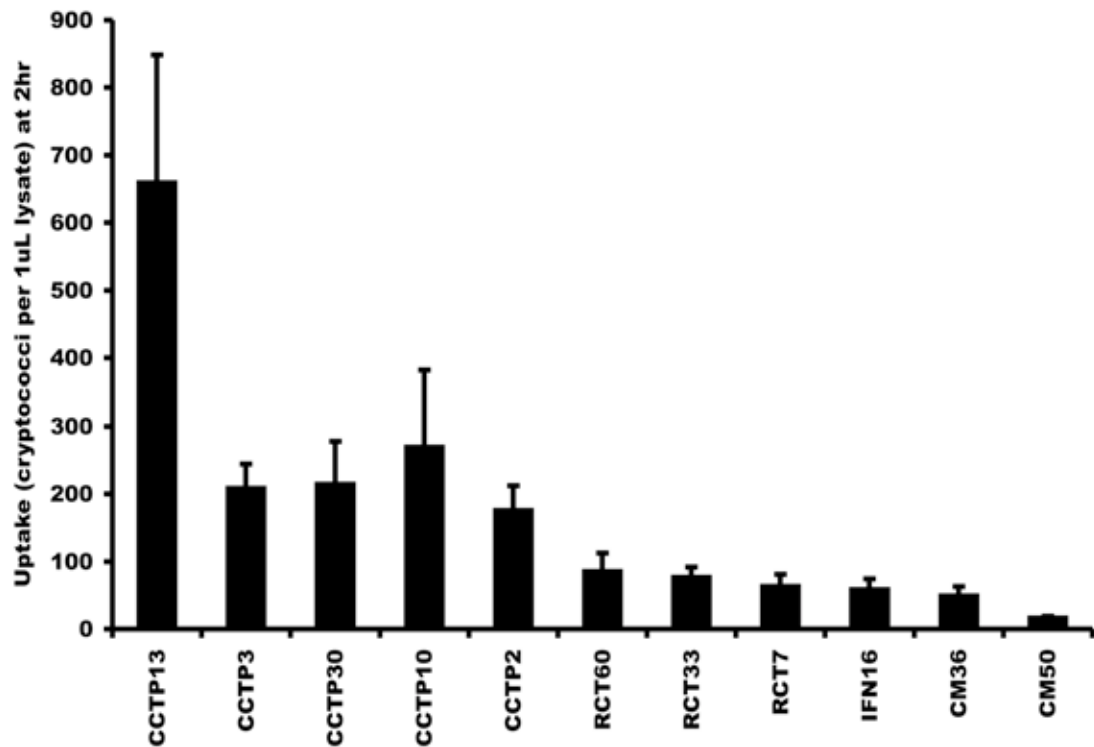
Figure 17: Cryptococci uptake rates by human primary macrophages
A panel of high and low uptake isolates in murine J774 macrophages were selected and tested for uptake in human monocyte-derived macrophages. Infection ratio, interval of exposure and determination of rate of uptake were conducted as described in Figure 15. As with J774 macrophages, the high uptake isolates (CTTP13, CTTP3, CCTP10, CTTP2) were better phagocytosed by human macrophages than the low uptake isolates (RCT60, RCT33, RCT7, IFN16 and CM36), suggesting that strain-dependent variation in 'ease of phagocytosis' is conserved between species. Error bars are standard error of the mean (n = 5 repeats).

4.1.1 Cryptococci uptake by macrophages is inversely correlated with IPR

In both cell types, cryptococci uptake and intracellular proliferation rate were negatively correlated, such that strains with a high basal rate of uptake showed lower intracellular proliferation rates (Figure 18).
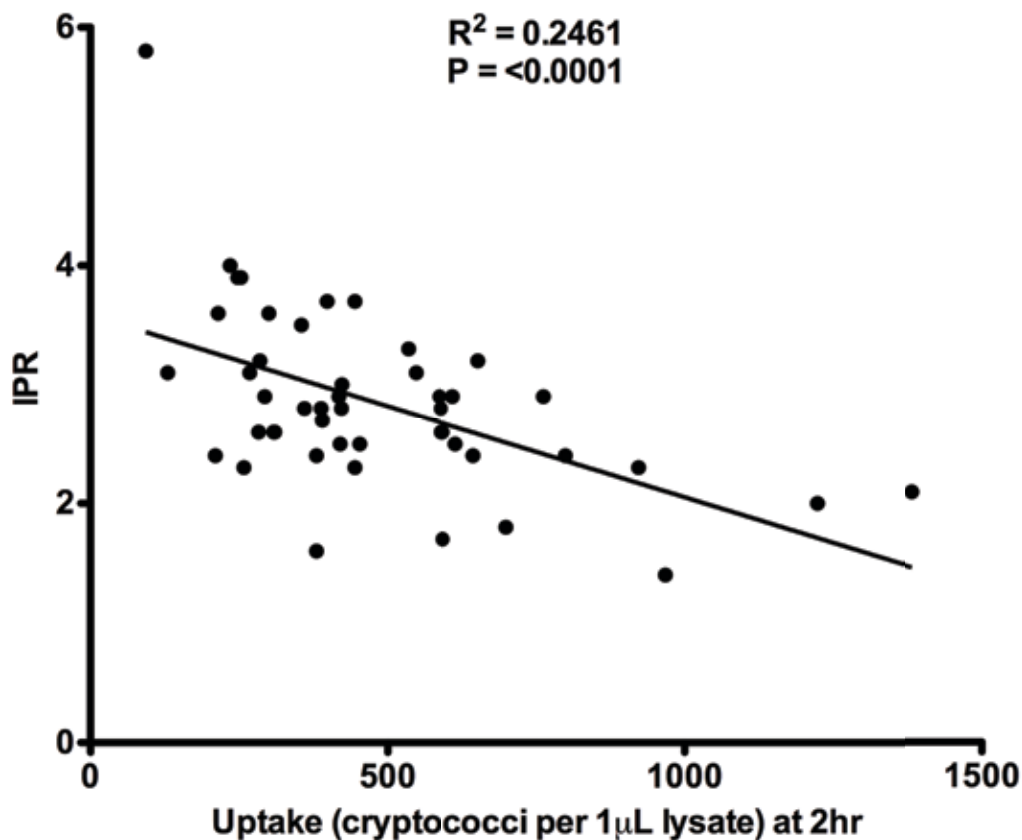
Figure 18: The association between uptake and Intracellular proliferation rate (IPR)

A regression analysis of isolates' rates of uptake and intracellular proliferation rates was performed to determine the correlation between these two variables. Uptake was inversely correlated to IPR, implying that high cryptococcal uptake by macrophages slows down the rate at which these cryptococci subsequently proliferate.

4.1.2 High uptake isolates better phagocytosed by macrophages in absence of opsonin

Opsonisation enhances the rate of cryptococcal phagocytosis by macrophages (Bolanos and Mitchell, 1989b; Mukherjee et al., 1995b; Vecchiarelli et al., 2002); hence we tested the cryptococcal uptake by macrophages in the absence of opsonisation. For both high and low uptake strains, the rate of uptake was reduced by ≥50%, although this was more profound for the low uptake isolates (Figure 19). The internalization of high uptake isolates in absence of opsonin was significantly higher than that of low uptake isolates, $P < 0.01$.
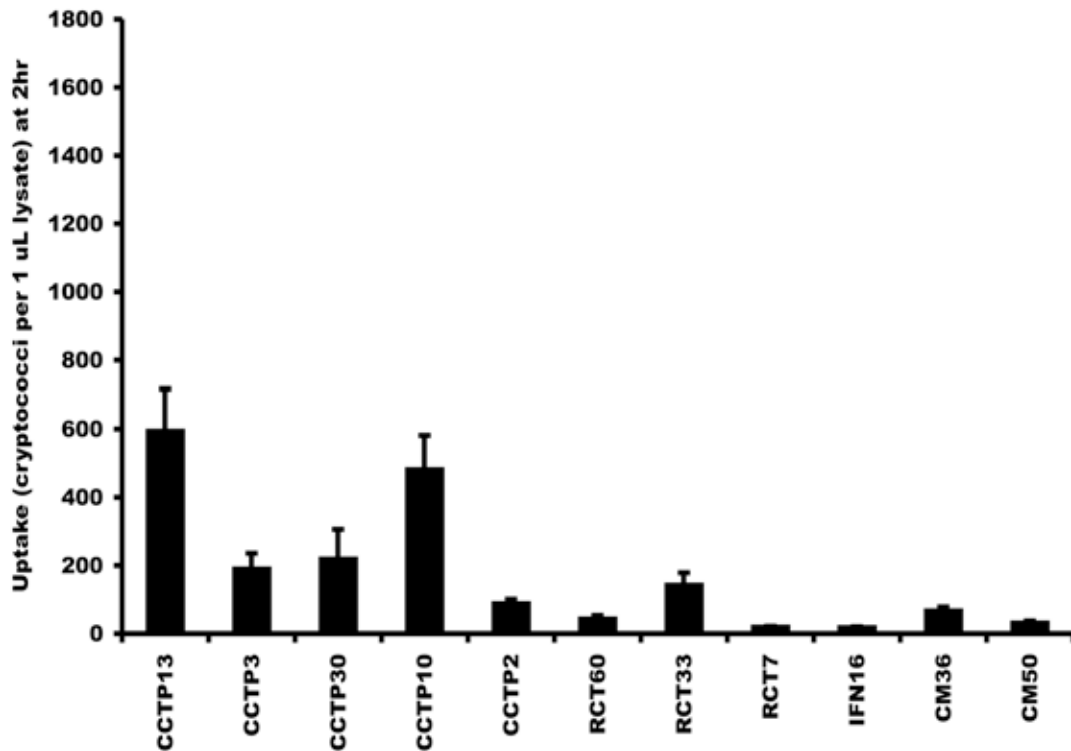
Figure 19: Rate of cryptococci uptake in absence of opsonin
A panel of high and low uptake isolates in murine J774 macrophages were selected
and tested for uptake in absence of the opsonin. Infection ratio, interval of exposure
and determination of rate of uptake were carried out as described in Figure 12A. Rate
of uptake was reduced for both sets of isolates but the high uptake isolates (CTTP13,
CTTP3, CCTP30, CCTP10, CTTP2) were still better phagocytosed than the low
uptake isolates (RCT60, RCT33, RCT7, IFN16 and CM36). Error bars are standard
error of the mean (n = 4 repeats).

4.2 Correlation of uptake and IPR with patient clinical parameters

4.2.1 Rate of uptake positively correlates with patient fungal burden

Uptake and intracellular proliferation profiles were analyzed against patient CSF parameters (glucose, protein, white blood cell count, pro-inflammatory cytokines and fungal burden) and clinical outcome to look for potential associations. Uptake was weakly positively correlated with high CSF fungal burden (Figure 20). In addition, there was seemingly strong correlation between uptake and CSF protein ($r^2 = 0.1283$, $P = 0.0134$), lymphocyte count ($r^2 = 0.1627$, $P = 0.0081$), white cell count ($r^2 = 0.1592$, $P = 0.0055$) driven by one high uptake isolate CCTP13 and disappears when the isolate is taken out of the analysis. However, the positive trend of association between high uptake and high CSF lymphocyte count; white cell count is retained when the data is categorized according to presence of inflammation (>5 white blood cells per mm^3 CSF, n = 23 patients) or absence of inflammation (≤5 white blood cells per mm^3 CSF, n = 24 patients).
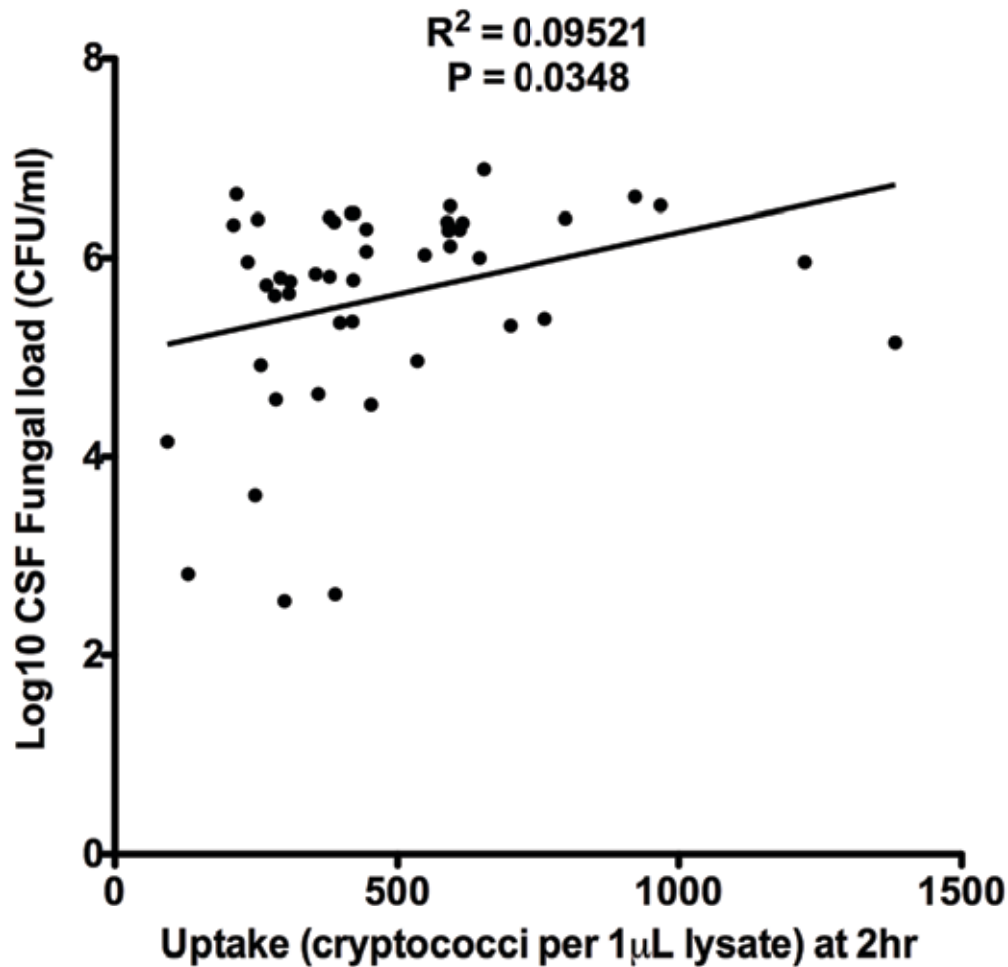
Figure 20: The correlation between rate of cryptococci uptake and patient CSF fungal burden

Linear regression was used to determine the association between uptake of isolates and baseline (before antifungal treatment) fungal burden of the patients. Patient fungal burden was determined by quantitative cryptococcal cultures of patient derived CSF as CFU/ml from which the log10 was calculated (Fungal burden data provided by Tihana Bicanic et al, St. Georges' University of London).

4.2.2 IPR inversely correlates with CSF fungal burden, CrAg and TNF-α

In contrast, intracellular proliferation (IPR) was weakly negatively correlated with CSF fungal burden, cryptococcal antigen (CrAg) and TNF-α levels (Figure 21, 22 and 23 respectively). The IPR correlations with patient CSF parameters are to some extent inverse of the positive association between uptake and CSF patient parameters.
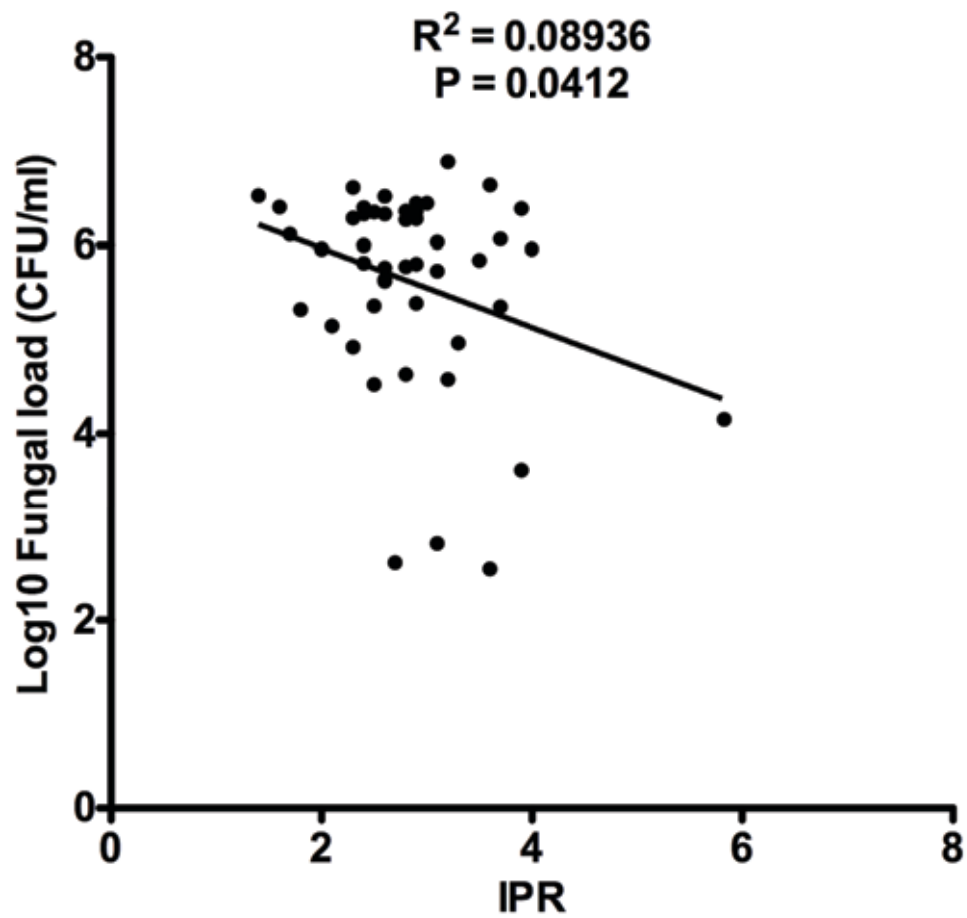
Figure 21: The association of IPR and CSF fungal burden
There was an inverse correlation between IPR and CSF fungal load. The association is particularly driven by one high IPR strain CM50, IPR = 5.83.
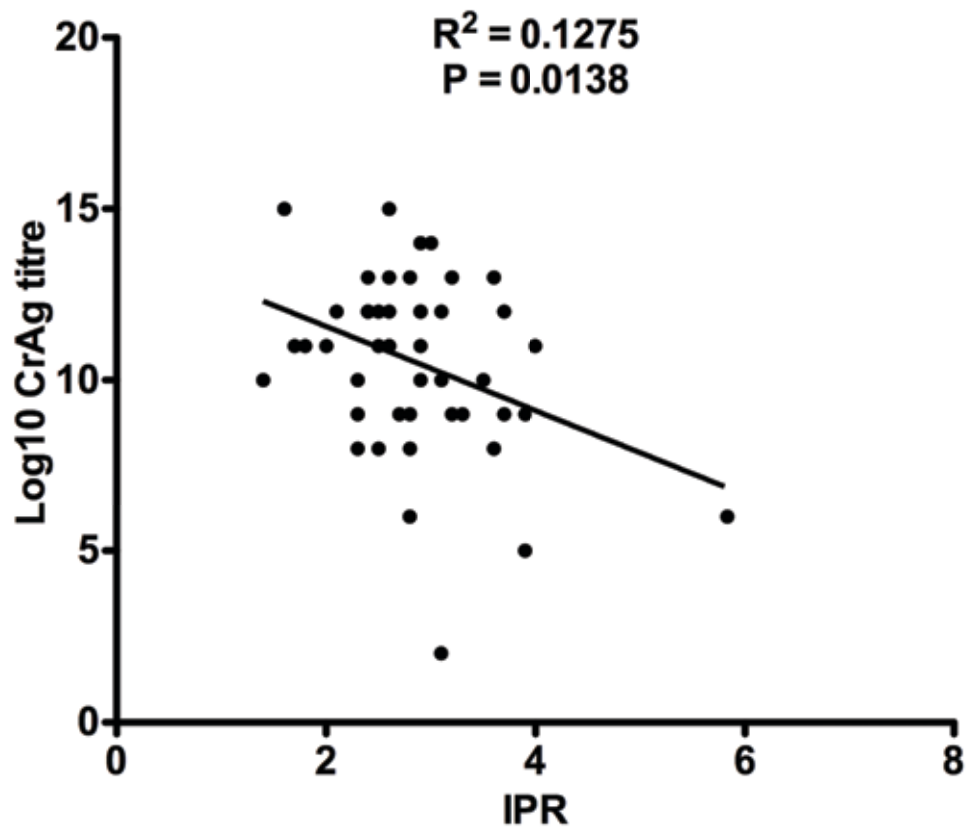
Figure 22: Association of IPR and CSF cryptococcal antigen (CrAg)
CrAg titre is the detection and measurement of soluble cryptococcal capsule in CSF or any other body fluids such as blood and urine. The higher the IPR, the lower the CrAg titre. Like fungal burden, the IPR – CSF CrAg association is driven by isolate CM50 (IPR = 5.83) and is lost when CM50 is removed from the analysis.
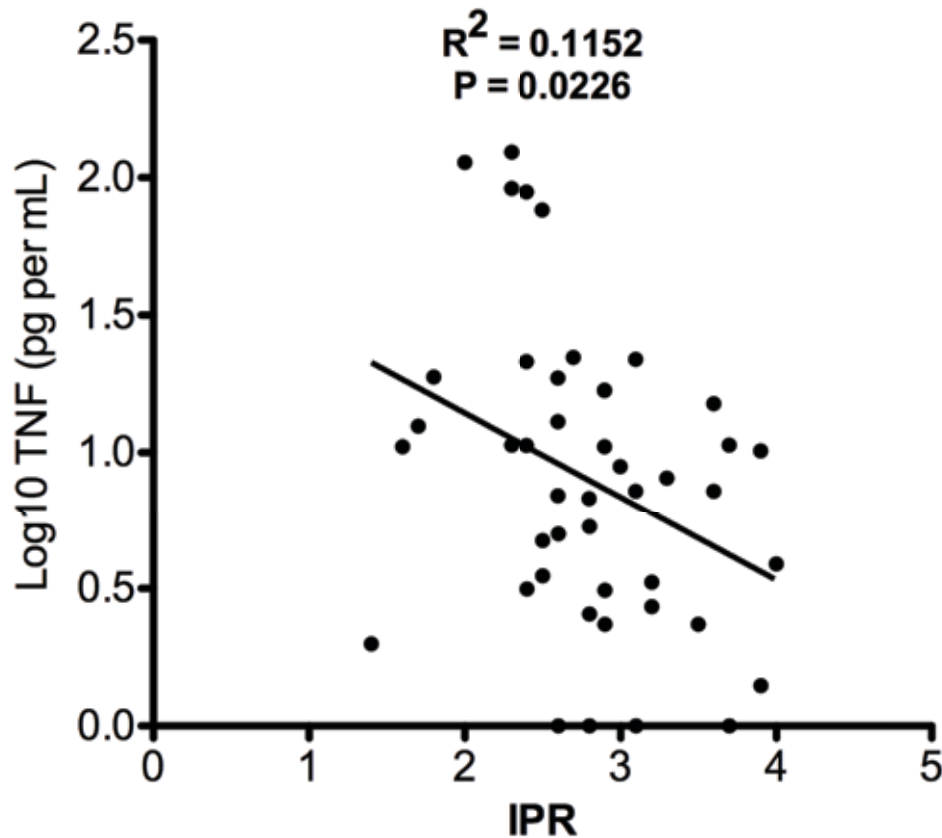
Figure 23: The correlation between IPR and CSF TNF-alpha profile
Linear regression analysis was performed on both uptake and IPR and CSF-cytokine levels. A significant negative correlation was found between IPR of the 46 including 41 African origin isolates and 5 Thailand isolates and baseline CSF TNF-α levels. The 6th Thailand isolate CM50 was the outlier and was not included in the analysis. The CSF TNF-α profile was previously determined by Immunosorbent enzyme linked assay (ELISA) of patient CSF (Bicanic et al, St Georges University of London).

4.3 Melanisation and capsule expression of the clinical isolates

4.3.1 Melanisation

Melanin is an antioxidant and therefore essential for *C. neoformans* to survive the lethal oxygen and nitrogen reactive species produced inside macrophages. We investigated the rate at which isolates produced melanin from the melanin precursor, L-DOPA (Figure 24), and tested this rate for association with cryptococcal uptake and IPR. High uptake isolates were faster melanizers that low uptake ones. Rate of melanization was positively correlated with uptake ($r^2 = 0.1$, P = 0.0293), implying that unlike low uptake isolates, high uptake isolates had higher ability to produce melanin (Figure 25).
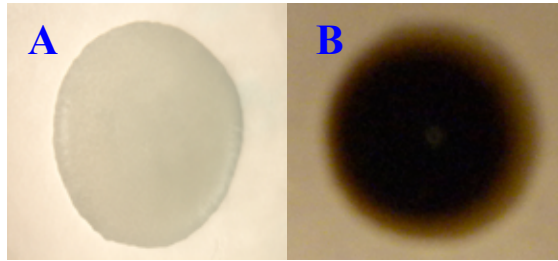
Figure 24: *C. neoformans* **melanisation on L-DOPA agar**
A) Non-melanised colony. B) Melanised colony. Both colonies were observed for 15 days with daily recording of browning rate.
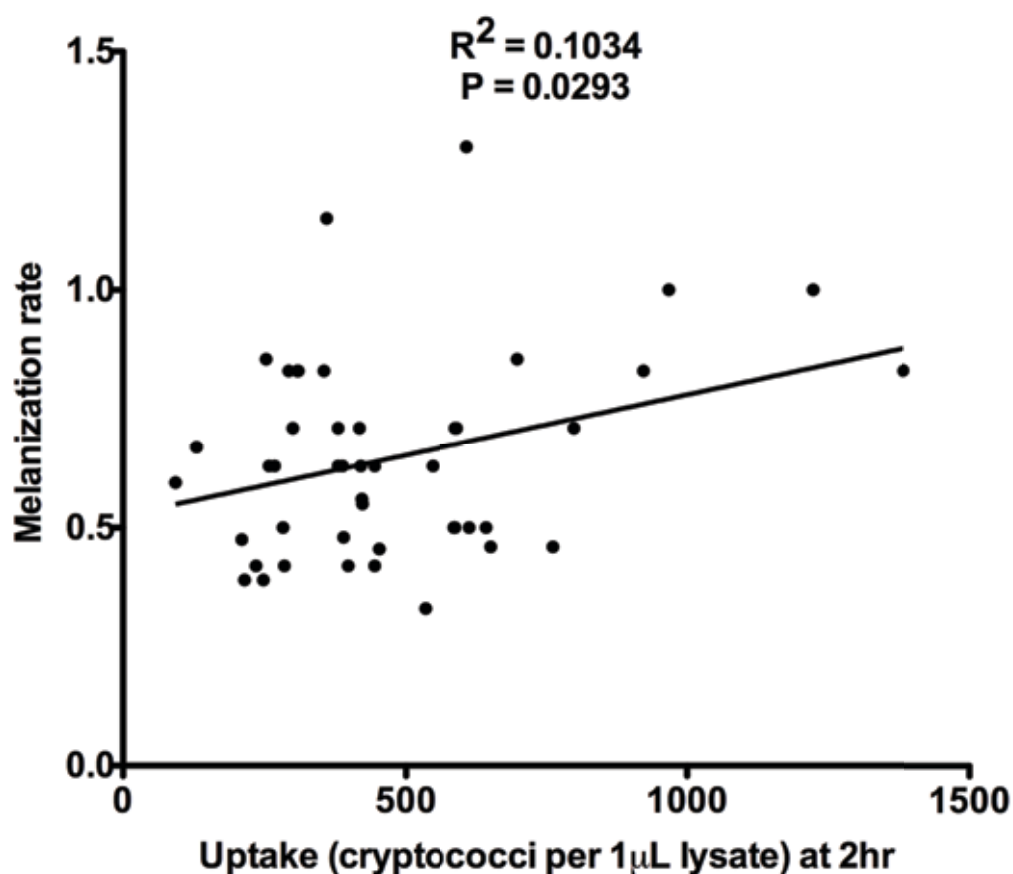
Figure 25: Association between uptake and melanin formation
Rate of melanin formation by isolates was determined by growth on L-DOPA agar. The melanisation rates were analyzed against uptake and IPR using linear regression. Rate of melanin formation was positively correlated with uptake and vice versa for IPR.

Passaging isolates in macrophages significantly increased the rate of melanisation P = 0.0002, suggesting that intracellular environment most likely upregulates expression of genes involved in melanin formation (Table 5).

Isolate	MR Extra.	MR Intra.
CCTP13	0.83	1.25
IFN1	0.33	1.13
IFN2	0.5	0.75
IFN4	0.83	1.7
IFN5	0.42	0.75
IFN6	0.71	0.75
IFN11	0.71	1.67
IFN12	0.5	1.25
IFN15	0.63	0.9
IFN16	0.39	0.75
IFN17	0.63	0.9
B3501	0.53	0.75
MIN	0.33	0.75
MAX	0.83	1.7
MEDIAN	0.58	1.23
P VALUE	0.0002	

Table 5: Effect of intracellular environment on melanisation rate
A set of clinical isolates and one laboratory reference *C. neoformans* serotype D strain B3501 were passaged in J774 macrophages for 24hr prior to melanization assay. Macrophages were washed to remove extracellular cryptococci and intracellular cryptococci released from macrophages by water lysis. 5μL of the lysate for each isolate was inoculated onto L-DOPA agar to determine the rate of melanin formation. By Mannwhitney U test, the intracellular melanisation rates (MR intra.) were significantly higher than the extracellular melanisation rates (MR extra.), P = 0.0002. Extracellular melanisation rate implies MR determined by inoculating L-DOPA with cryptococci directly from YPD culture medium.

4.3.2 Capsule expression

The capsule is a major virulence factor of *C. neoformans* and has been demonstrated to function as an antiphagocytic factor as well as an aid for intracellular survival (Zaragoza et al., 2008). We measured the capsule diameter of each isolate following growth in capsule induction medium and the capsule sizes were analyzed against the rate of uptake and IPR in macrophages. High uptake isolates exhibited low capsule expression as opposed to low uptake isolates with an inverse correlation with rate of uptake by macrophages (Figure 26). There was a trend but not significant positive association between capsule diameter and IPR (Figure 27).
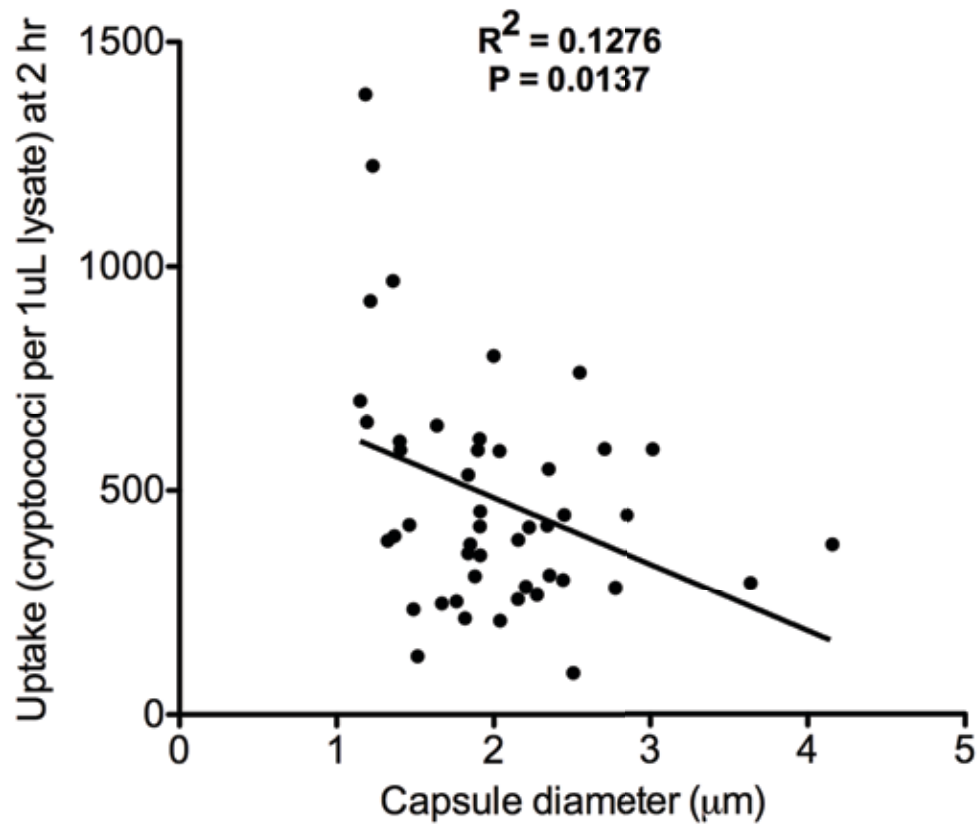
Figure 26: Association between uptake and capsule expression
Capsule diameters were determined by Image J measurement following growth of isolates in capsule induction medium. Capsule diameter (μm) was inversely correlated with uptake, implying that the high uptake isolates possess smaller capsules than low uptake isolates.
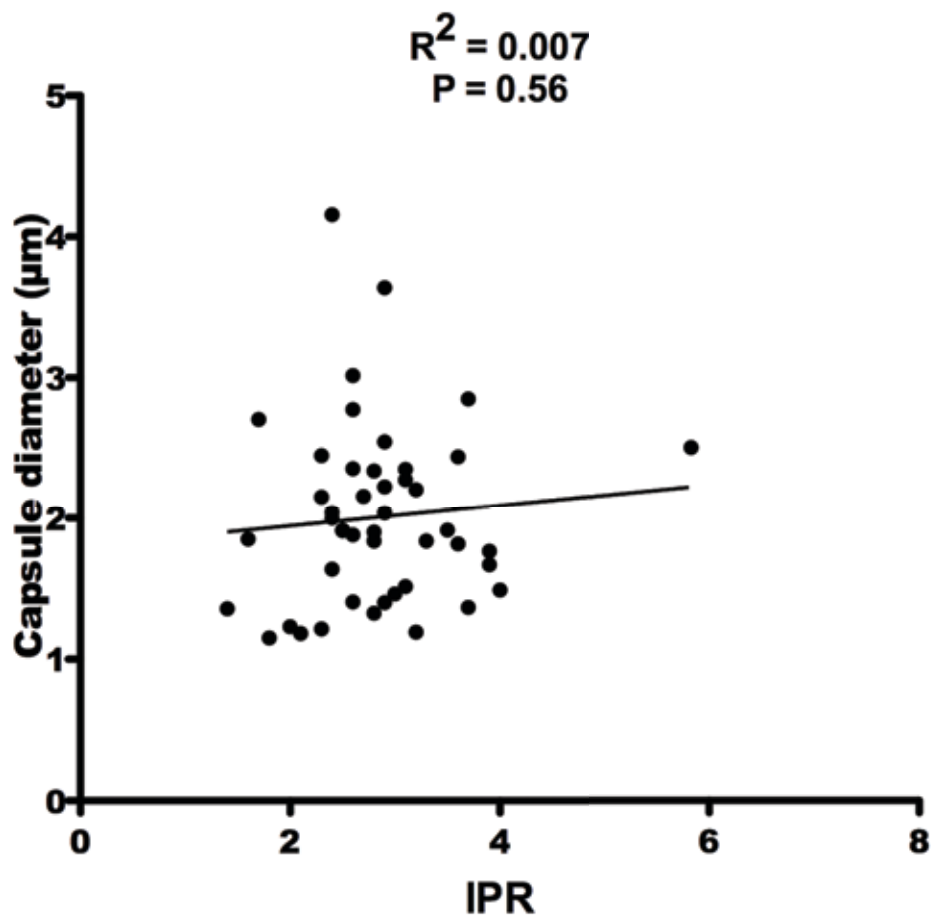
Figure 27: Association between IPR and capsule expression
Capsule diameters were determined by Image J measurement following growth of isolates in capsule induction medium. Capsule diameter (μm) was not significantly correlated with IPR but there was a trend of positive correlation between high IPR and high capsule diameter.

4.2.3 Iron utilization

Iron is important for *C. neoformans* pathogenicity because iron is crucial for elaboration of major virulence factors, capsule and melanin (Jung et al., 2006) In the human host, iron exists largely associated with intracellular proteins, such as haemoglobin and ferritin, or extracellular proteins, transferrin and lactoferrin, leaving only a very limited amount of free iron (Perkins-Balding et al., 2004). However, iron acquisition is essential for both bacterial and fungal pathogens' growth and elaboration of virulence factors (Jung and Kronstad, 2008; Schaible and Kaufmann, 2004). We therefore investigated a selection of the high and low uptake isolates for their ability to grow under iron-limited conditions and to utilize either transferrin or heme as the only source of iron. Both high and low uptake isolates grew poorly on low iron medium and much lower compared to the laboratory reference strain H99 (Figure 28A). High uptake isolates showed preferentially better growth on transferrin than the low uptake isolates, $P = 0.0408$ (Figure 28C). On the other hand, low uptake isolates utilized well on heme but not significantly better than high uptake isolates, $P = 0.0932$ (Figure 28D). All isolates showed high growth rates in rich medium YPD, however, the high uptake isolates' rates of growth were significantly higher than the low uptake ones $P = 0.026$ (Figure 28B). Growth rate data for individual isolates is given in Appendix 3.
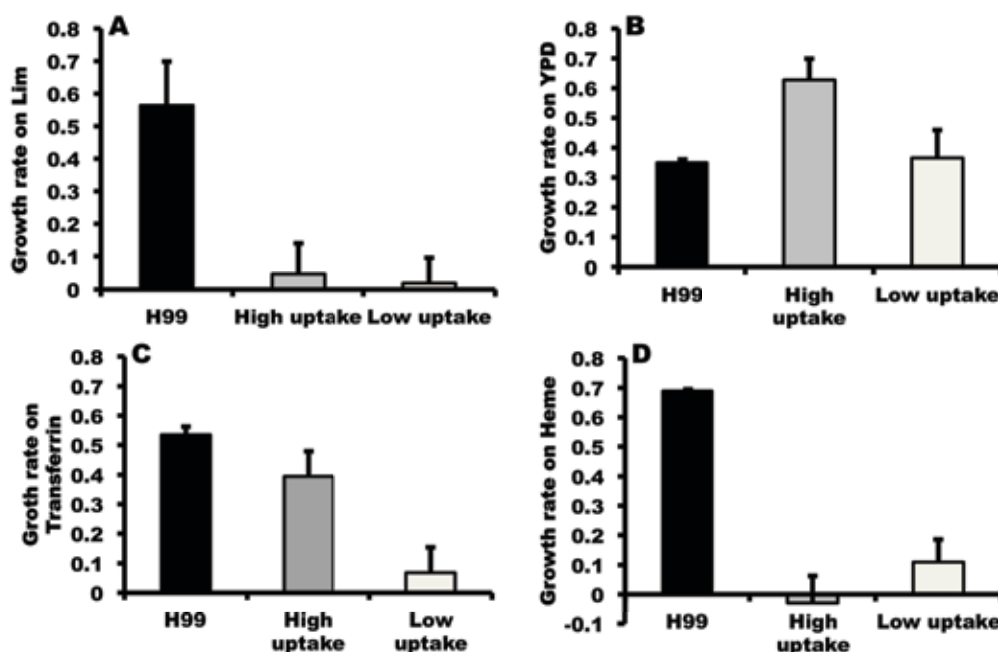
Figure 28: The growth phenotype of high and low uptake isolates in low iron conditions

Growth phenotypes of high uptake (n = 5 isolates) and low uptake (n = 6 isolates) were compared to that of the laboratory reference strain, H99. Prior to the assay, the iron reserves of all trains were reduced by 3-day growth in low iron medium. Cryptococci were then harvested and grown for 7 days in low iron medium (Lim), low iron medium with - transferrin as the only source of iron, heme as only source of iron); or in rich medium (YPD) as a control. Aliquots were taken every 24hr and plated for CFU counts, which were used to plot growth curves. Rate of growth was determined as the slope of the exponential growth curve for each isolate. A) Growth rate on low iron medium with both high and low growing poorly compared to H99. B) All isolates grew well in rich medium YPD with high uptake isolates performing better than H99. C) Growth rate on transferrin as source of iron, high uptake isolates grew better than low uptake isolates. D) Growth rate on heme as source of iron, low uptake isolates grew better on than high uptake. Compared to clinical isolates, H99 grew extraordinarily well on in low iron conditions and on transferrin and heme as sources of iron. High uptake isolates grew significantly better on transferrin than low uptake isolates and vice versa on heme. Both H99 and clinical isolates grew well on rich medium YPD. Error bars are standard error of the mean (n = 3 repeats).

4.4 Cryptococci survival and association with phagocytes in human whole blood

4.4.1 Survival in whole blood

The association between phagocyte-*Cryptococcus* interaction and CSF fungal burden may potentially be explained by the ability of cryptococci to exploit circulating phagocytes to disseminate to the brain. We therefore investigated the ability of both high and low uptake isolates to survive and associate with phagocytes in whole blood taken from healthy donors and infected within 5-10min from bleeding. 1 ml of blood was inoculated with a predetermined (8.73×10^3 CFU/ml by PBS plating) number of cryptoccocci per isolate and incubated at 37°C with minimal rotation for eight hours. At regular time points, 100 μl aliquots of the culture were plated on YPD agar and viable cryptococci determined as colony forming units. All isolates showed reduced viability after exposure to whole blood, with some being reduced to less than half the original inoculum within the first 10 – 30 min of exposure. After the initial hour of incubation there was little subsequent decrease in fungal CFU/ml (average of 6×10^3), which likely indicates the loss of unstable antifungal molecules (e.g. complement proteins) from blood after prolonged incubation (Figure 29).
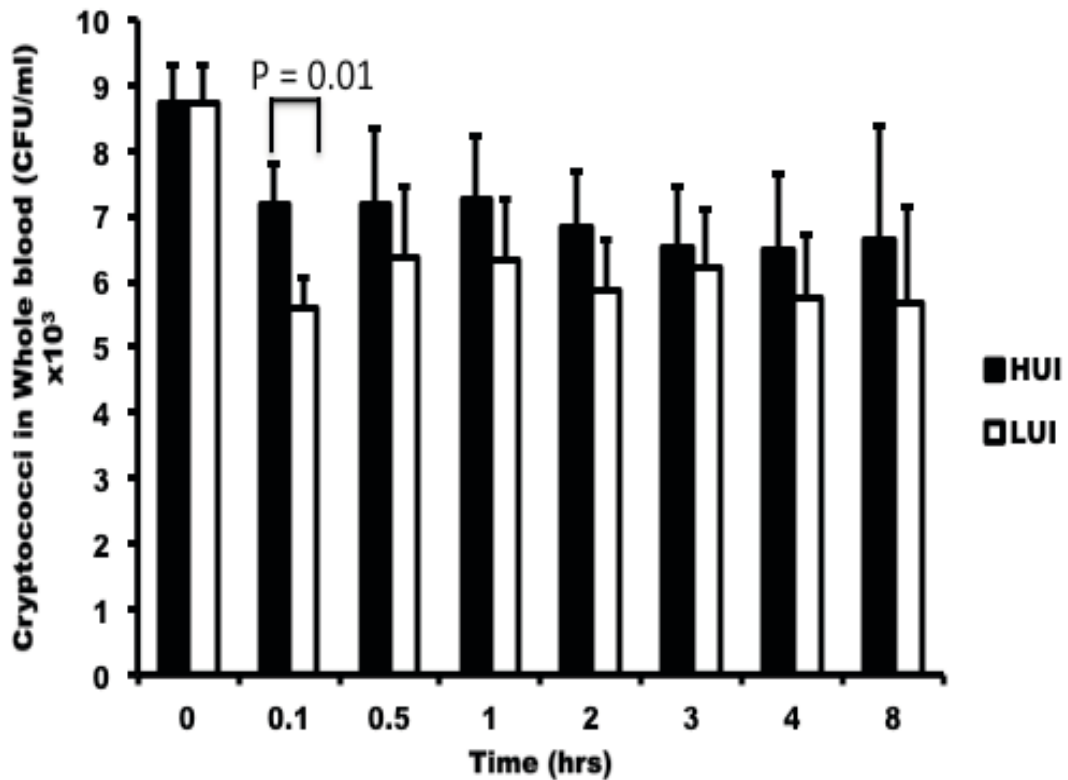
Figure 29: Survival of high uptake and low uptake isolates in whole blood from healthy donors across a time period of 8hrs

Whole blood was inoculated with 10^4 yeast cells of which 8.73×10^3 were determined viable through plating on YPD agar. The highest cryptococcal killing effect occurred within the first 10 – 30 min of which high uptake isolates (HIU, black bars, n = 4), survived significantly better than Low uptake isolates (LIU, black bars, n = 5), P = 0.01. From 1hr and on wards both HU and LU cryptococci survived at a relatively constant rate throughout the 8hr period with HUI showing a trend of better survival than LUI. Error bars are standard error of the mean, n = 6 donors.

4.3.2 Association with phagocytes in whole blood

We further investigated whether cryptococci were associated with phagocytes in whole blood and whether this occurred at the same rate for the low and high uptake isolates. Following 30 – 60 min of infection with FITC stained cryptococci, erythrocytes were removed by lysis and the remaining leukocyte population was analyzed by flow cytometry for association with cryptococci. At 60min, 2 – 4 % and 4 – 14% cryptococci were associated with monocytes and neutrophils respectively. However, there was no difference between low and high uptake cryptococci in association with the two sets of phagocytes 60 min (Figure 30 and 31).
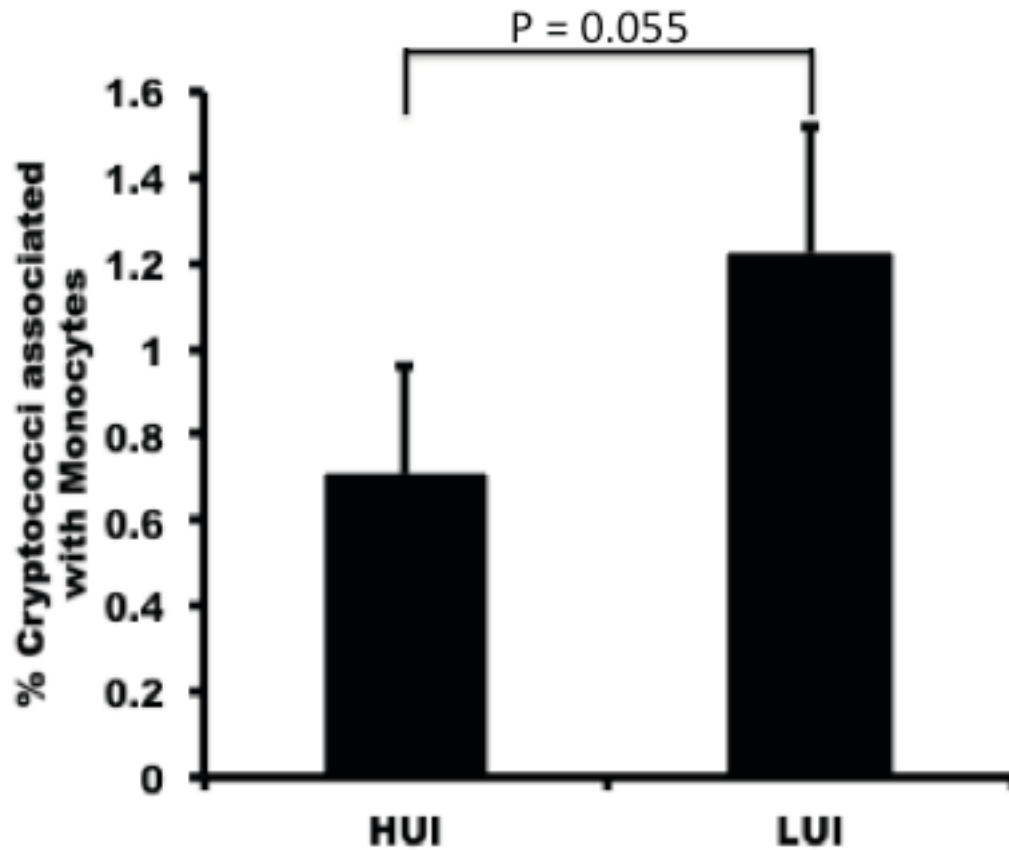
Figure 30: Percentage association of cryptococci with monocytes in whole blood
Fresh whole blood from healthy donors was incubated with FITC stained isolates and cryptococci (10^4 cells per 1ml of whole blood) for 60min. By flow cytometry the cryptococci associated with monocytes were determined using forward and side scatter. Unlike macrophages, Low uptake isolates (LUI), n = 5 exhibited higher but not significant rate of association with monocytes than High uptake isolates (HUI), n = 4. The high rate of association observed in the LUI is driven by isolate CM36 (See Appendix 3: Plot of all isolates). Error bars are standard error of the mean (n = 4 donors).
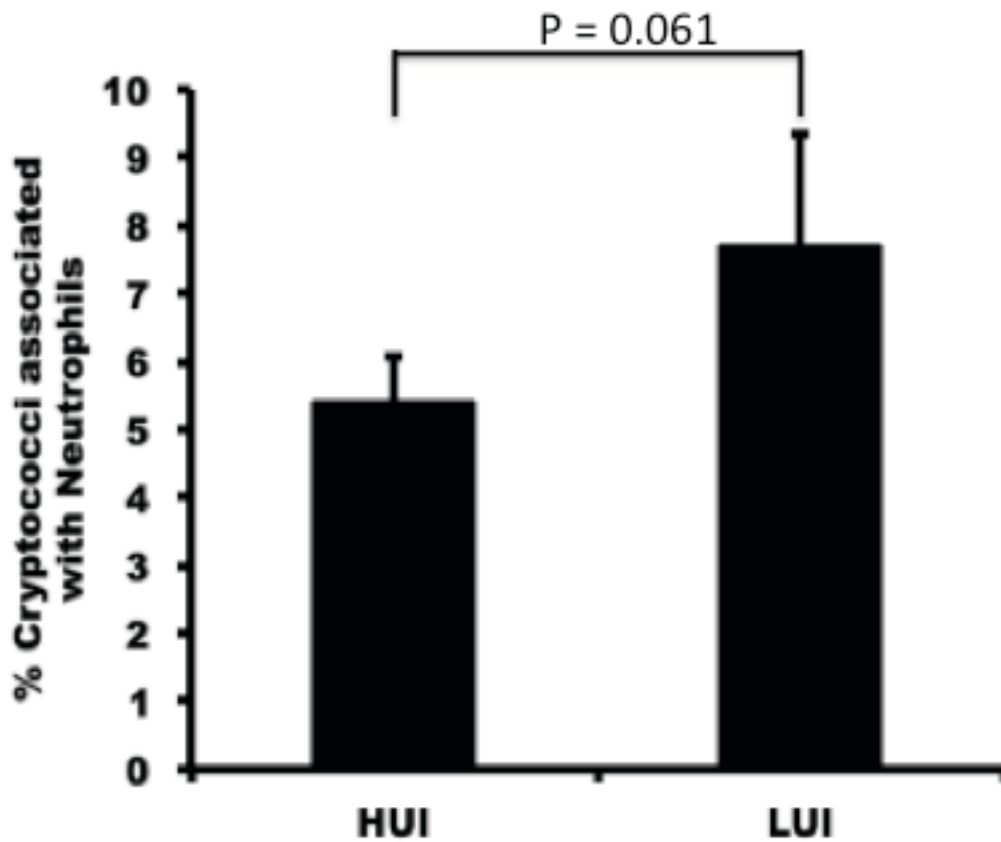
Figure 31: Percentage association of cryptococci with neutrophils in whole blood
Fresh whole blood from five healthy donors was incubated with FITC stained cryptococci (10^4 cells per 1ml of whole blood) for 60min. By flow cytometry the cryptococci associated with monocytes were determined using forward and side scatter. Like monocytes, Low uptake isolates (LUI), n = 5 exhibited higher but not significant rate of association with neutrophils than High uptake isolates (HUI), n = 4. The high rate of association observed in the LUI is driven by isolate CM50 (See Appendix 4: Plot of all isolates). Error bars are standard error of the mean (n = 4 donors).

4.5 Gene expression and cryptococci uptake by macrophages

To determine the genes that underly the difference in cryptococci uptake by macrophages, we tested 2 sets of isolates (4 high uptake and 4 low uptake isolates) for differential gene expression using RNAsequencing. Both high and low uptake isolates plus the reference strain H99 (Serotype A *C. neoformans var. grubii*, *Cnag*) were propagated in a pre-phagocytosis medium and RNA extracted for transcriptome sequencing. All sequences were aligned to the reference H99 genome yielding an average unique mapping rate of 81.8%. Pairwise comparison between isolates and H99 yielded between 776 – 2311 differentially expressed (DE) genes of which low uptake isolates had a slightly more DE genes to H99 than the high uptake isolates (Appendix 5). Sequence alignments betweem the high and low uptake isolates yielded a total of 6846 informative genes (genes that have atleast average reads across two samples in the comparison). By Fisher's exact test and filtering with absolute log2 fold change larger than 1 and 0.5% false discovery rate (q-value), 8 genes were found significantly differentially expressed between the high uptake and low uptake isolates (Figure 32).
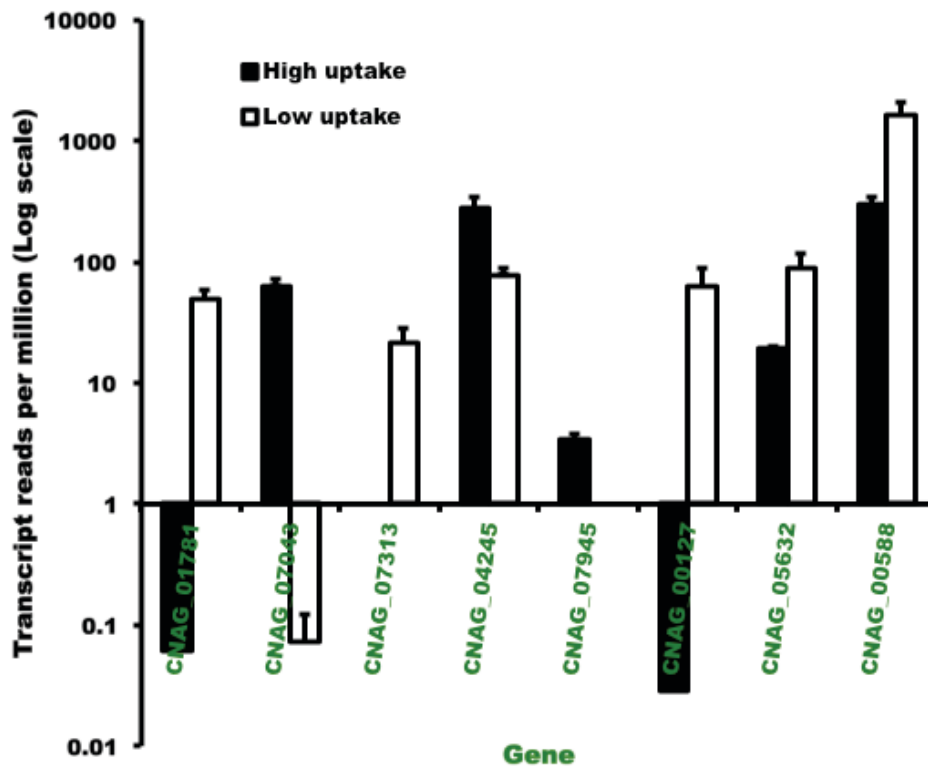
Figure 32: Differentially expressed genes between the high uptake and low uptake isolates

RNA was extracted from a set of high uptake (black bars) and low uptake (white bars) isolates before phagocytosis assay. By RNAsequencing 8 differentially expressed genes were determined of which 3 (CNAG 017040, CNAG 04245, CNAG 07945) are more expressed in the High uptake isolates whilst 5 (CNAG 01781, CNAG 07313, CNAG00127, CNAG 05632 and CNAG00588) were more expressed in low uptake isolates, P = <0.01 in all the 8 genes. Error bars are standard error of the mean. Eight isolates in total of which n = 4 for each set of isolates (high uptake and low uptake).

Out of the 8 differenntially-expressed genes, 3 (CNAG_04245, CNAG_05632 and CNAG_00588) had known function (Chinase, Mannose-6-phosphate receptor repeat and Racin superfamily respectively) Table.

GeneID	ProtID	Prot Function
CNAG_01781	AFR97983.1|	None
CNAG_07043	AFR98755.1|	None
CNAG_07313	AFR92263.1|	None
CNAG_04245	AFR96977.1	Chitinase
CNAG_07945	AFR98751.1	None (cystein dioxygenase)
CNAG_00127	AFR92264.1	None (but present in *C. gattii* and Myxococcus)
CNAG_05632	AFR99063.1	Mannose-6-phosphate receptor repeat
CNAG_00588	AFR92718.1	Ricin superfamily

Table 6: Differentially expressed genes and their protein function
Genes CNAG_04245, CNAG_05632 and CNAG_00588 encode Chitinase, Mannose-6-phosphate receptor repeat and Ricin superfamily. No known protein function encoded by genes CNAG_01781, CNAG_07043 and CNAG_07313; CNAG_07945 is thought to encode cysteine dioxgyenase while CNAG_00127 is present in *C. gattii and Myxococcus*.

4.6 Chapter IV Summary

The role of phagocytes in the pathogenesis human cryptococcosis remains a critical question to answer. The study of *C. gattii* isolates in our laboratory demonstrated that high Intracellular proliferation rate in macrophages is correlated with hypervirulence in a mouse model of cryptococcosis (Ma et al., 2009). In this chapter, we have shown that there is a link between macrophage – *Cryptococcus* interaction phenotype and patient clinical phenotype. By studying the uptake (phagocytosis) and Intracellular proliferation rates of *C. neoformans* isolates in macrophages, we show that there is association between high cryptococci uptake by macrophages and patient CSF fungal burden. In addition we demonstrate that Intracellular proliferation rate (IPR) is negatively correlated with patient CSF fungal burden, crytococcal antigen titre and levels of TNF-α. Uptake and IPR are inversely correlated implying that high uptake isolates have low IPR. The inverse relationship also implies that parameters like crytococcal antigen titre and levels of TNF-α could be positively correlated with uptake. Taken together, rate of cryptococci uptake by macrophages stands out as the positively associated factor with patient clinical phenotype. Therefore, the question is what could be the link between cryptococci uptake by macrophages and pathophysiology of cryptococcal meningitis? It could mean that either highly phagoctosed isolates have a high chance to dessiminate from the lungs (initial site of infection) to the brain using macrophages as Trojan horses or high uptake isolates are endowed with unique virulence traits that make them to efficiently survive and dessiminate in the host.

Testing the isolates by the known major virulence factors, capsule and melanin, we found that the high uptake isolates were high melanin formers but less capsulated demonstrated by the positive and inverse correlations between uptake and rate of melanin formation and capsule diameter respectively. This result suggests that the smaller the capsule the higher the rate of phagocytosis and rapid melanin formation is most likely crucial for surviving in the host and particulary the hostile intracellular environment. Passaging a set of isolates in macrophages significantly increased the rate of melanin formation implying that components of melanin formation pathway are vital and thus are highly expressed during intracellular survival. Efficient nutrient acquisition is important for pathogen survival in the host. By analysing Iron source utilization profiles, we show that high uptake isolates survive better in low iron medium and more efficient utilizers of transferrin as only Iron source than the low uptake isolates. The brain tissue is rich in transferrin (Dwork et al., 1988) and perhaps that is why high uptake isolates have high CSF fungal load because they proliferate in brain tissue rich in Transferrin. Exvivo analysis of high uptake and low uptake isolates in whole blood from healthy donors showed a significantly higher survival rate by high uptake isolates than low uptake ones in the first 10 - 30min of exposure to blood which faded with increase incubation time. This suggests that the crucial blood antimicrobial factors may have a short active life outside the donor and hence the defining killing effect occurs in the first few minutes. Interestingly, low uptake isolates show higher but not significant association with phagocytes in blood than the high uptake ones. This higher association efficiency particulary with neutrophils might contribute to the observed low survival in whole blood. Alternatively, it could be that the mechanism of association with blood phagocytes is different from tissue

macrophages and hence the discrimination between high and low uptake most likely occurs at the level of alveolar macrophages in the lungs.

The fact that there was consistent trend of cryptococci uptake by both mouse and human macrophages indicate that there is underlying genetic factors driving the difference in phagocytosis. Prephagocytois differential gene expression analysis revealed eight differentially expressed genes between high uptake and low uptake isolates. Three out of the eight genes encode proteins Chitinase, Mannose-6-phosphate receptor repeat and Ricin. Although these proteins might be important to *Cryptococcus* in certain aspects, none of them has been implicated in modulation of phagocytosis. Chitinase degrades chitin, a crucial component of the fungal cell wall and is thought to maintain the dynamic state of the fungal cell wall during growth and has been shown to be crucial sexual reproduction in *C. neoformans* (Baker et al., 2009) and also induces allergic inflammation in pulmonary cryptococcosis (Vicencio et al., 2008). Mannose-6-phosphate receptor is implicated in vesicle transport and endosome maturation (Qin et al., 2011) whilst ricin is a toxic lectin produced by caster plants but no known function has yet been described for *C. neoformans*. Genes underlying known antiphagocytic factors such as the capsule, antiphagocytic protein 1 and GATA family transcription factor (Gat201) were not differentially expressed between the two sets of isolates. This may mean that either the observed DE genes affect phagocytosis in ways that aren't yet illucidated or that pro-/anti-phagocytic gene expression occurs when cryptococci are exposed to macrophages and not before (in a macrophage free prephagocytosis medium), a reason why the difference in these genes could not be detected.

CHAPTER V: DISCUSSION

5.1 *C. neoformans* and the brain-microvascular endothelial cells

The mechanism by which *C. neoformans* associates with – and penetrates - the BBB remains a critical question in understanding the pathogenesis of CNS cryptococcosis. Considerable evidence shows that the penetration of the BBB by *C. neoformans* may occur via infected phagocytes (Charlier et al., 2009) or transcellularly through adherence and phagocytosis by the brain microvascular endothelial cells (Chang et al., 2004a; Shi et al., 2010). Determining the relative contribution of these different routes to CNS cryptococcosis requires quantitative analysis of the interaction between cryptococci and brain microvascular cells, data that are currently lacking. Here we have taken the first steps to address this shortfall by using both mouse and human brain endothelial cell models.

Our data indicate that adherence to, and phagocytosis of, cryptococci by brain microvascular endothelial cells is a rare event, although one that increases with extended periods of incubation. The rate of encapsulated and acapsular cryptococci association with bEnd3 cells remained low even with IFN-γ induction. IFN-γ treated and non-treated bEnd3 cells equally associated with cryptococci, an indication that the association of cryptococci with bEnd3 cells may be independent of IFN-γ induced expression cell adhesion molecules. These findings support recent observations in a mouse cryptococcosis model, which suggest that transmission across the BBB is a non-specific event dependent on trapping of cryptococci in narrow brain followed by phagocytosis after a significant time of contact with brain microvascular endothelial cells (Shi et al., 2010). This implies that the adherence to – and phagocytosis of - cryptococci by BMEC is a slow process involving single cryptococci binding at any

one time and thus that cryptococcal meningoencephalitis may be the result of a very small number of cryptococcal cells penetrating the BBB and subsequently proliferating to high numbers within the brain tissue (Lee et al., 2010). If so, then clinical approaches that reduce cryptococcal binding to endothelia even marginally may result in significant improvements to patient health.

Possession of a capsule is a major virulence factor in *C. neoformans* and the presence of a capsule modulates many aspects of the interaction between cryptococci and infected hosts (Syme et al., 1999; Zaragoza et al., 2008). *Cryptococcus* – endothelial cell interaction studies have demonstrated varying contribution of the capsule and or it absence to cryptococcal binding and uptake by BMEC (Charlier et al., 2005a; Fries et al., 2001; Guerrero et al., 2006; Ibrahim et al., 1995; Jain et al., 2006b). By studying isogenic pairs of wild type and acapsular cryptococci and different brain endothelial cell-lines, we have shown that binding and uptake of cryptococci by BMEC is capsule independent. In agreement with this finding, intravital imaging of cryptococcal traversal of the blood-brain barrier has demonstrated equivalent crossing of the blood-brain barrier by wild type and acapsular cryptococcal yeast cells (Shi et al., 2010), an observation that implies the dispensability of the capsule for cryptococcal penetration of the blood-brain barrier.

Our finding that neither opsonisation nor active signalling from the cryptococcal cell are required for uptake are in line with recent data suggesting that cryptococcal uptake into brain endothelia is mediated by binding of endothelial CD44 to hyaluronic acid on the yeast surface (Huang et al., 2011). Heat killing of the yeast is unlikely to disrupt this interaction, explaining why endothelial invasion by heat-killed

cryptococci is seen both in vitro (this study) and in vivo (Shi et al., 2010).
Interestingly, however, our data suggest that human derived endothelia (but not
murine bEnd3 cells) are capable of killing intracellular cryptococci. Presumably
crossing the BBB intact thus requires one or more of the virulence factors used by
cryptococci to resist phagosomal killing (Ma et al., 2009), explaining why heat-killed
cryptococci can enter endothelial cells but are not seen to transmigrate.

5.2 Macrophages and clinical cryptococcosis

In the second part of this thesis we have used an *in vitro* model of phagocyte –
Cryptococcus interaction to explore the impact of this interaction on clinical
parameters and thus on clinical outcome. Our results show that high cryptococcal
uptake by macrophages is correlated with high cerebral spinal fluid fungal burden.
The significance of this association is weak (P = 0.035), but given the fact there are
numerous other factors that together underlie the patient's clinical outcome, even a
relatively weak association is likely to indicate an important phenotype for the
pathogenesis of cryptococcal meningitis. Interestingly, patients with high CSF fungal
burden are most likely to die by 10 weeks from diagnosis (Bicanic et al., 2009). Thus
our data would suggest that high phagocytic uptake is ultimately an indicator of poor
prognosis for cryptococcal meningitis patients. This counterintuitive correlation may
have two (non-exclusive) potential explanations. Firstly, high uptake isolates may
disseminate faster into the brain by using macrophages as vectors. Once in the brain,
the cryptococci-laden macrophages may either expel or lyse to release cryptococci
into neuro-cerebral tissue. Unlike low uptake isolates, macrophages exposed to high
uptake isolates were often observed highly loaded with cryptococci at 2hr of

incubation, suggesting that such isolates are likely to generate a high force of infection into neural tissue, even in the absence of opsonin. The macrophage intracellular environment provides a protective niche to grow and spread to other cells and tissues for which *C. neoformans* apparently employs the "get in fast" strategy. Monocytes from HIV patients are less able to internalize cryptococci (Monari et al., 1997) so cryptococci that are more rapidly taken up by these macrophages may have an advantage in disseminating into the brain. Indeed, studies have shown that that cryptococci-laden monocytes (Chretien et al., 2002), and or perivascular macrophages (Shinoe et al., 2006) are seen circulating or lodged in the perivascular spaces of in the brain capillaries respectively. Secondly, intracellular cryptococci are more slowly cleared by antifungal treatment, since most antifungals show poor cellular penetration. Thus high uptake strains may disseminate more rapidly to other tissues by 'hijacking' host phagocytes and are additionally protected from the worst effects of therapy during their journey to the brain.

The nature of the host cytokine response is important in determining the fate of cryptococcal infection as well influencing clinical outcome. For instance, the presence of IFN-γ in the CSF improves both rates of fungal clearance and clinical outcome (Bicanic et al., 2009a). We tested the association of cryptococcal uptake, IPR and patient CSF cytokine (IFN-γ, IL-6 and TNF-α) levels. These analyses revealed intracellular proliferation rate and CSF TNF-α levels to be negatively correlated, implying that the higher the intracellular proliferation rate the lower CSF TNF levels. TNF-α is a macrophage produced pro-inflammatory cytokine and has been implicated in restricting intracellular proliferation of *M. tuberculosis* in macrophages as well as promoting granuloma formation responsible for containing *M. tuberculosis* infection

(Bean et al., 1999). Thus the presence of intracellular cryptococci may suppress TNF-α production by macrophages resulting in lower levels of the cytokine. Interestingly, the high IPR isolates were also found to express larger capsules and studies have shown that the polysaccharide capsule negatively modulates monocyte/macrophage cytokine production by inhibiting pro-inflammatory cytokines and enhancing anti-inflammatory cytokine production (Reviewed in Vecchiarelli and Monari, 2012). The paucity of pro-inflammatory cytokines observed in CM patients (Boulware et al., 2010), may be partly explained by intracellular cryptococci inhibiting cytokine production by macrophages. Kawakami et al demonstrated that cryptococci could inhibit TNF-α production by macrophages both *in vivo* and *in vitro* (Kawakami et al., 1996; Kawakami et al., 1997). These observations concur with a study, which implicated brain macrophages/microglia as the most reactive cells in CM pathology and any deficiency in their effector functions results in accumulation of cryptococci in the brain (Lee et al., 1996).

Capsule expression and melanin are crucial virulence factors in the pathogenicity of *C. neoformans*. The capsule is involved in evasion and modulation of the immune response whereas melanin functions as an antioxidant, protecting the fungus from reactive oxygen species generated by phagocytes (Garcia-Rodas and Zaragoza, 2012; Jacobson and Tinnell, 1993; Vecchiarelli and Monari, 2012). We characterized all the isolates used in Chapter IV for capsule expression and rate of melanin production. Our results show that the capsule diameter is inversely correlated with high cryptococci uptake by macrophages. This suggests that hypocapsulated isolates are more successfully engulfed by macrophages than the hypercapsulated ones, confirming the role of the capsule in resisting phagocytosis. The results are in

agreement with earlier phagocytosis studies, which showed that cryptococci phagocytosis by alveolar macrophages was inversely related to capsule size (Bolanos and Mitchell, 1989b) and further demonstrated that large encapsulated strains were not taken up in absence of serum (Bolanos and Mitchell, 1989a). While resisting phagocytosis is a strategy deployed by some strains of *C. neoformans* to evade the fungicidal effects of the immune response, hypocapsulation most likely offers an alternative means of evading the immune response by hiding inside phagocytes such as macrophages and monocytes. Studies have shown the cryptococcal capsule enlarges during infection and intracellular survival (Zaragoza et al., 2008) but there seems to be a population of evolutionarily hypocapsulated strains existing in the environment with an ability to infect and cause disease in the human host without altering their capsule size. Such hypocapsulated strains were first reported in the Lancet, 1985 as a cause of cryptococcal meningitis (CM) in AIDS patients (Bottone et al., 1985). Bottone, further argues that the impaired immune response immune in AIDS imposes less selective pressure on *C. neoformans* and hence, the retention of poorly encapsulated cells (Bottone et al., 1986). These observations were further supported by a study in which a capsule-deficient isolate from the brain of a CM patient did not form capsule for 2 weeks in the inoculated murine peritoneal cavity. The same study showed this capsule-deficient isolate was highly phagocytosed by phagocytes *in vitro* (Sugiura et al., 2005). Patient CSF cultures were always negative, suggesting that the isolate's susceptibility to phagocytosis prevented detection by growth culture since it may have been hidden inside phagocytes (Sugiura et al., 2005). Unlike capsule expression, rate of melanisation was positively correlated with cryptococcal uptake into macrophages, an indication that the high uptake isolates are fast melanin formers. The rate of melanin formation was significantly increased ($P =$

0.0002) when isolates were passaged in macrophages, suggesting that the intracellular environment has an impact on the expression of melanin forming genes. This is most likely an evolved trait, selected for by environmental phagocytes such as amoebae; strains that are inherently 'easily eaten' must have alternative means, such as melanisation, for surviving within soil predators. Interestingly, the high uptake, fast melanin forming and high fungal burden isolates were less encapsulated, suggesting that *C. neoformans* employs multiple and varied virulence strategies to adapt to and colonize host tissues - in this case, with capsule deficiency being compensated for by high melanin formation.

The mechanism to explain why highly phagocytosed isolates are responsible for high CSF fungal burden remains unclear. It could be that, in addition to trafficking more successfully to the CSF, such strains grow more rapidly under limited nutrient supply or they are better survivors. To this end, we tested the high uptake and low uptake isolates' ability to grow on limited iron supply and specific sources of iron. Our results show that both sets of isolates are sensitive to low iron conditions, although the high uptake isolates grew slightly better in these conditions. In contrast, the laboratory reference strain H99 grew extremely well on low iron, a remarkable trait that sets it apart from other recently isolated clinical strains of the same species and serotype. H99 was isolated in 1978 from the CSF of a Hodgkin's disease patient (Morrow et al., 2012) and is currently the reference genome for serotype A *C. neoformans*.

High uptake strains showed a preference for growth on transferrin as a source of iron while the low uptake isolates grew better on heme. Transferrin is widely available in human brain tissue with the choroid plexus being the main producer of brain

transferrin (Dwork et al., 1988). Therefore an ability to efficiently utilize transferrin as a source of iron might explain why high uptake isolates are responsible for high fungal burden possibly due to high growth rates in CSF. *C. neoformans* take up iron from transferrin using the high affinity permease/ferroxidase system and mutants in this uptake mechanism were unable to grow on transferrin as a source of iron and exhibited less virulence with poor dissemination to the brain in a murine model of cryptococcosis (Jung et al., 2009). It is important to note that there were within-group variations for iron source utilization capabilities with CCTP3, CCTP10 and CCTP13 of the high uptake group being outstanding for transferrin use while RCT7, RCT33 and IFN16 in the low uptake group being outstanding for heme utilization. These isolates are good candidates for studying the transferrin and heme utilization mechanisms.

Last but not the least we tested the isolates for their survival in whole blood from healthy donors. Both high and low uptake cryptococci exhibited relatively unhampered survival in whole blood, although the high uptake isolates showed significant (P = 0.01) resistance to killing by blood in the first 30 min of incubation compared to the low uptake isolates. We thus hypothesized that high uptake isolates associate quickly with blood phagocytes, particularly monocytes, which offer them protection from fungicidal proteins like complement. A flow cytometry analysis of cryptococci-phagocyte association showed a generally equal rate of association with monocytes and neutrophils by both high uptake and low uptake isolates. Interestingly, however, low uptake isolates seemed to associate better with both monocytes and neutrophils than did high uptake isolates (Figure 30 and 30). These observations suggest that the cryptococci-blood phagocyte association mechanism may be different

from that of tissue macrophages. The distinction between the easily and poorly phagocytosed cryptococci is most likely very important within the lungs, when *C. neoformans* first encounters alveolar macrophages. This encounter may subsequently define rates of dissemination with the high uptake isolates disseminating faster to the brain, suggesting that the rate of brain involvement may largely depend on the rate of pulmonary phagocytosis of cryptococci. This hypothesis could be tested in the murine inhalation model to confirm the dissemination rates and brain fungal burden in mice infected with high uptake and low uptake isolates.

6.0 Conclusion

Cryptococcal infection of the brain is the end result of a journey through hurdles imposed by the host. Entering the highly protected environment of the brain requires cryptococci to overcome barriers in the lung, circulatory system and, most significantly, the blood-brain barrier. Alveolar macrophages are key in the pulmonary response to cryptococci and the ability of cryptococci to survive and replicate inside these macrophages creates a path for transmission from the lung to systemic circulation. Cryptococci are endowed with protective strategies such as the production of capsule and melanin to downplay the antimicrobial activity of phagocytic cells such as monocytes and neutrophils as well as of complement proteins. At the brain gate, the blood-brain barrier, cryptococci can gain entry hidden inside phagocytes, by being engulfed directly by the brain microvascular endothelial cells or by inducing damage to tight junctions to pave the way between brain endothelial cells. Once in the brain, the fungus proliferates, resulting in devastating inflammation of the meninges and brain parenchyma (meningoencaphalitis). The fact that the probability of survival from cryptococcal meningoencephalitis is less than a half, even with treatment, makes improved diagnostic and therapeutic developments, as well as interventions focusing on the pulmonary and pre-brain systemic life of *C. neoformans*, critical in order to reduce mortality from this disease.

6.1 Future perspectives

Our current understanding of the underlying mechanisms in the pathogenesis of cryptococcosis largely stem from animal models of infection. Indeed through mammalian/non-mammalian and tissue culture models, various aspects of

cryptococcosis including pathogen virulence, manipulation of host immune response and penetration of blood brain barrier have been illustrated (Sabiiti et al., 2012). The challenge, however, is to what extent observations made in these models can explain what happens in the human host. For every infection, colonization, disease progression and clinical outcome are mutually modulated by interplay between pathogen and host factors, which makes it challenging to decipher the human host factors by studying the pathogen in a different host. Fortunately, over the past decade there has been an appreciable increase in clinical research on cryptococcosis and thus we envision that future research will see more clinical analysis, which will bridge the gap between laboratory models of infection and patient clinical parameters. Direct clinical analysis of samples and general underlying physiological parameters of patients will provide reference for observations made in laboratory models of infection.

Del Poeta and Casadevall have recently contextualized a series of major unanswered questions in cryptococcosis (Del Poeta and Casadevall, 2012), ranging from the nature of the infectious propagule to the possibility of predicting the likelihood of haematogenous dissemination to the brain. In addition, there remain critical unanswered questions about the behaviour of cryptococci in the environment. For instance, what are the nutritional requirements for cryptococcal growth in soil, pigeon excreta or on trees (Casadevall and Perfect, 1998; Chowdhary et al., 2012; Sorrell et al., 1996), and what is the nature of the relationship between plants and *Cryptococcus*? For instance Waikedere et al have shown that essential oils extracted from two species of Heartwood tree, *Callitris neocaledonica* and *C. sulcata* can inhibit growth of various human fungal pathogens including *C. neoformans*

(Waikedre et al., 2012). Thus research into understanding *C. neoformans* in its natural environment will be crucial in developing better control measures as well as identifying new anti-cryptococcal compounds.

In addition, understanding the molecular basis of the host-pathogen interaction will be crucial for effective management of cryptococcal disease as well as discovering novel therapeutic targets. Despite having relatively similar level of exposure to potentially *Cryptococcus* infested environments, not all immunosuppressed people develop cryptococcosis (Del Poeta and Casadevall, 2012). Identifying host (genetic) factors that underlie differences in susceptibility to cryptococcal infection is thus a major priority. Equally important will be pathogen transcriptomics and proteomics, especially of clinical isolates, to uncover virulence factors responsible for disease in different groups of patients.

The damage caused by cryptococcal meningoencaphalitis is in most cases irreparable with mortality reaching 100% in some cohorts even with antifungal treatment (Mwaba P. et al. , 2001). While rabbits have to be therapeutically immunosuppressed by repeated treatment with steroids for meningoencephalitis to take effect (Lee et al., 2010; Perfect et al., 1980; Rude et al., 2002), the effects of cryptococci in the human brain are equally devastating to both the immunodeficient and immunocompetent patients (Lee et al., 2011). To this end, the ultimate prize for the future will be to prevent, rather than cure, cryptococcal infections.
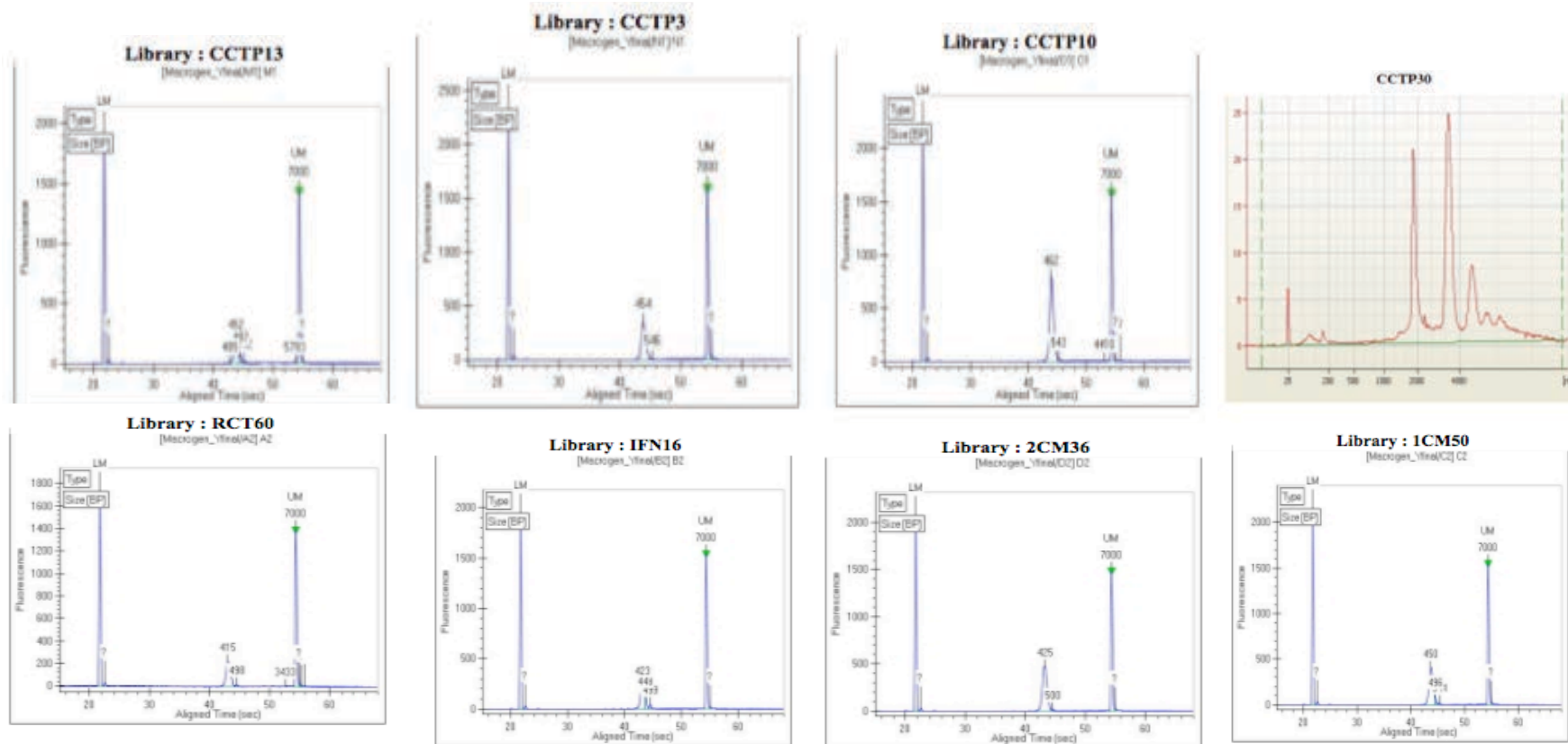
APPENDIX

Appendix 1: Melanisation scores

Isolate	Daily melanization score (Mean)															MR
	1	2	3	4	5	6	7	8	9	10	11	12	13	14	15	
CM20	0.5	1.5	2.3	3	3.5	3.75	3.8	4	4.5	4.8	5	5	5	5	5	0.56
CM24	0.5	2	3.5	4	4.5	4.75	5	5	5	5	5	5	5	5	5	1.15
CM36	0.8	2.5	3.3	3.3	3.25	3.5	4.5	4.5	5	5	5	5	5	5	5	0.67
CM50	0.8	2.5	3	3	3.5	3.75	3.8	4.25	4.8	5	5	5	5	5	5	0.595
CM52	0.5	1.5	2.8	3.8	4.25	4.5	4.8	4.75	5	5	5	5	5	5	5	0.86
CM64	0.8	1.8	3.8	4	4.25	4.5	4.8	5	5	5	5	5	5	5	5	0.86
CCTP2	0	0.3	1.3	2.2	3.3	4	4.5	4.8	5	5	5	5	5	5	5	0.71
CCTP3	0	1.8	3	4	4.5	4.8	4.8	5	5	5	5	5	5	5	5	1
CCTP10	0	0.8	2	3.1	4.3	4.6	4.8	5	5	5	5	5	5	5	5	0.83
CCTP12	0	0.2	1.3	2	2.7	4	4.5	4.8	5	5	5	5	5	5	5	0.71
CCTP13	0	0.8	1.8	3.2	4	4.5	4.6	5	5	5	5	5	5	5	5	0.83
CCTP25	0	0	0.2	0.5	1.3	2.2	2.5	3.2	3.3	3.8	4.3	4.5	4.5	4.5	4.8	0.42
CCTP26	0	0.3	0.6	1.4	2.1	3	3.6	3.9	4.3	4.5	4.9	5	5	5	5	0.5
CCTP29	0	0.3	0.7	2.3	3.5	3.8	4.7	5	5	5	5	5	5	5	5	0.42
CCTP30	1.5	2.9	3.6	4.3	4.8	4.9	5	5	5	5	5	5	5	5	5	1
CCTP49	0.5	1.3	2.5	2.8	3.5	4	4	4	4.3	4.3	4.5	4.5	4.5	4.8	5	0.48
CCTP52	0.5	1.8	2.3	3	3.25	3.5	3.8	4	4	4.3	4.5	4.5	4.5	5	5	0.48
IFN1	0	0.2	0.3	0.8	1.7	2.3	2.8	3.3	3.8	3.8	4	4.3	4.3	4.3	4.8	0.33
IFN2	0.2	0.5	0.8	1.5	2.2	2.5	2.8	3.8	4.2	4.7	5	5	5	5	5	0.5
IFN4	0.5	2.5	3.5	3.6	4.3	4.5	4.8	4.8	4.8	5	5	5	5	5	5	0.83
IFN5	0	0.2	0.5	0.7	0.8	1.2	2	2.3	3.3	3.5	4.2	4.3	4.7	4.8	4.8	0.42
IFN6	0	0	0.3	1.3	2	2.7	3.7	3.7	3.7	3.8	4.2	4.5	4.5	4.7	4.8	0.71
IFN8	0.2	1.8	3.3	3.5	4.2	4.3	4.7	4.8	4.8	5	5	5	5	5	5	0.71
IFN9	0	0.3	2	2.5	3.2	3.6	4.1	4.2	4.3	4.3	4.7	4.8	4.8	5	5	0.46
IFN10	0	0.3	0.8	1.8	3.1	3.7	4	4.7	4.7	4.7	4.8	5	5	5	5	0.63
IFN11	0	0.2	1	1.5	2.7	3.7	4.5	4.8	5	5	5	5	5	5	5	0.71
IFN12	0	0.2	0.5	1.2	1.5	1.8	2.2	2.7	3.3	3.7	3.8	4.2	4.3	4.3	4.7	0.5
IFN15	0	1	1.7	2.3	3	3.7	4.2	4.7	4.8	5	5	5	5	5	5	0.63
IFN16	0.2	0.5	1.2	1.7	2.3	2.3	2.7	2.8	3.5	3.7	4	4.3	4.7	4.7	4.7	0.39
IFN17	0.2	1.3	2.7	3.3	3.8	4.2	4.2	4.5	4.7	5	5	5	5	5	5	0.63
IFN18	0	0.7	1.7	2.7	3.5	3.8	4	4.5	4.7	4.7	5	5	5	5	5	0.63
IFN19	0	0.2	0.7	1.3	1.7	2.2	2.7	3.8	3.8	4	4.5	5	5	5	5	0.455
IFN24	0.2	0.2	2.3	3.3	4	4.8	5	5	5	5	5	5	5	5	5	0.83
RCT3	0	0.5	1.5	2.7	3.2	4	4.3	4.7	4.7	5	5	5	5	5	5	0.63
RCT6	0.5	1.8	2.8	3	3.5	3.75	4.3	4.5	4.8	5	5	5	5	5	5	0.63
RCT7	0	0.3	1.2	1.5	2.3	3	3.2	3.5	4	4	4.2	4.7	4.8	4.8	5	0.42
RCT21	0.5	1.5	3.3	4	4	4.5	4.5	4.5	5	5	5	5	5	5	5	0.83
RCT24	0	0.2	0.7	1.8	3.3	4.3	4.7	4.8	5	5	5	5	5	5	5	0.71
RCT33	0	0.3	1	1.3	2.2	2.7	3.2	3.5	3.67	3.8	4.2	4.7	4.8	5	5	0.39
RCT36	0	1	2	2.7	3.5	4	4.3	4.8	4.8	5	5	5	5	5	5	0.63
RCT44	0.2	1.8	3.5	4.7	4.8	5	5	5	5	5	5	5	5	5	5	1.3
RCT50	0	0.3	1.7	2	2.3	3.2	3.7	3.8	4.3	4.7	4.8	4.8	4.4	5	5	0.5
RCT51	0	0	0.7	1.3	2.1	3.2	3.5	4	4.2	4.7	4.7	4.8	4.8	4.8	5	0.5
RCT52	0	0.5	1.3	1.7	2.7	3.3	3.8	4.2	4.3	4.7	5	5	5	5	5	0.5
RCT54	0.5	1.8	3.5	3.8	4	4.5	4.5	4.75	5	5	5	5	5	5	5	0.83
RCT55	0	0.5	1.5	2	2.7	3	3	3.7	4	4.3	4.7	4.7	4.8	5	5	0.46
RCT60	0.2	1.2	1.8	2.3	2.8	3.5	3.7	4	4.5	4.8	4.8	4.8	4.8	5	5	0.55
H99	0.2	3.5	4.7	5	5	5	5	5	5	5	5	5	5	5	5	1.67
B3501	0	0	0.17	0.5	1.33	2.17	3.33	4.33	4.83	5	5	5	5	5	5	0.53

The red and blue coloured numbers are melanisation rates of H99 (laboratory reference strain) and RCT44 (highest MR in the set of clinical isolates) respectively. Like in the low iron medium growth phenotype, strain H99 again shows remarkably higher rate of melanisation than the clinical isolates. Scores are mean of 3 repeats for CCTP and RCT isolates and 2 repeats of CM isolates.

Appendix 2: The bioanalysis results of RNA extracts before RNA sequencing

Appendix 2A: Graphs showing the 18s and 28s picks of RNA samples determined by the Bioanalyzer. The first pick on the left side in all graphs represents the ladder. 2CM36 = CM36, 1CM50 = CM50.

	Library name	Sample name	Library type	Volume (μL)	Conc. (ng/μL)	Size (bp)	RIN	Result
1	CCTP13	CCTP13	RNA library	60	49	452	9.7	Pass
2	CCTP3	CCTP3	RNA library	60	56	454	9.8	Pass
3	CCTP10	CCTP10	RNA library	60	62	464	9.6	Pass
4	CCTP30	CCTP30	RNA library	30	101	ND	9.6	Pass
5	RCT60	RCT60	RNA library	60	62	415	8.4	Pass
6	IFN16	IFN16	RNA library	60	56	423	9.5	Pass
7	CM36	CM36	RNA library	60	98	450	9.8	Pass
8	CM50	CM50	RNA library	60	43	425	9.4	Pass
9	H99	H99	RNA library	60	44	464	9.5	Pass

Appendix 2B: The quantity and RNA integrity (RIN) of the RNA samples.

Appendix 3: Growth rates in low iron and rich media

Isolate	Growth rate on different media			
	Lim	**Transferrin**	**Heme**	**YPD**
CCTP2	-0.0066	0.2612	0.0958	0.7154
CCTP3	0.2064	0.43335	-0.1353	0.6775
CCTP10	-0.0211	0.6096	-0.1476	0.6894
CCTP13	0.0213	0.5707	0.06	0.7247
CCTP30	0.03857	0.0961	-0.0213	0.3324
H99	0.5643	0.5351	0.6861	0.3499
RCT7	0.1589	0.3776	0.1935	0.4124
RCT33	0.1646	0.2014	-0.02003	0.6144
RCT60	-0.224	-0.2311	-0.0374	0.1772
IFN16	0.3041	0.2427	0.30275	0.3935
CM36	-0.1355	-0.0405	0.0082	0.1636
CM50	-0.17	-0.2125	0.3035	0.3804

Appendix 4: Non-grouped plot of percentage association of cryptococci with monocytes in whole blood
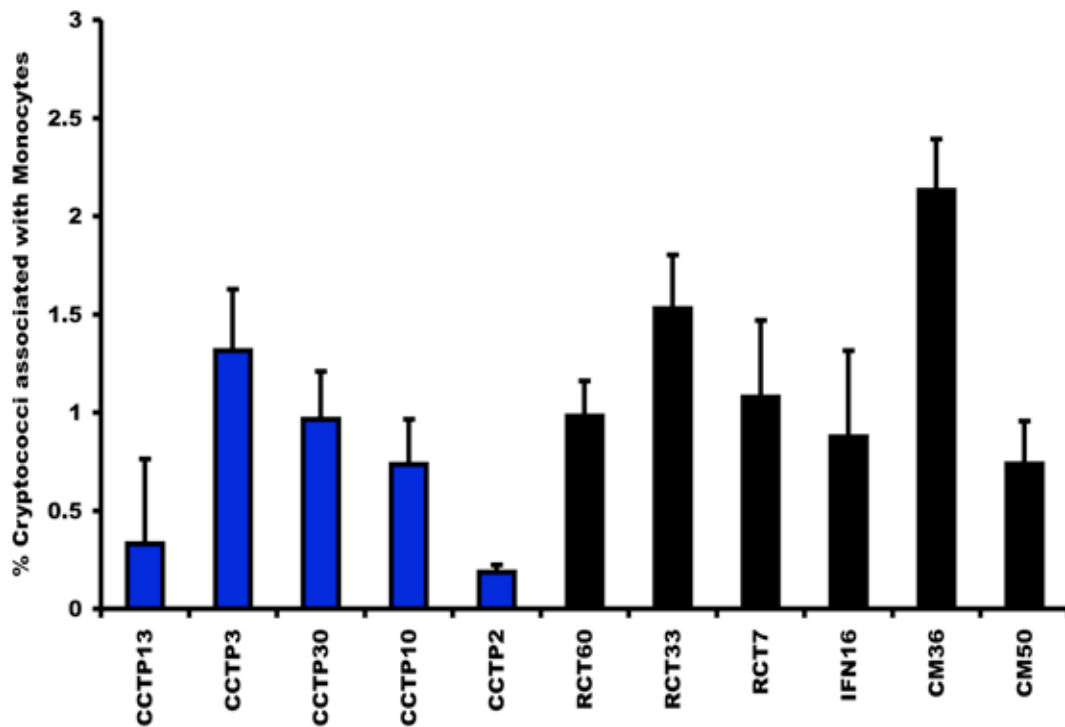
Fresh whole blood from healthy donors was incubated with FITC stained cryptococci (10^4 cells per 1ml of whole blood) for 60min. By flow cytometry the cryptococci associated with monocytes were determined using forward and side scatter. Unlike macrophages, there was generally no difference between high (blue bars) and low (black bars) uptake isolates' association with monocytes in whole blood. Error bars are standard error of the mean (n = 4 donors).

Appendix 5: Non-grouped plot of percentage association of cryptococci with neutrophils in whole blood
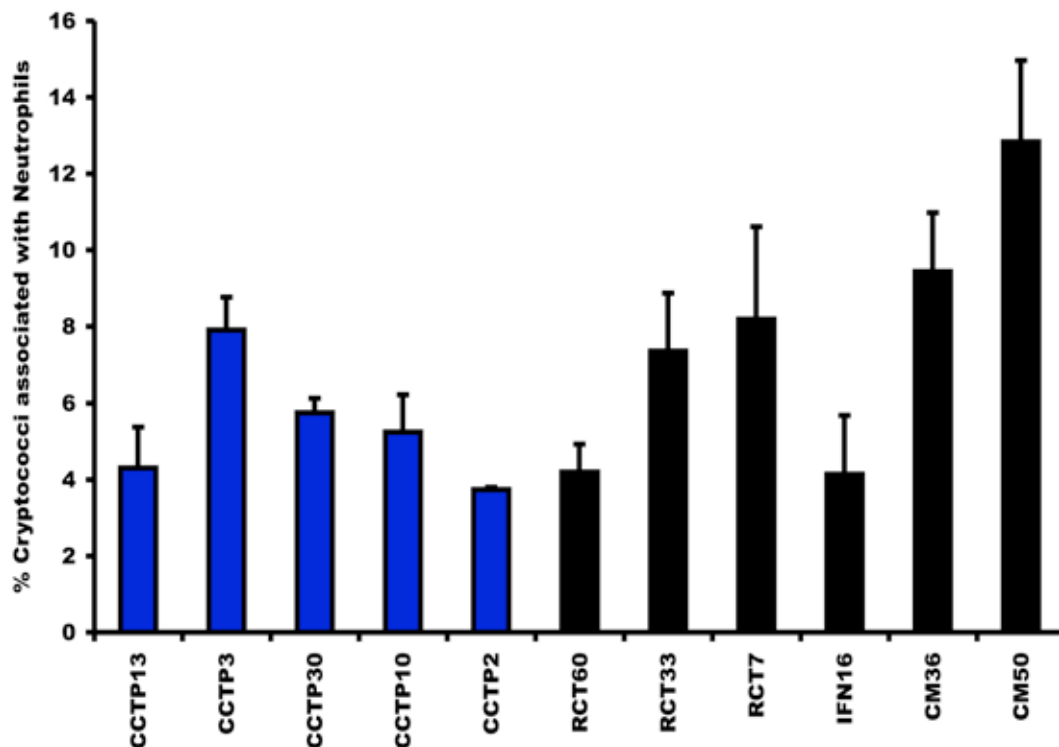
Fresh whole blood from five healthy donors was incubated with FITC stained cryptococci (10^4 cells per 1ml of whole blood) for 60min. By flow cytometry the cryptococci associated with monocytes were determined using forward and side scatter. As with monocytes, there was generally no difference between high (blue bars) and low (black bars) isolates' association with neutrophils in whole blood. Error bars are standard error of the mean (n = 5 donors).

Appendix 6: Gene expression comparison between clinical isolates and reference strain H99

Comparison	Statistical method	Informative genes	Significant genes	UP_all	UP_2-4	UP_ gte4	Down_all	Down_ 2-4	Down_ gte
Low vs High	QuasiSeq	6846	8	3	1	2	5	2	3
CCTP10 vs H99	Fisher's exact test	6838	933	178	136	42	755	574	181
CCTP13 vs H99	Fisher's exact test	6834	1249	1124	977	147	125	69	56
CCTP3 vs H99	Fisher's exact test	6849	776	482	349	133	294	240	54
CCTP30 vs H99	Fisher's exact test	6849	1343	347	269	78	996	790	206
CM50 vs H99	Fisher's exact test	6837	1421	194	151	43	1227	976	251
CM36 vs H99	Fisher's exact test	6834	1353	319	270	49	1034	760	274
IFN16 vs H99	Fisher's exact test	6844	2311	1085	880	205	1226	926	300
RCT60 vs H99	Fisher's exact test	6845	1602	572	448	124	1030	860	170

The overall differentially expressed genes between the Low and High uptake isolates (green row). High uptake (Orange highlighted rows) and low uptake (Yellow rows) isolates pairwise comparisons with H99 respectively. UP_all = the number of genes exhibiting upregulated profile in high uptake isolates, UP_2-4 = number genes exhibiting 2-4 fold upregulated profile in high uptake group relative to low uptake group, UP_gte4 = number genes exhibiting 4 fold upregulated profile high uptake group relative to low uptake group, DOWN_all = number genes exhibiting

downregulated profile high uptake group relative to low uptake group, DOWN_2-4 = number genes exhibiting 2-4 fold down regulated profile in high uptake isolates relative to low uptake group, and DOWN_gte4 = number genes exhibiting 4 fold down regulated profile in high uptake isolates relative to low uptake group.

Appendix 7: List of isolate charcteristics grouped by median uptake by macrophages

Isolate	Uptake	IPR	Mel. Rate	Cap. Diam.	Mating type	MLST	VN type
CM50	93	5.8	0.595	2.5057	α	6	VNI
CM36	130	3.1	0.67	1.51404	α	6	VNI
CCTP52	210	2.4	0.475	2.03923	α	52	VNII
IFN16	215	3.6	0.39	1.81586	ND	ND	ND
RCT7	235	4.0	0.42	1.48954	α	51	VNI
RCT33	248	3.9	0.39	1.66877	α	51	VNI
CM64	253	3.9	0.855	1.7632	α	6	VNI
IFN18	258	2.3	0.63	2.15289	ND	ND	ND
IFN10	268	3.1	0.63	2.27428	ND	ND	ND
IFN2	283	2.6	0.5	2.77378	ND	ND	ND
IFN5	285	3.2	0.42	2.20404	ND	ND	ND
IFN4	293	2.9	0.83	3.63826	ND	ND	ND
IFN8	300	3.6	0.71	2.43963	ND	ND	ND
RCT54	308	2.6	0.83	1.87994	α	75	VNI
RCT21	310	2.6	0.83	2.35467	α	56	VNB
IFN24	355	3.5	0.83	1.91326	ND	ND	ND
CM24	360	2.8	1.15	1.83635	α	6	VNI
RCT3	380	1.6	0.63	1.85091	α	51	VNI
IFN11	380	2.4	0.71	4.15688	ND	ND	ND
RCT36	388	2.8	0.63	1.32467	ND	Diploid	VNI
CCTP49	390	2.7	0.48	2.15618	α	66	VNII
CCTP29	398	3.7	0.42	1.36735	α	51	VNI
IFN6	418	2.9	0.71	2.22468	ND	ND	ND
RCT6	420	2.5	0.63	1.91132	α	6	VNI
CM20	423	2.8	0.56	2.33921	α	6	VNI
RCT60	423	3.0	0.55	1.46208	α	76	VNI
CCTP25	445	2.3	0.42	2.44792	α	51	VNI
IFN17	445	3.7	0.63	2.85066	ND	ND	ND
IFN19	453	2.5	0.455	1.91361	ND	ND	ND
IFN1	535	3.3	0.33	1.83685	ND	ND	ND
IFN15	548	3.1	0.63	2.34907	ND	ND	ND
RCT50	588	2.9	0.5	2.03683	α	74	VNI
RCT24	590	2.8	0.71	1.89935	α	1	VNI
RCT52	590	2.6	0.5	1.4045	α	32	VNI
CCTP12	593	2.6	0.71	3.01612	α	58	VNI
CCTP26	593	1.7	0.61	2.70432	α	51	VNI
RCT44	610	2.9	1.3	1.40128	α	54	VNI
IFN12	615	2.5	0.5	1.91023	ND	ND	ND
RCT51	645	2.4	0.5	1.63739	α	23	VNI
RCT55	653	3.2	0.46	1.19248	α	51	VNI
CM52	700	1.8	0.855	1.15001	α	6	VNI
IFN9	763	2.9	0.46	2.54598	ND	ND	ND
CCTP2	800	2.4	0.71	1.99937	α	37	VNI
CCTP10	923	2.3	0.83	1.2151	α	57	VNI
CCTP30	968	1.4	1	1.35794	α	5	VNI
CCTP3	1223	2.0	1	1.23091	α	5	VNI
CCTP13	1383	2.1	0.83	1.18299	α	5	VNI

The table represents all the 47 isolates with determined phenotypes (Uptake, IPR, melanisation rate, Mel. Rate, capsule diameter (Cap. Diam) divided into two groups by the Median (420) of uptake. Upper division is (yellow) is uptake below 420

cryptococci/µl lysate whilst the lower division (orange) are those whose rate of uptake is higher than 420 cryptococci/µl lysate. Interestingly the three highest uptake (CCTP3, CCTP30 and CCTP13) isolates belong to same MLST 5 while the two lowest uptake isolates (CM36 and CM50) are both MLST 6.

References

Abraham, M., Matthews, M.S. and John, T.J. (1997) Environmental isolation of *Cryptococcus neoformans var. neoformans* from Vellore. **Indian J Med Res**, 106: 458-459.

Alvarez, M. and Casadevall, A. (2007) Cell-to-cell spread and massive vacuole formation after *Cryptococcus neoformans* infection of murine macrophages. **BMC Immunol**, 8: 16.

Alvarez, M. and Casadevall, A. (2006) Phagosome extrusion and host-cell survival after *Cryptococcus neoformans* phagocytosis by macrophages. **Curr Biol**, 16 (21): 2161-2165.

Avraham, H.K., Jiang, S., Lee, T.H., et al. (2004) HIV-1 Tat-mediated effects on focal adhesion assembly and permeability in brain microvascular endothelial cells. **J Immunol**, 173 (10): 6228-6233.

Baker, L.G., Specht, C.A. and Lodge, J.K. (2009) Chitinases are essential for sexual development but not vegetative growth inCryptococcus neoformans. **Eukaryot cell**, 8 (11): 1692-705.

Balankura, P. (1974) Isolation of *Cryptococcus neoformans* from soil contaminated with pigeon droppings in Bangkok. **J Med Assoc Thai**, 57 (3): 158-159.

Bean, A.G., Roach, D.R., Briscoe, H., et al. (1999) Structural deficiencies in granuloma formation in TNF gene-targeted mice underlie the heightened susceptibility to aerosol *Mycobacterium tuberculosis* infection, which is not compensated for by lymphotoxin. **J Immunol**, 162 (6): 3504-3511.

Bicanic, T., Brouwer, A.E., Meintjes, G., et al. (2009a) Relationship of cerebrospinal fluid pressure, fungal burden and outcome in patients with cryptococcal meningitis undergoing serial lumbar punctures. **AIDS**, 23 (6): 701-706.

Bicanic, T. and Harrison, T.S. (2005) Cryptococcal meningitis. **Br Med Bull**, 72: 99-118.

Bicanic, T., Meintjes, G., Wood, R., et al. (2007) Fungal burden, early fungicidal activity, and outcome in cryptococcal meningitis in antiretroviral-naive or antiretroviral-experienced patients treated with amphotericin B or fluconazole. **Clin Infect Dis**, 45 (1): 76-80.

Bicanic, T., Muzoora, C., Brouwer, A.E., et al. (2009b) Independent association between rate of clearance of infection and clinical outcome of HIV-associated cryptococcal meningitis: analysis of a combined cohort of 262 patients. **Clin Infect Dis**, 49 (5): 702-709.

Bicanic, T., Wood, R., Meintjes, G., et al. (2008) High-dose amphotericin B with flucytosine for the treatment of cryptococcal meningitis in HIV-infected patients: a randomized trial. **Clin Infect Dis**, 47 (1): 123-130.

Boekhout, T., van Belkum, A., Leenders, A.C., et al. (1997) Molecular typing of *Cryptococcus neoformans*: taxonomic and epidemiological aspects. **Int J Syst Bacteriol**, 47 (2): 432-442.

Bolanos, B. and Mitchell, T.G. (1989a) Phagocytosis and killing of *Cryptococcus neoformans* by rat alveolar macrophages in the absence of serum. **J Leukoc Biol**, 46 (6): 521-528.

Bolanos, B. and Mitchell, T.G. (1989b) Phagocytosis of *Cryptococcus neoformans* by rat alveolar macrophages. **J Med Vet Mycol**, 27 (4): 203-217.

Bottone, E.J., Toma, M., Johansson, B.E., et al. (1986) Poorly encapsulated *Cryptococcus neoformans* from patients with AIDS. I: Preliminary observations. **AIDS Res**, 2 (3): 211-218.

Bottone, E.J., Toma, M., Johansson, B.E., et al. (1985) Capsule-deficient *Cryptococcus neoformans* in AIDS patients. **Lancet**, 1 (8425): 400.

Botts, M.R., Giles, S.S., Gates, M.A., et al. (2009) Isolation and characterization of *Cryptococcus neoformans* spores reveal a critical role for capsule biosynthesis genes in spore biogenesis. **Eukaryot Cell**, 8 (4): 595-605.

Boulware, D.R., Bonham, S.C., Meya, D.B., et al. (2010) Paucity of initial cerebrospinal fluid inflammation in cryptococcal meningitis is associated with subsequent immune reconstitution inflammatory syndrome. **J Infect Dis**, 202 (6): 962-970.

Boven, L.A., Middel, J., Verhoef, J., et al. (2000) Monocyte infiltration is highly associated with loss of the tight junction protein zonula occludens in HIV-1-associated dementia. **Neuropathol Appl Neurobiol**, 26 (4): 356-360.

Bovers, M., Hagen, F. and Boekhout, T. (2008) Diversity of the *Cryptococcus neoformans-Cryptococcus gattii* species complex. **Rev Iberoam Micol**, 25 (1): S4-12.

Brouwer, A.E., Rajanuwong, A., Chierakul, W., et al. (2004) Combination antifungal therapies for HIV-associated cryptococcal meningitis: a randomised trial. **Lancet**, 363 (9423): 1764-1767.

Byrnes, E.J. and Heitman, J. (2009) *Cryptococcus gattii* outbreak expands into the Northwestern United States with fatal consequences. **F1000 Biol Rep**, 1: 62.

Callejas, A., Ordonez, N., Rodriguez, M.C., et al. (1998) First isolation of *Cryptococcus neoformans var. gattii*, serotype C, from the environment in Colombia. **Med Mycol**, 36 (5): 341-344.

Casadevall, A., Cassone, A., Bistoni, F., et al. (1998) Antibody and/or cell-mediated immunity, protective mechanisms in fungal disease: an ongoing dilemma or an unnecessary dispute? **Med Mycol**, 36 (Suppl 1): 95-105.

Casadevall, A., Freundlich, L.F., Marsh, L., et al. (1992) Extensive allelic variation in *Cryptococcus neoformans*. **J Clin Microbiol**, 30 (5): 1080-1084.

Casadevall, A. and Perfect, J.R. (1998) *Cryptococcus neoformans*. Washington, DC: ASM press.

Casadevall, A., Rosas, A.L. and Nosanchuk, J.D. (2000) Melanin and virulence in *Cryptococcus neoformans*. **Curr Opin Microbiol**, 3 (4): 354-358.

Chakrabarti, A., Jatana, M., Kumar, P., et al. (1997) Isolation of *Cryptococcus neoformans var. gattii* from Eucalyptus camaldulensis in India. **J Clin Microbiol**, 35 (12): 3340-3342.

Chang, Y.C., Bien, C.M., Lee, H., et al. (2007) Sre1p, a regulator of oxygen sensing and sterol homeostasis, is required for virulence in *Cryptococcus neoformans*. **Mol Microbiol**, 64 (3): 614-629.

Chang, Y.C., Stins, M.F., McCaffery, M.J., et al. (2004a) Cryptococcal yeast cells invade the central nervous system via transcellular penetration of the blood-brain barrier. **Infect Immun**, 72 (9): 4985-4995.

Chang, Y.C., Wang, Z., Flax, L.A., et al. (2011) Glycosaminoglycan binding facilitates entry of a bacterial pathogen into central nervous systems. **PLoS Pathog**, 7 (6): e1002082.

Chang, Y.C., Wright, L.C., Tscharke, R.L., et al. (2004b) Regulatory roles for the homeodomain and C2H2 zinc finger regions of *Cryptococcus neoformans* Ste12alphap. **Mol Microbiol**, 53 (5): 1385-1396.

Charlier, C., Chretien, F., Baudrimont, M., et al. (2005a) Capsule structure changes associated with *Cryptococcus neoformans* crossing of the blood-brain barrier. **Am J Pathol**, 166 (2): 421-432.

Charlier, C., Chretien, F., Lortholary, O., et al. (2005b) [Early capsule structure changes associated with *Cryptococcus neoformans* crossing of the blood-brain barrier]. **Med Sci (Paris)**, 21 (8-9): 685-687.

Charlier, C., Nielsen, K., Daou, S., et al. (2009) Evidence of a role for monocytes in dissemination and brain invasion by *Cryptococcus neoformans*. **Infect Immun**, 77 (1): 120-127.

Chau, T.T., Mai, N.H., Phu, N.H., et al. (2010) A prospective descriptive study of cryptococcal meningitis in HIV uninfected patients in Vietnam - high prevalence of Cryptococcus neoformans var grubii in the absence of underlying disease. **BMC Infect Dis**, 10: 199.

Chen, L.C., Blank, E.S. and Casadevall, A. (1996) Extracellular proteinase activity of *Cryptococcus neoformans*. **Clin Diagn Lab Immunol**, 3 (5): 570-574.

Chen, S.C., Muller, M., Zhou, J.Z., et al. (1997) Phospholipase activity in *Cryptococcus neoformans*: a new virulence factor? **J Infect Dis**, 175 (2): 414-420.

Chen, S.H., Stins, M.F., Huang, S.H., et al. (2003) *Cryptococcus neoformans* induces alterations in the cytoskeleton of human brain microvascular endothelial cells. **J Med Microbiol**, 52: 961-970.

Chowdhary, A., Rhandhawa, H.S., Prakash, A., et al. (2012) Environmental prevalence of Cryptococcus neoformans and *Cryptococcus gattii* in India: an update. **Crit Rev Microbiol**, 38 (1): 1-16.

Chretien, F., Lortholary, O., Kansau, I., et al. (2002) Pathogenesis of cerebral *Cryptococcus neoformans* infection after fungemia. J Infect Dis, 186 (4): 522-530.

Chun, C.D., Brown, J.C. and Madhani, H.D. (2011) A major role for capsule-independent phagocytosis-inhibitory mechanisms in mammalian infection by *Cryptococcus neoformans*. **Cell Host Microbe**, 9 (3): 243-251.

Chun, C.D. and Madhani, H.D. (2010) Ctr2 links copper homeostasis to polysaccharide capsule formation and phagocytosis inhibition in the human fungal pathogen *Cryptococcus neoformans*. **PloS One**, 5 (9): e12503.

Correale, J. and Villa, A. (2009) Cellular Elements of the Blood-Brain Barrier. **Neurochem Res**, 34: 2067-2077.

Cox, G.M., McDade, H.C., Chen, S.C., et al. (2001) Extracellular phospholipase activity is a virulence factor for *Cryptococcus neoformans*. **Mol Microbiol**, 39 (1): 166-175.

Cox, G.M., Mukherjee, J., Cole, G.T., et al. (2000) Urease as a virulence factor in experimental cryptococcosis. **Infect Immun**, 68 (2): 443-448.

Datta, K., Bartlett, K.H., Baer, R., et al. (2009) Spread of *Cryptococcus gattii* into Pacific Northwest region of the United States. **Emerg Infect Dis**, 15 (8): 1185-1191.

De Jesus, M., Chow, S.K., Cordero, R.J., et al. (2010) Galactoxylomannans from *Cryptococcus neoformans varieties neoformans* and *grubii* are structurally and antigenically variable. **Eukaryotic cell**, 9 (7): 1018-1028.

Del Poeta, M. and Casadevall, A. (2012) Ten challenges on *Cryptococcus* and cryptococcosis. **Mycopathologia**, 173 (5-6): 303-310.

Dietrich, J.B. (2002) The adhesion molecule ICAM-1 and its regulation in relation with the blood-brain barrier. **J Neuroimmunol**, 128 (1-2): 58-68.

Djordjevic, J.T. (2010) Role of phospholipases in fungal fitness, pathogenicity, and drug development - lessons from *Cryptococcus neoformans*. **Front Microbiol**, 1: 125.

Drevets, D.A. (1999) Dissemination of *Listeria monocytogenes* by infected phagocytes. **Infect Immun**, 67 (7): 3512-3517.

Drevets, D.A. and Leenen, P.J. (2000) Leukocyte-facilitated entry of intracellular pathogens into the central nervous system. **Microbes Infect**, 2 (13): 1609-1618.

Drevets, D.A., Leenen, P.J. and Greenfield, R.A. (2004) Invasion of the central nervous system by intracellular bacteria. **Clin Microbiol Rev**, 17 (2): 323-347.

Dromer, F., Ronin, O. and Dupont, B. (1992) Isolation of *Cryptococcus neoformans* var. gattii from an Asian patient in France: evidence for dormant infection in healthy subjects. **J Med Vet Mycol**, 30 (5): 395-397.

Dromer, F., Salamero, J., Contrepois, A., et al. (1987) Production, characterization, and antibody specificity of a mouse monoclonal antibody reactive with *Cryptococcus neoformans* capsular polysaccharide. **Infect Immun**, 55 (3): 742-748.

Dwork, A.J., Schon, E.A. and Herbert, J. (1988) Nonidentical distribution of transferrin and ferric iron in human brain. **Neuroscience**, 27 (1): 333-345.

Eckert, T.F. and Kozel, T.R. (1987) Production and characterization of monoclonal antibodies specific for *Cryptococcus neoformans* capsular polysaccharide. **Infect Immun**, 55 (8): 1895-1899.

Emery, H.S., Shelburne, C.P., Bowman, J.P., et al. (1994) Genetic study of oxygen resistance and melanization in *Cryptococcus neoformans*. **Infect Immun**, 62 (12): 5694-5697.

Fan, W., Kraus, P.R., Boily, M.J., et al. (2005) *Cryptococcus neoformans* gene expression during murine macrophage infection. **Eukaryot Cell**, 4 (8): 1420-1433.

Feldmesser, M., Kress, Y. and Casadevall, A. (2001a) Dynamic changes in the morphology of *Cryptococcus neoformans* during murine pulmonary infection. **Microbiology**, 147: 2355-2365.

Feldmesser, M., Tucker, S. and Casadevall, A. (2001b) Intracellular parasitism of macrophages by *Cryptococcus neoformans*. **Trends Microbiol**, 9 (6): 273-278.

Fortes, S.T., Lazera, M.S., Nishikawa, M.M., et al. (2001) First isolation of Cryptococcus neoformans var. gattii from a native jungle tree in the Brazilian Amazon rainforest. **Mycoses**, 44 (5): 137-140.

Franzot, S.P., Fries, B.C., Cleare, W., et al. (1998) Genetic relationship between *Cryptococcus neoformans* var. neoformans strains of serotypes A and D. **J Clin Microbiol**, 36 (8): 2200-2204.

Franzot, S.P., Salkin, I.F. and Casadevall, A. (1999) Cryptococcus neoformans var. grubii: separate varietal status for *Cryptococcus neoformans* serotype A isolates. J **Clin Microbiol**, 37 (3): 838-840.

Fries, B.C., Taborda, C.P., Serfass, E., et al. (2001) Phenotypic switching of *Cryptococcus neoformans* occurs in vivo and influences the outcome of infection. **J Clin Invest**, 108 (11): 1639-1648.

Ganendren, R., Carter, E., Sorrell, T., et al. (2006) Phospholipase B activity enhances adhesion of *Cryptococcus neoformans* to a human lung epithelial cell line. **Microbes Infect**, 8 (4): 1006-1015.

Garcia-Hermoso, D., Janbon, G. and Dromer, F. (1999) Epidemiological evidence for dormant *Cryptococcus neoformans* infection. **J Clin Microbiol**, 37 (10): 3204-3209.

Garcia-Rodas, R. and Zaragoza, O. (2012) Catch me if you can: phagocytosis and killing avoidance by *Cryptococcus neoformans*. **FEMS Immunol Med Microbiol**, 64 (2): 147-161.

Geunes-Boyer, S., Beers, M.F., Perfect, J.R., et al. (2012) Surfactant Protein D facilitates *Cryptococcus neoformans* infection. **Infect Immun**, 80 (7): 2444-53.

Ghannoum, M.A. (2000) Potential role of phospholipases in virulence and fungal pathogenesis. **Clin Mcrobiol Rev**, 13 (1): 122-43.

Giles, S.S., Dagenais, T.R., Botts, M.R., et al. (2009) Elucidating the pathogenesis of spores from the human fungal pathogen *Cryptococcus neoformans*. **Infect Immun**, 77 (8): 3491-3500.

Goldman, D., Song, X., Kitai, R., et al. (2001a) *Cryptococcus neoformans* induces macrophage inflammatory protein 1alpha (MIP-1alpha) and MIP-1beta in human microglia: role of specific antibody and soluble capsular polysaccharide. **Infect Immun**, 69 (3): 1808-1815.

Goldman, D.L., Khine, H., Abadi, J., et al. (2001b) Serologic evidence for Cryptococcus neoformans infection in early childhood. **Pediatrics**, 107 (5): E66.

Goldman, D.L., Lee, S.C., Mednick, A.J., et al. (2000) Persistent *Cryptococcus neoformans* pulmonary infection in the rat is associated with intracellular parasitism, decreased inducible nitric oxide synthase expression, and altered antibody responsiveness to cryptococcal polysaccharide. **Infect Immun**, 68 (2): 832-838.

Goodison, S., Urquidi, V. and Tarin, D. (1999) CD44 cell adhesion molecules. **Mol Pathol**, 52 (4): 189-196.

Gordon, S.B. and Read, R.C. (2002) Macrophage defences against respiratory tract infections. **Br Med Bull**, 61: 45-61.

Guerrero, A., Jain, N., Goldman, D.L., et al. (2006) Phenotypic switching in *Cryptococcus neoformans*. **Microbiology**, 152 3-9.

Heitman Joseph, Kozel Thomas R, Kwon-Chung Kyung J, Perfect John R, Casadevall Arturo (ed.) (2010) *Cryptococcus*: From Human Pathogen to Model Yeast. Washington, DC.: ASM Press.

Hernandez, A.D. (1989) Cutaneous cryptococcosis. **Dermatol Clin**, 7 (2): 269-274.

Hu, G., Cheng, P.Y., Sham, A., et al. (2008) Metabolic adaptation in *Cryptococcus neoformans* during early murine pulmonary infection. **Mol Microbiol**, 69 (6): 1456-1475.

Hu, G., Wang, J., Choi, J., et al. (2011) Variation in chromosome copy number influences the virulence of *Cryptococcus neoformans* and occurs in isolates from AIDS patients. **BMC Genomics**, 12: 526.

Huang, S.H., Long, M., Wu, C.H., et al. (2011) Invasion of *Cryptococcus neoformans* into Human Brain Microvascular Endothelial Cells Is Mediated through the Lipid Rafts-Endocytic Pathway via the Dual Specificity Tyrosine Phosphorylation-regulated Kinase 3 (DYRK3). **J Biol Chem**, 286 (40): 34761-34769.

Ibrahim, A.S., Filler, S.G., Alcouloumre, M.S., et al. (1995) Adherence to and damage of endothelial cells by *Cryptococcus neoformans* in vitro: role of the capsule. **Infect Immun**, 63 (11): 4368-4374.

Jacobson, E.S. and Tinnell, S.B. (1993) Antioxidant function of fungal melanin. **J Bacteriol,** 175 (21): 7102-7104.

Jain, N., Guerrero, A. and Fries, B.C. (2006a) Phenotypic switching and its implications for the pathogenesis of *Cryptococcus neoformans*. **FEMS Yeast Res**, 6 (4): 480-488.

Jain, N., Li, L., McFadden, D.C., et al. (2006b) Phenotypic switching in a *Cryptococcus neoformans var. gattii* strain is associated with changes in virulence and promotes dissemination to the central nervous system. **Infect Immun**, 74 (2): 896-903.

Jain, N., Wickes, B.L., Keller, S.M., et al. (2005) Molecular epidemiology of clinical *Cryptococcus neoformans* strains from India. **J Clin Microbiol**, 43 (11): 5733-5742.

Jarvis, J.N., Boulle, A., Loyse, A., et al. (2009) High ongoing burden of cryptococcal disease in Africa despite antiretroviral roll out. **AIDS**, 23 (9): 1182-1183.

Johnston, S.A. and May, R.C. (2010) The human fungal pathogen *Cryptococcus neoformans* escapes macrophages by a phagosome emptying mechanism that is inhibited by Arp2/3 complex-mediated actin polymerisation. **PLoS Pathog**, 6 (8): e1001041.

Jong, A., Wu, C.H., Shackleford, G.M., et al. (2008) Involvement of human CD44 during *Cryptococcus neoformans* infection of brain microvascular endothelial cells. **Cell Microbiol**, 10 (6): 1313-1326.

Jong, A.Y., Stins, M.F., Huang, S.H., et al. (2001) Traversal of *Candida albicans* across human blood-brain barrier in vitro. **Infect Immun**, 69 (7): 4536-4544.

Jong, A.Y., Wu, C.H., Jiang, S., et al. (2007) HIV-1 gp41 ectodomain enhances Cryptococcus neoformans binding to HBMEC. **Biochem Biophys Res Commun**, 356 (4): 899-905.

Jung, W.H., Hu, G., Kuo, W., et al. (2009) Role of ferroxidases in iron uptake and virulence of Cryptococcus neoformans. **Eukaryotic cell,** 8 (10): 1511-1520.

Jung, W.H. and Kronstad, J.W. (2008) Iron and fungal pathogenesis: a case study with Cryptococcus neoformans. **Cell Microbiol**, 10 (2): 277-284.

Jung, W.H., Sham, A., Lian, T., et al. (2008) Iron source preference and regulation of iron uptake in *Cryptococcus neoformans*. **PLoS Pathog**, 4 (2): e45.

Jung, W.H., Sham, A., White, R., et al. (2006) Iron regulation of the major virulence factors in the AIDS-associated pathogen Cryptococcus neoformans. **PLoS Biol**, 4 (12): e410.

Kambugu, A., Meya, D.B., Rhein, J., et al. (2008) Outcomes of cryptococcal meningitis in Uganda before and after the availability of highly active antiretroviral therapy. **Clin Infect Dis**, 46 (11): 1694-1701.

Kanmogne, G.D., Schall, K., Leibhart, J., et al. (2007) HIV-1 gp120 compromises blood-brain barrier integrity and enhances monocyte migration across blood-brain barrier: implication for viral neuropathogenesis. **J Cereb Bood Flow Metab**, 27 (1): 123-134.

Kawakami, K., Qifeng, X., Tohyama, M., et al. (1996) Contribution of tumour necrosis factor-alpha (TNF-alpha) in host defence mechanism against *Cryptococcus neoformans*. **Clin Exp Immunol**, 106 (3): 468-474.

Kawakami, K., Zhang, T., Qureshi, M.H., et al. (1997) *Cryptococcus neoformans* inhibits nitric oxide production by murine peritoneal macrophages stimulated with interferon-gamma and lipopolysaccharide. **Cell Immunol**, 180 (1): 47-54.

Kechichian, T.B., Shea, J. and Del Poeta, M. (2007) Depletion of alveolar macrophages decreases the dissemination of a glucosylceramide-deficient mutant of *Cryptococcus neoformans* in immunodeficient mice. **Infect Immun**, 75 (10): 4792-4798.

Khosravi, A.R. (1997) Isolation of *Cryptococcus neoformans* from pigeon (Columbia livia droppings in northern Iran. **Mycopathologia**, 139 (2): 93-95.

Kidd, S.E., Hagen, F., Tscharke, R.L., et al. (2004) A rare genotype of *Cryptococcus gattii* caused the cryptococcosis outbreak on Vancouver Island (British Columbia, Canada). **Proc Natl Acad Sci USA**, 101 (49): 17258-17263.

Kim, K.S. (2008) Mechanisms of microbial traversal of the blood-brain barrier. **Nat Rev Microbiol**, 6 (8): 625-634.

Kim, T.A., Avraham, H.K., Koh, Y.H., et al. (2003) HIV-1 Tat-mediated apoptosis in human brain microvascular endothelial cells. **J Immunol,** 170 (5): 2629-2637.

Kishi, K., Homma, S., Kurosaki, A., et al. (2006) Clinical features and high-resolution CT findings of pulmonary cryptococcosis in non-AIDS patients. **Respir Med**, 100 (5): 807-812.

Knoke, M. and Schwesinger, G. (1994) One hundred years of cryptococcosis. **Mycoses**, 37 (Suppl 1): 28-33.

Kozel, T.R. and Pfrommer, G.S. (1986) Activation of the complement system by *Cryptococcus neoformans* leads to binding of iC3b to the yeast. **Infect Immun**, 52 (1): 1-5.

Kozel, T.R., Pfrommer, G.S., Guerlain, A.S., et al. (1988) Strain variation in phagocytosis of *Cryptococcus neoformans*: dissociation of susceptibility to phagocytosis from activation and binding of opsonic fragments of C3. **Infect Immun**, 56 (11): 2794-2800.

Kozel, T.R., Wilson, M.A., Pfrommer, G.S., et al. (1989) Activation and binding of opsonic fragments of C3 on encapsulated *Cryptococcus neoformans* by using an alternative complement pathway reconstituted from six isolated proteins. **Infect Immun**, 57 (7): 1922-1927.

Kretschmer, M., Wang, J. and Kronstad, J.W. (2012) Peroxisomal and mitochondrial beta-oxidation influence the virulence of the pathogenic fungus *Cryptococcus neoformans*. **Eukaryot cell**, 11 (8): 1042-54.

Kwon-Chung, K. (1976a) Morphogenesis of *Filobasidiella neoformans*, the sexual state of *Cryptococcus neoformans*. **Mycologia**, 68 (4): 821-833.

Kwon-Chung, K. (1976b) A new species of *Filobasidiella*, the sexual state of *Cryptococcus neoformans* B and C serotypes. **Mycologia**, 68 (4): 943-946.

Kwon-Chung, K. and Bennett, J.E. (1984a) Epidemiologic differences between the two varieties of *Cryptococcus neoformans*. **Am J Epidemiol**, 120 (1): 123-130.

Kwon-Chung, K. and Bennett, J.E. (1984b) High prevalence of *Cryptococcus neoformans var. gattii* in tropical and subtropical regions. **Zentralbl Bakteriol Mikrobiol Hyg A**, 257 (2): 213-218.

Kyung J. Kwon-Chung, Teun Boekhout, Jack W. Fell and Mara Diaz (2002) Proposal to Conserve the Name *Cryptococcus gattii* against *C. hondurianu*s and *C. bacillisporus* (Basidiomycota, Hymenomycetes, Tremellomycetidae). **Taxon**, 51 (4): 804-806.

Lachenmaier, S.M., Deli, M.A., Meissner, M., et al. (2011) Intracellular transport of *Toxoplasma gondii* through the blood-brain barrier. **J Immunol**, 232 (1-2): 119-130.

Lagrou, K., Van Eldere, J., Keuleers, S., et al. (2005) Zoonotic transmission of *Cryptococcus neoformans* from a magpie to an immunocompetent patient. **J Intern Med**, 257 (4): 385-388.

Lee, A., Toffaletti, D.L., Tenor, J., et al. (2010) Survival defects of *Cryptococcus neoformans* mutants exposed to human cerebrospinal fluid result in attenuated virulence in an experimental model of meningitis. **Infect Immun**, 78 (10): 4213-4225.

Lee, S.C., Dickson, D.W. and Casadevall, A. (1996) Pathology of cryptococcal meningoencephalitis: analysis of 27 patients with pathogenetic implications. **Hum Pathol**, 27 (8): 839-847.

Lee, S.C., Kress, Y., Zhao, M.L., et al. (1995) *Cryptococcus neoformans* survive and replicate in human microglia. Lab Invest, 73 (6): 871-879.

Lee, Y.C., Wang, J.T., Sun, H.Y., et al. (2011) Comparisons of clinical features and mortality of cryptococcal meningitis between patients with and without human immunodeficiency virus infection. **J Microbiol Immunol Infect**, 44 (5): 338-345.

Lengeler, K.B., Wang, P., Cox, G.M., et al. (2000) Identification of the MATa mating-type locus of *Cryptococcus neoformans* reveals a serotype A MATa strain thought to have been extinct. **Proc Natl Acad Sci USA**, 97 (26): 14455-14460.

Levitz, S.M., Selsted, M.E., Ganz, T., et al. (1986) In vitro killing of spores and hyphae of *Aspergillus fumigatus* and *Rhizopus oryzae* by rabbit neutrophil cationic peptides and bronchoalveolar macrophages. **J Infect Dis**, 154 (3): 483-489.

Lin, X. and Heitman, J. (2006) The biology of the *Cryptococcus neoformans* species complex. **Annu Rev Microbiol**, 60: 69-105.

Lin, X., Huang, J.C., Mitchell, T.G., et al. (2006) Virulence attributes and hyphal growth of *C. neoformans* are quantitative traits and the MATalpha allele enhances filamentation. **PLoS Genet**, 2 (11): e187.

Lin, X., Hull, C.M. and Heitman, J. (2005) Sexual reproduction between partners of the same mating type in *Cryptococcus neoformans*. **Nature**, 434 (7036): 1017-1021.

Lin, X., Patel, S., Litvintseva, A.P., et al. (2009) Diploids in the *Cryptococcus neoformans* serotype A population homozygous for the alpha mating type originate via unisexual mating. **PLoS Pathog**, 5 (1): e1000283.

Litvintseva, A.P., Carbone, I., Rossouw, J., et al. (2011) Evidence that the human pathogenic fungus *Cryptococcus neoformans* var. grubii may have evolved in Africa. PloS One, 6 (5): e19688.

Litvintseva, A.P., Lin, X., Templeton, I., et al. (2007) Many globally isolated AD hybrid strains of *Cryptococcus neoformans* originated in Africa. **PLoS Pathog**, 3 (8): e114.

Litvintseva, A.P., Thakur, R., Vilgalys, R., et al. (2006) Multilocus sequence typing reveals three genetic subpopulations of *Cryptococcus neoformans var. grubii* (serotype A), including a unique population in Botswana. **Genetics**, 172 (4): 2223-2238.

Liu, P.Y., Yang, Y. and Shi, Z.Y. (2009) Cryptococcal liver abscess: a case report of successful treatment with amphotericin-B and literature review. **Jpn J Infect Dis**, 62 (1): 59-60.

Lortholary, O. (2007) Management of cryptococcal meningitis in AIDS: the need for specific studies in developing countries. **Clin Infect Dis**, 45 (1): 81-83.

Loyse, A., Wainwright, H., Jarvis, J.N., et al. (2010) Histopathology of the arachnoid granulations and brain in HIV-associated cryptococcal meningitis: correlation with cerebrospinal fluid pressure. **AIDS**, 24 (3): 405-410.

Ma, H., Croudace, J.E., Lammas, D.A., et al. (2007) Direct cell-to-cell spread of a pathogenic yeast. **BMC Immunol**, 8: 15.

Ma, H., Croudace, J.E., Lammas, D.A., et al. (2006) Expulsion of live pathogenic yeast by macrophages. **Curr Biol**, 16 (21): 2156-2160.

Ma, H., Hagen, F., Stekel, D.J., et al. (2009) The fatal fungal outbreak on Vancouver Island is characterized by enhanced intracellular parasitism driven by mitochondrial regulation. **Proc Natl Acad Sci USA**, 106 (31): 12980-12985.

Mahmoud, Y.A. (1999) First environmental isolation of *Cryptococcus neoformans var. neoformans* and *var. gatti* from the Gharbia Governorate, Egypt. **Mycopathologia**, 148 (2): 83-86.

Maruvada, R., Zhu, L., Pearce, D., et al. (2012) *Cryptococcus neoformans* phospholipase B1 activates host cell Rac1 for traversal across the blood-brain barrier. **Cell Microbiol**, 14(10): 1544-53.

McQuiston, T.J. and Williamson, P.R. (2012) Paradoxical roles of alveolar macrophages in the host response to *Cryptococcus neoformans*. **J Infect Chemother**, 18 (1): 1-9.

Messer, S.A., Moet, G.J., Kirby, J.T., et al. (2009) Activity of contemporary antifungal agents, including the novel echinocandin anidulafungin, tested against *Candida spp.*, *Cryptococcus spp.*, and *Aspergillus spp.*: report from the SENTRY Antimicrobial Surveillance Program (2006 to 2007). **J Clin Microbiol**, 47 (6): 1942-1946.

Meya, D.B., Manabe, Y.C., Castelnuovo, B., et al. (2010) Cost-effectiveness of serum cryptococcal antigen screening to prevent deaths among HIV-infected persons with a CD4+ cell count < or = 100 cells/microL who start HIV therapy in resource-limited settings. **Clin Infect Dis**, 51 (4): 448-455.

Meyohas, M.C., Roux, P., Bollens, D., et al. (1995) Pulmonary cryptococcosis: localized and disseminated infections in 27 patients with AIDS. **Clin Infect Dis**, 21 (3): 628-633.

Miller, M.F., Mitchell, T.G., Storkus, W.J., et al. (1990) Human natural killer cells do not inhibit growth of *Cryptococcus neoformans* in the absence of antibody. *Infect Immun*, 58 (3): 639-645.

Mitchell, T.G. and Perfect, J.R. (1995) Cryptococcosis in the era of AIDS--100 years after the discovery of *Cryptococcus neoformans*. **Clin Microbiol Rev**, 8 (4): 515-548.

Molez, J.F. (1998) The historical question of acquired immunodeficiency syndrome in the 1960s in the Congo River basin area in relation to cryptococcal meningitis. The **Am J Trop Med Hyg**, 58 (3): 273-276.

Monari, C., Baldelli, F., Pietrella, D., et al. (1997) Monocyte dysfunction in patients with acquired immunodeficiency syndrome (AIDS) versus *Cryptococcus neoformans*. **J Infect**, 35 (3): 257-263.

Montenegro, H. and Paula, C.R. (2000) Environmental isolation of *Cryptococcus neoformans var. gattii* and *C. neoformans var. neoformans* in the city of Sao Paulo, Brazil. **Med Mycol**, 38 (5): 385-390.

Montoya, J.G. and Liesenfeld, O. (2004) Toxoplasmosis. **Lancet**, 363 (9425): 1965-1976.

Mora, D.J., da Cunha Colombo, E.R., Ferreira-Paim, K., et al. (2012) Clinical, epidemiological and outcome features of patients with cryptococcosis in uberaba, minas gerais, Brazil. **Mycopathologia**, 173 (5-6): 321-327.

Morrow, C.A., Lee, I.R., Chow, E.W., et al. (2012) A unique chromosomal rearrangement in the *Cryptococcus neoformans var. grubii* type strain enhances key phenotypes associated with virulence. **mBio**, 3 (2): e00310-11.

Mukherjee, J., Cleare, W. and Casadevall, A. (1995a) Monoclonal antibody mediated capsular reactions (Quellung) in *Cryptococcus neoformans*. **J Immunol Methods**, 184 (1): 139-143.

Mukherjee, S., Lee, S.C. and Casadevall, A. (1995b) Antibodies to *Cryptococcus neoformans* glucuronoxylomannan enhance antifungal activity of murine macrophages. **Infect Immun**, 63 (2): 573-579.

Mwaba P., Mwansa J., Chintu C. et al. (2001) Clinical presentation, natural history, and cumulative death rates of 230 adults with primary cryptococcal meningitis in Zambian AIDS patients treated under local conditions. **Postgrad Med J**, 77 (914): 769-73

Naslund, P.K., Miller, W.C. and Granger, D.L. (1995) *Cryptococcus neoformans* fails to induce nitric oxide synthase in primed murine macrophage-like cells. **Infect Immun**, 63 (4): 1298-1304.

Ngamskulrungroj, P., Chang, Y., Sionov, E., et al. (2012) The Primary Target Organ of *Cryptococcus gattii* Is Different from That of *Cryptococcus neoformans* in a Murine Model. **mBio**, 3 (3): 10.1128/mBio.00103-12.

Ngamskulrungroj, P., Gilgado, F., Faganello, J., et al. (2009) Genetic diversity of the Cryptococcus species complex suggests that *Cryptococcus gattii* deserves to have varieties. **PloS One**, 4 (6): e5862.

Nicola, A.M., Albuquerque, P., Martinez, L.R., et al. (2012) Macrophage Autophagy in Immunity to *Cryptococcus neoformans* and *Candida albicans*. **Infect Immun**, 80(9): 3065-76.

Nielsen, K., Cox, G.M., Litvintseva, A.P., et al. (2005) *Cryptococcus neoformans* {alpha} strains preferentially disseminate to the central nervous system during coinfection. **Infect Immun**, 73 (8): 4922-4933.

Nottet, H.S., Bar, D.R., van Hassel, H., et al. (1997) Cellular aspects of HIV-1 infection of macrophages leading to neuronal dysfunction in in vitro models for HIV-1 encephalitis. **J Leukoc Biol**, 62 (1): 107-116.

Noverr, M.C., Cox, G.M., Perfect, J.R., et al. (2003) Role of PLB1 in pulmonary inflammation and cryptococcal eicosanoid production. I**nfect Immun**, 71 (3): 1538-1547.

Nussbaum, J.C., Jackson, A., Namarika, D., et al. (2010) Combination flucytosine and high-dose fluconazole compared with fluconazole monotherapy for the treatment of cryptococcal meningitis: a randomized trial in Malawi. **Clin Infect Dis**, 50 (3): 338-344.

Okagaki, L.H. and Nielsen, K. (2012) Titan Cells Confer Protection from Phagocytosis in *Cryptococcus neoformans* Infections. **Eukaryot cell**, 11 (6): 820-826.

Okagaki, L.H., Strain, A.K., Nielsen, J.N., et al. (2010) Cryptococcal cell morphology affects host cell interactions and pathogenicity. **PLoS Pathog**, 6 (6): e1000953.

Olszewski, M.A., Noverr, M.C., Chen, G.H., et al. (2004) Urease expression by *Cryptococcus neoformans* promotes microvascular sequestration, thereby enhancing central nervous system invasion. **Am J Pathol**, 164 (5): 1761-1771.

Osterholzer, J.J., Surana, R., Milam, J.E., et al. (2009) Cryptococcal urease promotes the accumulation of immature dendritic cells and a non-protective T2 immune response within the lung. **Am J Pathol**, 174 (3): 932-943.

Park, B.J., Wannemuehler, K.A., Marston, B.J., et al. (2009) Estimation of the current global burden of cryptococcal meningitis among persons living with HIV/AIDS. **AIDS**, 23 (4): 525-530.

Perfect, J.R., Dismukes, W.E., Dromer, F., et al. (2010) Clinical practice guidelines for the management of cryptococcal disease: 2010 update by the infectious diseases society of America. **Clin Infect Dis**, 50 (3): 291-322.

Perfect, J.R., Lang, S.D. and Durack, D.T. (1980) Chronic cryptococcal meningitis: a new experimental model in rabbits. **Am J Pathol**, 101 (1): 177-194.

Perkins-Balding, D., Ratliff-Griffin, M. and Stojiljkovic, I. (2004) Iron transport systems in Neisseria meningitidis. **Microbiol Mol Biol Rev**, 68 (1): 154-171.

Pfeiffer, T.J. and Ellis, D.H. (1992) Environmental isolation of *Cryptococcus neoformans var. gattii* from Eucalyptus tereticornis. **J Med Vet Mycol**, 30 (5): 407-408.

Philpott, C.C. (2006) Iron uptake in fungi: a system for every source. **Biochim Biophys Acta**, 1763 (7): 636-645.

Pirofski, L., Lui, R., DeShaw, M., et al. (1995) Analysis of human monoclonal antibodies elicited by vaccination with a *Cryptococcus neoformans* glucuronoxylomannan capsular polysaccharide vaccine. **Infect Immun**, 63 (8): 3005-3014.

Polacheck, I., Hearing, V.J. and Kwon-Chung, K. (1982) Biochemical studies of phenoloxidase and utilization of catecholamines in *Cryptococcus neoformans*. **J Bacteriol**, 150 (3): 1212-1220.

Polacheck, I., Platt, Y. and Aronovitch, J. (1990) Catecholamines and virulence of *Cryptococcus neoformans*. **Infect Immun**, 58 (9): 2919-2922.

Ponta, H., Sherman, L. and Herrlich, P.A. (2003) CD44: from adhesion molecules to signalling regulators. **Nat Rev Mol Cell Biol**, 4 (1): 33-45.

Price, M.S., Betancourt-Quiroz, M., Price, J.L., et al. (2011) *Cryptococcus neoformans* Requires a Functional Glycolytic Pathway for Disease but Not Persistence in the Host. **mBio**, 2 (3): e00103-11.

Pukkila-Worley, R. and Alspaugh, J.A. (2004) Cyclic AMP signaling in *Cryptococcus neoformans*. **FEMS Yeast Res**, 4 (4-5): 361-367.

Qin, Q.M., Luo, J., Lin, X., et al. (2011) Functional analysis of host factors that mediate the intracellular lifestyle of Cryptococcus neoformans. **PLoS Pathog**, 7 (6): e1002078.

Rodrigues, M.L., Alviano, C.S. and Travassos, L.R. (1999) Pathogenicity of *Cryptococcus neoformans*: virulence factors and immunological mechanisms. **Microbes Infect**, 1 (4): 293-301.

Rude, T.H., Toffaletti, D.L., Cox, G.M., et al. (2002) Relationship of the glyoxylate pathway to the pathogenesis of *Cryptococcus neoformans*. **Infect Immun**, 70 (10): 5684-5694.

Saag, M.S., Graybill, R.J., Larsen, R.A., et al. (2000) Practice guidelines for the management of cryptococcal disease. **Clin Infect Dis**, 30 (4): 710-718.

Sabiiti, W. and May, R.C. (2012) Capsule independent uptake of the fungal pathogen *Cryptococcus neoformans* into brain microvascular endothelial cells. **PloS One**, 7 (4): e35455.

Sabiiti, W., May, R.C. and Pursall, E.R. (2012) Experimental models of cryptococcosis. **Int J Microbiol**, 2012: 626745.

Salas, S.D., Bennett, J.E., Kwon-Chung, K., et al. (1996) Effect of the laccase gene CNLAC1, on virulence of *Cryptococcus neoformans*. **J Exp Med**, 184 (2): 377-386.

Santangelo, R., Zoellner, H., Sorrell, T., et al. (2004) Role of extracellular phospholipases and mononuclear phagocytes in dissemination of cryptococcosis in a murine model. I**nfect Immun**, 72 (4): 2229-2239.

Schaible, U.E. and Kaufmann, S.H. (2004) Iron and microbial infection. **Nat Rev Microbiol**, 2 (12): 946-953.

Schop, J. (2007) Protective immunity against *Cryptococcus neoformans* infection. **Mcgill J Med**, 10 (1): 35-43.

Schroder, A., Kland, R., Peschel, A., et al. (2006) Live cell imaging of phagosome maturation in Staphylococcus aureus infected human endothelial cells: small colony variants are able to survive in lysosomes. **Med Microbiol Immunol**, 195 (4): 185-194.

Sethna, S.B., Wagle, A.P. and Rahalkar, P.W. (1973) Isolation of *Cryptococcus neoformans* from pigeon habitats in Poona area. **Hindustan Antibiot Bull**, 16 (2-3): 115-117.

Severo, C.B., Xavier, M.O., Gazzoni, A.F., et al. (2009) Cryptococcosis in children. **Paediatr Respir Rev**, 10 (4): 166-171.

Shao, X., Mednick, A., Alvarez, M., et al. (2005) An innate immune system cell is a major determinant of species-related susceptibility differences to fungal pneumonia. **J Immunol**, 175 (5): 3244-3251.

Shi, M., Li, S.S., Zheng, C., et al. (2010) Real-time imaging of trapping and urease-dependent transmigration of *Cryptococcus neoformans* in mouse brain. **J Clin Invest**, 120 (5): 1683-1693.

Shinoe, T., Wanaka, A., Nikaido, T., et al. (2006) The pro-apoptotic human BH3-only peptide harakiri is expressed in cryptococcus-infected perivascular macrophages in HIV-1 encephalitis patients. **Neurosci Lett**, 393 (2-3): 102-107.

Sia, R.A., Lengeler, K.B. and Heitman, J. (2000) Diploid strains of the pathogenic basidiomycete *Cryptococcus neoformans* are thermally dimorphic. **Fungal Genet Biol**, 29 (3): 153-163.

Siddiqui, A.A., Shattock, R.J. and Harrison, T.S. (2006) Role of capsule and interleukin-6 in long-term immune control of *Cryptococcus neoformans* infection by

specifically activated human peripheral blood mononuclear cells. **Infect Immun**, 74 (9): 5302-5310.

Silva, F.D., Rossi, D.C., Martinez, L.R., et al. (2011) Effects of microplusin, a copper-chelating antimicrobial peptide, against *Cryptococcus neoformans*. **FEMS Microbiol Lett**, 324 (1): 64-72.

Simwami, S.P., Khayhan, K., Henk, D.A., et al. (2011) Low diversity *Cryptococcus neoformans var. grubii* multilocus sequence types from Thailand are consistent with an ancestral African origin. **PLoS Pathog**, 7 (4): e1001343.

Singh, N., Alexander, B.D., Lortholary, O., et al. (2008) Pulmonary cryptococcosis in solid organ transplant recipients: clinical relevance of serum cryptococcal antigen. **Clin Infect Dis**, 46 (2): e12-8.

Singh, N., Forrest, G. and AST Infectious Diseases Community of Practice (2009) Cryptococcosis in solid organ transplant recipients. **Am J Transplant**, 9 (Suppl 4) S192-8.

Sirinavin, S., Intusoma, U. and Tuntirungsee, S. (2004) Mother-to-child transmission of *Cryptococcus neoformans*. **Pediatr Infect Dis J**, 23 (3): 278-279.

Sorrell, T.C. (2001) *Cryptococcus neoformans var. gattii*. **Med Mycol**, 39 (2): 155-168.

Sorrell, T.C., Brownlee, A.G., Ruma, P., et al. (1996) Natural environmental sources of *Cryptococcus neoformans var. gattii*. **J Clin Microbiol**, 34 (5): 1261-1263.

Springer, D.J. and Chaturvedi, V. (2010) Projecting global occurrence of *Cryptococcus gattii*. **Emerg Infect Dis**, 16 (1): 14-20.

Staib, F. (1981) The perfect state of *Cryptococcus neoformans*, *Filobasidiella neoformans*, on pigeon manure filtrate agar. **Zentralbl Bakteriol A**, 248 (4): 575-578.

Stano, P., Williams, V., Villani, M., et al. (2009) App1: an antiphagocytic protein that binds to complement receptors 3 and 2. **J Immunol**, 182 (1): 84-91.

Steele, K.T., Thakur, R., Nthobatsang, R., et al. (2010) In-hospital mortality of HIV-infected cryptococcal meningitis patients with *C. gattii* and *C. neoformans* infection in Gaborone, Botswana. **Med Mycol**, 48 (8): 1112-5.

Steenbergen, J.N. and Casadevall, A. (2003) The origin and maintenance of virulence for the human pathogenic fungus *Cryptococcus neoformans*. **Microbes Infect**, 5 (7): 667-675.

Stie, J., Bruni, G. and Fox, D. (2009) Surface-associated plasminogen binding of *Cryptococcus neoformans* promotes extracellular matrix invasion. PLoS One, 4 (6): e5780.

Sugiura, Y., Homma, M. and Yamamoto, T. (2005) Difficulty in diagnosing chronic meningitis caused by capsule-deficient *Cryptococcus neoformans*. **J Neurol Neurosurg Psychiatry**, 76 (10): 1460-1461.

Sukroongreung, S., Kitiniyom, K., Nilakul, C., et al. (1998) Pathogenicity of basidiospores of *Filobasidiella neoformans var. neoformans*. **Med Mycol**, 36 (6): 419-424.

Syme, R.M., Bruno, T.F., Kozel, T.R., et al. (1999) The capsule of *Cryptococcus neoformans* reduces T-lymphocyte proliferation by reducing phagocytosis, which can be restored with anticapsular antibody. **Infect Immun**, 67 (9): 4620-4627.

Todaro-Luck, F., Reiss, E., Cherniak, R., et al. (1989) Characterization of *Cryptococcus neoformans* capsular glucuronoxylomannan polysaccharide with monoclonal antibodies. **Infect Immun**, 57 (12): 3882-3887.

Tucker, S.C. and Casadevall, A. (2002) Replication of *Cryptococcus neoformans* in macrophages is accompanied by phagosomal permeabilization and accumulation of vesicles containing polysaccharide in the cytoplasm. **Proc Natl Acad Sci USA**, 99 (5): 3165-3170.

Valdez, P.A., Vithayathil, P.J., Janelsins, B.M., et al. (2012) Prostaglandin E2 suppresses antifungal immunity by inhibiting interferon regulatory factor 4 function and interleukin-17 expression in T cells. **Immunity**, 36 (4): 668-679.

van Duin, D., Casadevall, A. and Nosanchuk, J.D. (2002) Melanization of *Cryptococcus neoformans* and Histoplasma capsulatum reduces their susceptibilities to amphotericin B and caspofungin. Antimicrob Agents Chemother, 46 (11): 3394-3400.

van, d.W., Coenjaerts, F.E., Vaandrager, A.B., et al. (2004) Aggregation of *Cryptococcus neoformans* by surfactant protein D is inhibited by its capsular component glucuronoxylomannan. **Infect Immun**, 72 (1): 145-153.

Vecchiarelli, A., Dottorini, M., Pietrella, D., et al. (1994) Role of human alveolar macrophages as antigen-presenting cells in Cryptococcus neoformans infection. **Am J Respir Cell Mol Biol**, 11 (2): 130-137.

Vecchiarelli, A. and Monari, C. (2012) Capsular Material of *Cryptococcus neoformans*: Virulence and Much More. **Mycopathologia**, 176 (5-6): 375-386 .

Vecchiarelli, A., Pietrella, D., Bistoni, F., et al. (2002) Antibody to *Cryptococcus neoformans* capsular glucuronoxylomannan promotes expression of interleukin-12Rbeta2 subunit on human T cells in vitro through effects mediated by antigen-presenting cells. **Immunology**, 106 (2): 267-272.

Velagapudi, R., Hsueh, Y.P., Geunes-Boyer, S., et al. (2009) Spores as infectious propagules of *Cryptococcus neoformans*. **Infect Immun**, 77 (10): 4345-4355.

Vicencio, A.G., Narain, S., Du, Z., et al. (2008) Pulmonary cryptococcosis induces chitinase in the rat. **Respir Res**, 9: 40.

Voelz, K., Johnston, S.A., Rutherford, J.C., et al. (2010) Automated Analysis of Cryptococcal Macrophage Parasitism Using GFP-Tagged Cryptococci. **PloS One**, 5 (12): e15968.

Vu, K., Weksler, B., Romero, I., et al. (2009) Immortalized human brain endothelial cell line HCMEC/D3 as a model of the blood-brain barrier facilitates in vitro studies of central nervous system infection by *Cryptococcus neoformans*. **Eukaryot Cell**, 8 (11): 1803-1807.

Waikedre, J., Vitturo, C.I., Molina, A., et al. (2012) Antifungal Activity of the Essential Oils of Callitris neocaledonica and C. sulcata Heartwood (Cupressaceae). **Chem Biodivers**, 9 (3): 644-653.

Waterman, S.R., Hacham, M., Hu, G., et al. (2007) Role of a CUF1/CTR4 copper regulatory axis in the virulence of *Cryptococcus neoformans*. **J Clin Invest**, 117 (3): 794-802.

Weksler, B.B., Subileau, E.A., Perriere, N., et al. (2005) Blood-brain barrier-specific properties of a human adult brain endothelial cell line. **FASEB J**, 19 (13): 1872-1874.

Wickes, B.L., Mayorga, M.E., Edman, U., et al. (1996) Dimorphism and haploid fruiting in *Cryptococcus neoformans*: association with the alpha-mating type. Proc **Natl Acad Sci USA**, 93 (14): 7327-7331.

Williamson, P.R. (1997) Laccase and melanin in the pathogenesis of *Cryptococcus neoformans*. **Front Biosci**, 2 e99-107.

Williamson, P.R. (1994) Biochemical and molecular characterization of the diphenol oxidase of *Cryptococcus neoformans*: identification as a laccase. **J Bacteriol**, 176 (3): 656-664.

Wright, L.C., Payne, J., Santangelo, R.T., et al. (2004) Cryptococcal phospholipases: a novel lysophospholipase discovered in the pathogenic fungus *Cryptococcus gattii*. **Biochem J**, 384 377-384.

Wright, L.C., Santangelo, R.M., Ganendren, R., et al. (2007) Cryptococcal lipid metabolism: phospholipase B1 is implicated in transcellular metabolism of macrophage-derived lipids. **Eukaryot cell**, 6 (1): 37-47.

Wu, B., Liu, H., Huang, J., et al. (2009) Pulmonary cryptococcosis in non-AIDS patients. **Clin Invest Med**, 32 (1): E70-7.

Xie, S., Sao, R., Braun, A., et al. (2012) Difference in *Cryptococcus neoformans* cellular and capsule size in sequential pulmonary and meningeal infection: a postmortem study. **Diagn Microbiol Infect Dis**, 73 (1): 49-52.

Yamamoto, Y., Kohno, S., Noda, T., et al. (1995) [Isolation of *Cryptococcus neoformans* from environments (pigeon excreta) in Nagasaki]. **Kansenshogaku Zasshi**, 69 (6): 642-645.

Zaragoza, O., Chrisman, C.J., Castelli, M.V., et al. (2008) Capsule enlargement in *Cryptococcus neoformans* confers resistance to oxidative stress suggesting a mechanism for intracellular survival. **Cell Microbiol**, 10 (10): 2043-2057.

Zaragoza, O., Garcia-Rodas, R., Nosanchuk, J.D., et al. (2010) Fungal cell gigantism during mammalian infection. **PLoS Pathog**, 6 (6): e1000945.

Zaragoza, O., Rodrigues, M.L., De Jesus, M., et al. (2009) The capsule of the fungal pathogen *Cryptococcus neoformans*. **Adv Appl Microbiol**, 68 133-216.

Zhang, Y., Wang, F., Tompkins, K.C., et al. (2009) Robust Th1 and Th17 immunity supports pulmonary clearance but cannot prevent systemic dissemination of highly virulent *Cryptococcus neoformans* H99. **Am J Pathol**, 175 (6): 2489-2500.

Zhu, L.P., Wu, J.Q., Xu, B., et al. (2010) Cryptococcal meningitis in non-HIV-infected patients in a Chinese tertiary care hospital, 1997-2007. **Med Mycol**, 48 (4): 570-579.

Zhu, X. and Williamson, P.R. (2004) Role of laccase in the biology and virulence of *Cryptococcus neoformans*. **FEMS Yeast Res**, 5 (1): 1-10.

Capsule Independent Uptake of the Fungal Pathogen *Cryptococcus neoformans* into Brain Microvascular Endothelial Cells

Wilber Sabiiti, Robin C. May*

Institute of Microbiology & Infection, School of Biosciences, College of Life and Environmental Sciences, University of Birmingham, Birmingham, United Kingdom

Abstract

Cryptococcosis is a life-threatening fungal disease with a high rate of mortality among HIV/AIDS patients across the world. The ability to penetrate the blood-brain barrier (BBB) is central to the pathogenesis of cryptococcosis, but the way in which this occurs remains unclear. Here we use both mouse and human brain derived endothelial cells (bEnd3 and hCMEC/D3) to accurately quantify fungal uptake and survival within brain endothelial cells. Our data indicate that the adherence and internalisation of cryptococci by brain microvascular endothelial cells is an infrequent event involving small numbers of cryptococcal yeast cells. Interestingly, this process requires neither active signalling from the fungus nor the presence of the fungal capsule. Thus entry into brain microvascular endothelial cells is most likely a passive event that occurs following 'trapping' within capillary beds of the BBB.

Introduction

Cryptococcosis is a life-threatening disease caused primarily by the human fungal pathogen *Cryptococcus neoformans*. Cryptococcal infection can potentially occur in any part of the human body (reviewed in [1]), although central nervous system (CNS) cryptococcosis accounts for most clinical presentation. Globally, fatalities due to cryptococcal meningitis were recently estimated at over 600,000 cases per year of which 504000 (81%) occur in Sub-Saharan Africa [2]. The victims of cryptococcal infection are predominantly immunocompromised people infected with *C. neoformans*, although there is an increasing incidence of immuno-competent cryptococcosis caused by *C. gattii* [3–7]. HIV/AIDS is the major predisposing condition for cryptococcosis with 10–15% HIV patients acquiring cryptococcal infection, although prolonged glucocorticosteroid therapy and solid organ transplantation are increasingly becoming important [8,9].

The route of cryptococcal infection is believed to be through inhalation of airborne basidiospores or desiccated yeast cells from an environmental source to the lungs. The fungal yeast cells may stay dormant in the host, and can potentially disseminate to all body organs but there is a high propensity of dissemination to the brain [10]. Once in the brain the fungus causes meningoenceph-alitis, a severe form of the disease, which is uniformly fatal if untreated [11]. Even with the most effective antifungal therapy, the fatality rate remains high in HIV-associated crytococcosis (10–25% and >40% in rich and poor settings respectively [12–17] Dissemination to the brain requires that *C. neoformans* penetrate the normally impermeable blood-brain barrier (BBB) [18]. The BBB is

made of microvascular endothelial cells supported by astrocytic foot processes, pericytes and neuronal processes [19]. Brain microvascular endothelial cells form strong tight junctions, which present a formidable barrier to any invading pathogens [18–20]. The mechanism by which *C. neoformans* penetrates this barrier is not currently understood, although several possibilities have been proposed, including passage between neighbouring endothelial cells (paracellular entry), carriage into the CNS within infected phagocytes (Trojan Horse model), or uptake by and traversal through endothelial cells (transcytosis) [21,22]. In the transcellular model of traversal, adherence to and uptake of cryptococci by brain microvascular endothelial cells (BMEC) must occur before transit into the brain. In support of this model, Chang et al used electron microscopy to demonstrate that cryptococcal yeast cells could adhere to and become internalised by brain microvascular endothelial cells [23].

Several pathogen-generated microbial factors including urease, laccase, capsule and hyaluronic acid have been implicated in modulating the *Cryptococcus* – blood-brain barrier interaction [24,25]. The capsule is a major virulence factor and its role in pathogen – phagocyte interaction and systemic dissemination of *Cryptococcus* is well documented [26]. However, the role of capsule in regulating CNS invasion remains unclear. Capsule associated structural changes such as phenotypic switching (rough to smooth) have been reported to enhance crossing of the blood-brain barrier [27–31], but a recent study using intravital real time imaging demonstrated that encapsulated and acapsular strains of *C. neoformans* had an equal ability to associate with – and transmigrate across - the microvascular endothelium into the brain [32].

Despite these recent advances, however, there are currently no quantitative data on cryptococcal uptake by brain endothelial cells in the presence and absence of capsule. Here we report the first attempts to address this, by using an *in vitro* brain endothelial cell culture to quantify association and uptake of cryptococci.

Materials and Methods

Yeast culture

Two sets of isogenic *C. neoformans* strains, serotype A H99 and its isogenic acapsular strain cap59 and serotype D B3501 with its isogenic acapsular strain B4131 were used. Strains were propagated on YPD agar (1% yeast extract, 1% peptone, 2% dextrose and 1% agar) at 25°C. Prior to experimentation, cultures of both strains were grown in YPD broth (1% yeast extract, 1% peptone and 2% dextrose) at 25°C with rotation at 20 RPM overnight. The yeast cells were washed with sterile phosphate buffered saline (PBS) and stained with 0.5 mg/ml FITC for 30 min with shaking (Labrolller, Labnet Inc.) at room temperature. The required infection inoculum (of 2×10^6 yeast cells) was determined by counting using a haemocytometer.

Tissue culture

Two types of brain microvascular endothelial cell-lines, the immortalized mouse brain derived endothelial (bEnd3) cells and the human brain capillary microvascular endothelial cells (hCMEC/D3) were used. The bEnd3 cells were grown to monolayer confluence in 24 well tissue culture plates (Greiner, UK) containing Dulbecco's modified Eagle's medium (DMEM, Sigma Aldrich) supplemented with 10% foetal bovine serum (FBS), I% streptomycin/penicillin and 2 mM L-glutamine, 1% non-essential aminoacids, 1% Sodium pyruvate and 5 µM 2-Mercaptoethanol. HCMEC/D3 cells were grown in endothelial growth medium 2 (EGM-2, Lonza, UK) in 24 well tissue culture plates precoated with Calf Skin collagen (Sigma UK). Seeding plates with 10^5 endothelial cells per well, ensured even growth of a cell monolayer. The culture was maintained at 37°C with 5%CO$_2$ for 4–6 days to obtain a fully matured cell monolayer. For microscopic examination, 13 mm sterile glass coverslips (collagen coated for hCMEC/D3 cells) were inserted into the 24 well plates before seeding with endothelial cells, allowing the monolayer to grow on the coverslip, which could then be easily transferred for microscopy. Prior to infection, tissue culture growth medium was replaced with serum free medium and incubated for 1 hr at 37°C. The cultures were then inoculated with 2×10^6 yeast cells per well, producing an approximate infection ratio of 1: 3 (target: effector). Infections were allowed to proceed for either 2 hr or 4 hrs, as described, at 37°C with 5% CO$_2$. To ensure that the infection media did not have a negative effect on cryptococcal growth, cryptococci (10^5 yeast cells/ml) were directly inoculated into bEnd3 and or hCMEC/D3 infection medium and growth recorded over 24 hrs.

Quantification of yeast cell association with, and internalization by, BMEC cells

The rate of cryptococcal yeast cell association with brain microvascular endothelial cells (BMEC), bEnd3 and hCMEC/D3 was determined both microscopically and using CFU counts. In the former, dual colour fluorescence microscopy (Nikon Eclipse T*i* - S, Japan) was used to determine associated (adherent and internalized) yeast cells. After infection, the non-adherent yeast cells were removed by washing four times with sterile PBS and the extracellular adherent yeast cells stained for 10–15 min with 20 µg/ml calcoflour white (adapted from [33]) at room temper-

ature. Since mammalian cells are impermeable to calcofluor white, internalized yeast retained the green FITC signal while adherent cells stained blue. Nine random fields per coverslip were viewed and the internalized and non-internalized yeasts therein counted. Association (total number of yeast cells –attached or internalized by BMEC) and internalization were determined and compared to the original inoculum.

Since this microscopic approach did not distinguish between live and dead cryptococci, we exploited colony forming unit (CFU) assays to determine the viability of cryptococci that had been internalised by cells of the BBB. After removal of non-adherent cryptococci by extensive washing, endothelial cells were lysed with 200 µl sterile water for 15 min at 37°C to release internalized cryptococci and the lysate plated on YPD agar for colony counts (CFU assay). The associated cryptococci were determined as the ratio of cryptococcal yeast cells (CFU/ml) to the original inoculum.

Thus, by comparing data derived both from microscopy (which distinguishes internalised from attached cryptococci, but not live from dead cells) and from CFU counts (which have the opposite profile) we were able to accurately estimate both uptake and survival of cryptococci. The results were recorded as endothelial cell associated cryptococci per well, which is equivalent to cryptococci per coverslip for microscopy and CFU/ml for colony counts.

Opsonisation

Antibodies to *Cryptococcus* have been reported to exist in circulation as early as childhood [34]. Furthermore, phagocytosis studies using macrophages have shown that internalization of cryptococcal yeast cells is enhanced by antibody and or complement mediated opsonisation [35–37]. However, no studies have investigated whether adherence and uptake of cryptococci by BMEC requires opsonisation. To address this, opsonised and non-oposonized live and heat killed H99 cryptococci were incubated with BMEC for 2 hr and 4 hr at 37°C. Opsonisation was done by adding 5 µg/ml the capsule specific 18B7 mouse IgG (a kind gift from Arturo Casadevall) to 200 µl aliquot of yeast cells and rotated (Labroller, Labnet Inc, US) at room temperature for 30 min prior to infection. The rate of association and internalization was determined as described above.

Role of viability in *Cryptococcus* – BMEC association and internalization

We tested whether dead cryptococci adhere and are internalized by BMEC at the same rate as live cells. 1 ml aliquots of both encapsulated and non-capsulated cryptococci were heated at 65°C for 15 min prior to infection. Adherent and internalized yeasts were determined microscopically. To determine if the yeast culture was completely killed, 20 µl aliquots were plated on YPD agar and no growth was observed.

Fixed endothelial cell control

As a negative control, mature endothelial cell (bEnd3 and hCMEC/D3) monolayers were fixed with 250 µl PFA 4% in PBS for 10 min at room temperature, rinsed five times with PBS and then inoculated with 2×10^6 cryptococci per ml. As for the live endothelial cell monolayers, the fixed monolayers were incubated with cryptococci for 2 hr and 4 hr at 37°C with 5% CO$_2$ and washed four times to remove non-adherent yeast cells. 200 µl sterile water was used to lyse the endothelial cells with additional scraping to remove any remaining endothelial cell associated

cryptococci. The lysate was plated on YPD agar at 25°C and colony counts were made after 48 hr.

Statistical analysis

Non-parametric Mann-Whitney U Test and Wilcoxon Signed Ranks Test were used to measure the significance of adherence at different conditions and time points. Mann-Whitney U Test was applied to compare the means of test different setups, for instance comparing the mean association of encapsulated and acapsular strain to bEnd3 and or hCMEC/D3 cells. Wilcoxon Signed ranks test was applied to compare means of the same setup at different time points, for example comparing the mean association of encapsulated H99 strain or the acapsular mutant with endothelial cells after 2 hrs and 4 hrs of incubation at 37°C.

Results

Cryptococcal association with and internalization by the murine brain endothelial cell line bEnd3

We exposed the mouse brain endothelial cell line bEnd3 to wildtype *C. neoformans* H99 and its isogenic acapsular derivative, cap59 [38]. The two strains were tested for their rate of binding and internalization by BMEC and whether the presence or absence of capsule has an effect on this interaction. After two hours of exposure to bEnd3 cells at 37°C, 8.8×10^3 (0.43%) of inoculated wild type (H99) cryptococci had adhered strongly to the endothelial layer, rising to 2.0×10^4 (1.2%) after four hours. Similarly, 1.6×10^4 (0.8%) of the acapsular cryptococci had associated with bEnd3 cells at 2 hr rising to 2.5×10^4 (1.23%) after four hours of incubation at 37°C (Figure 1A). In contrast, binding to paraformaldehyde-fixed BMEC monolayers was negligible at all time points tested (Figure S1). By using calcofluor staining to discriminate surface bound from internalised crypto-cocci, we determined that 3.1×10^3 (35% of associated) and 4.4×10^3 (28% of associated) wild type and acapsular cryptococci, respectively, had been internalised by 2 hours at 37°C, rising to 8.1×10^3 (40%) and 8.6×10^3 (35%) respectively by 4 hrs (Figure 1B). Importantly, for both strains, microscopic yeast cell counts and live CFU counts gave the same rate of association for both H99 and cap59, suggesting that there is no significant drop in cryptococcal viability upon adherence to or uptake by bEnd3 cells.

Effect of opsonisation on *Cryptococcus* – BMEC association and internalization

Since most individuals produce circulating antibodies to cryptococci by late childhood [34], we investigated whether opsonisation of cryptococci with antibody increases the association and internalization with brain endothelial cells. However, there were no significant differences between opsonised and non-opsonised yeast in either adherence or uptake at either time point tested (Figure 2A and B), suggesting binding and uptake by brain endothelial cells is opsonin independent.

Cryptococcal association and internalization by human brain endothelial cells, hCMEC/D3

To test whether the rates of adherence and uptake that we had observed in bEnd3 cells were species specific, we repeated our analyses using the human brain endothelial derived cell-line, hCMEC/D3. As with bEnd3 cells, both microscopic and CFU counts showed that encapsulated H99 and its isogenic acapsular mutant cap59 associated and were engulfed at the same rate, P = >0.05 at 2 hr and 4 hr of infection respectively (Figure 3A and B). To determine whether the interaction varies from strain to strain, we tested a different pair of *C. neoformans* serotype D strains; encapsulated B3501 and its isogenic acapsular strain B4131. Like the H99/cap59 isogenic pair, both B3501 and B4131 strains associated and were internalized at the same rate with hCMEC/ D3 cells (Figure 4A and B).

However, unlike bEnd3 cells, we observed a significant decrease over time in cryptococcal CFU counts for both strains. Microscopic counts revealed that association and internalization for both strains increases with time of incubation, suggesting a loss of viability by cryptococci during association with hCMEC/D3 cells (Figure 3A and 4A). One potential explanation for this result is that hCMEC/D3 cells may generate a more antimicrobial environment for cryptococci following uptake than that produced by bEnd3 cells. Thus bEnd3 cells and hCMEC/D3 cells bind and engulf cryptococci at similar rates, but only hCMEC/D3 cells are able to significantly reduce cryptococcal viability following uptake.

Viability of cryptococci is not a prerequisite for association and internalization by BMEC

Lastly, we investigated whether the uptake of cryptococci into BMEC requires active signals from the pathogen. However, heat-killed H99 retained the ability to bind and enter both mouse bEnd3 and human hCMEC/D3 cells at a similar rate to live yeast (Figure 5A and C). Although viable cryptococci showed higher association efficiency in bEnd3 cells, there was no significant difference between internalization of viable and heat-killed cryptococci in both bEnd3 and hCMEC/D3 cells. (Figure 5B and D), suggesting that uptake is a passive process that occurs independently of yeast cell viability.

Discussion

The mechanism by which *C. neoformans* associates with – and penetrates - the BBB remains a critical question in understanding the pathogenesis of CNS cryptococcosis. Considerable evidence shows that the penetration of the BBB by *C. neoformans* may occur via infected phagocytes [21,39] or transcellularly through adherence and phagocytosis by the brain microvascular endothe-lial cells [22,32]. Determining the relative contribution of these different routes to CNS cryptococcosis requires quantitative analysis of the interaction between cryptococci and brain microvascular cells, data that are currently lacking. Here we take the first steps to address this shortfall by using both mouse and human brain endothelial cell models.

Our data indicate that cryptococcal association with brain microvascular endothelial cells is a relatively infrequent event, although one that increases with extended periods of incubation. In both cell lines, mouse and human, less than 2% of encapsulated and acapsular cryptococci were strongly bound by 4 hrs of incubation. However, once bound, the probability of being internalized is high (typically >40% within four hours). These findings support recent observations in a mouse cryptococcosis model, which suggest that transmission across the BBB is a non-specific event dependent on trapping of cryptococci in narrow brain capillaries followed by phagocytosis into brain microvascular endothelial cells [32]. This implies that the adherence to – and phagocytosis of - cryptococci by BMEC is a slow process involving single cryptococci binding at any one time. We thus hypothesize that cryptococcal meningoencephalitis may be the result of a very small number of cryptococcal cells penetrating the BBB and subsequently proliferating to high numbers within the brain tissue. If so, then clinical approaches that reduce cryptococcal binding to endothelia even marginally may result in significant improvements to patient health. On the other hand, the low transcellular uptake
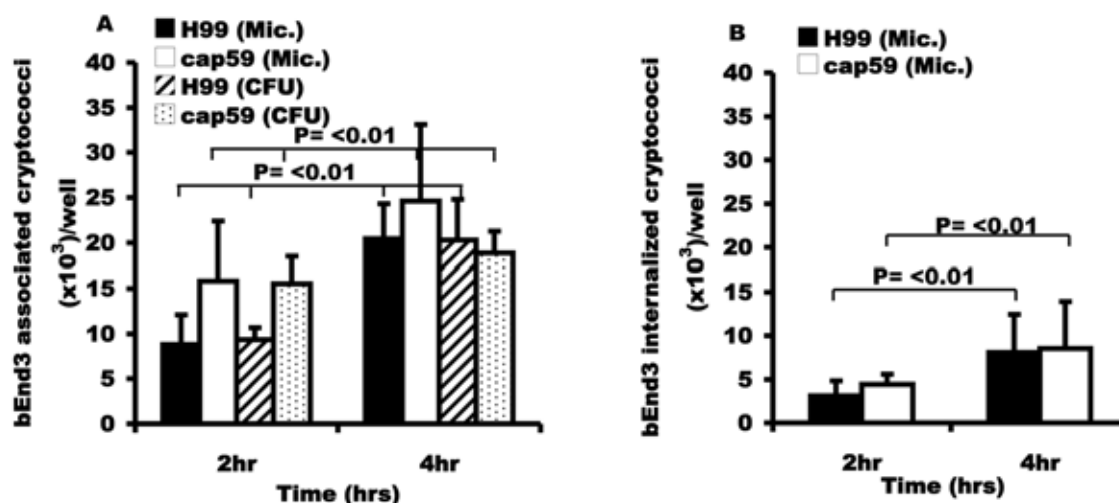
Figure 1. Binding and uptake of H99 and cap59 to the murine brain endothelial cell line, bEnd3. BEnd3 cells were exposed to wild type H99 and its acapsular derivative cap59 for 2 hr and 4 hr at 37°C. (A) The rate of association (bound and internalized cryptococci) was determined both by microscopy and live CFU counts. The rate of association increased significantly in a time dependent manner, (P<0.01 for both strains). However, there was no difference in association of encapsulated H99 or acapsular cap59 cells (P=0.1 and 0.5 at 2 hr and 4 hr respectively). (B) Internalization of the two strains, H99 and cap59 by bEnd3 cells as determined by fluorescence microscopy. Internalized cryptococci (pre-stained with FITC) were distinguished from extracellular adherent ones by counter labelling with calcofluor white after infection. Intracellular cryptococci retained the FITC green signal while extracellular cells acquired the blue signal from calcofluor. The number of phagocytosed cryptococci increased significantly in a time dependent manner, (P<0.01 for both strains). However, there was no difference in internalization of encapsulated H99 and acapsular cap59, (P=0.5 and 0.8 at 2 hr and 4 hr respectively). Error bars are standard error of the mean, n=5 repeats.
doi:10.1371/journal.pone.0035455.g001

suggests that *C. neoformans* might engage multiple entry mechanisms into the brain.

Possession of a capsule is a major virulence factor in *C. neoformans* and the presence of a capsule modulates many aspects of the interaction between cryptococci and infected hosts [40,41]. *Cryptococcus* – endothelial cell interaction studies have yielded

conflicting results regarding how capsule impacts on cryptococcal binding and uptake by BMEC [27,29–31,42]. By studying isogenic pairs of wild type and acapsular cryptococci and different brain endothelial cell-lines, we have shown that binding and uptake of cryptococci by BMEC is capsule independent. In agreement with this finding, intravital imaging of cryptococcal traversal of the
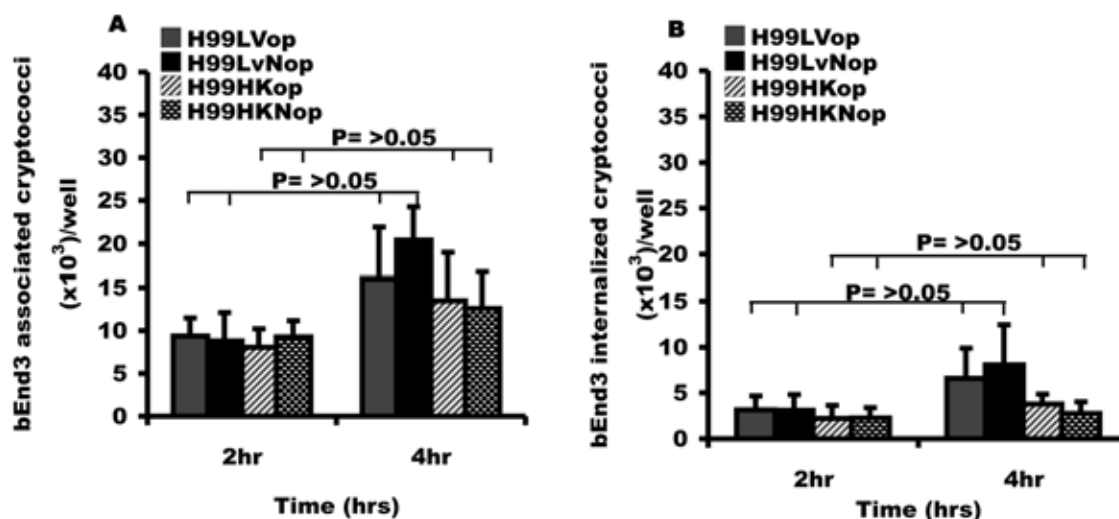

Figure 2. Effect of opsonisation on cryptococcal binding and uptake by bEnd3 cells. Live (LV) and heat-killed (HK) H99 cryptococci were opsonised with mouse derived anti-capsule IgG antibody, 18B7 and the rate of adherence and internalization was determined by fluorescence microscopy. (A) Association of opsonised (op) and non-opsonised (Nop) cryptococci with bEnd3 cells. Rate of association of opsonised and non-opsonised H99LV cryptococci was similar, P=0.8 and 0.4 at 2 hr and 4 hr respectively. Similarly, there was no difference between opsonised and non-opsonised heat-killed H99 cryptococci, P=0.9 and 0.5 at 2 hr and 4 hr respectively. (B) Rate of internalization of opsonised and non-opsonised cryptococci internalized by bEnd3 cells. The number of internalized H99LV cryptococci was similar, regardless of opsonisation status (P=0.9 at both 2 hr and 4 hr). Similarly, there was no difference between opsonised and non-opsonised heat-killed H99 cryptococci, P=0.5 and 0.4 at 2 hr and 4 hr respectively. Error bars are standard error of the mean, n=5 repeats.
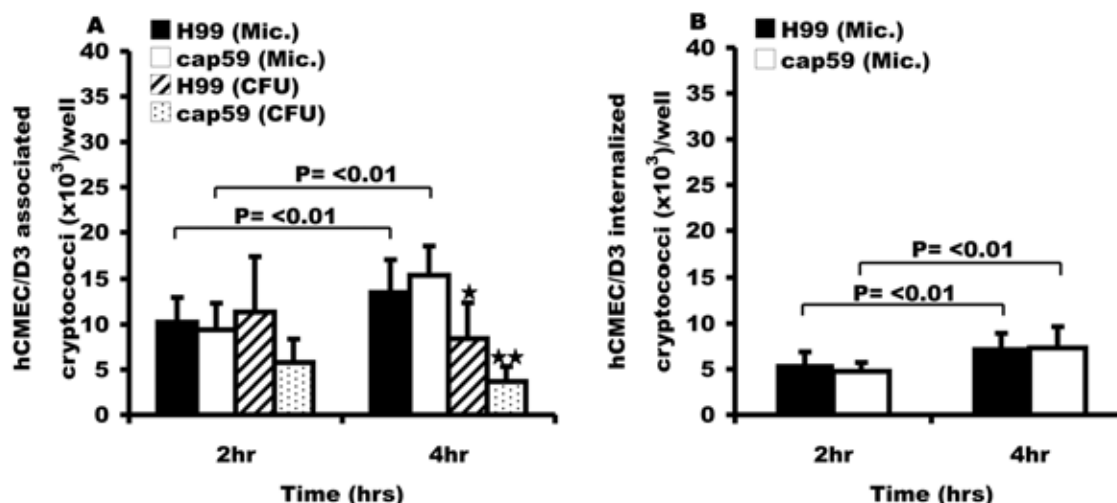doi:10.1371/journal.pone.0035455.g002

Figure 3. Binding and uptake of H99 and cap59 with human brain endothelial cell line, hCMEC/D3. Like bEnd3 cells, hCMEC/D3 cells were exposed to the *C. neoformans* serotype A isogenic strains, wild type H99 and acapsular derivative cap59 for 2 hr and 4 hr at 37°C. Microscopic (Mic.) and live CFU counts were performed to determine the association and survival of cryptococci. (A) Association efficiency of H99 and cap59 cryptococci with hCMEC/D3 cells. As opposed to microscopic counts, live CFU counts showed a time dependent decrease in the number of associated cryptococci by 4 hr of incubation, ★ = P<0.05 and ★★ = P<0.01 for H99 and cap59 respectively, suggesting a drop in viability of the hCMEC/D3 associated H99 and cap59 cryptococci. There was no difference in association of encapsulated H99 and acapsular cap59, P = 0.7 and 0.6 at 2 hr and 4 hr respectively. (B) Internalization of encapsulated H99 and acapsular cap59 cryptococci by human brain endothelial cell line, hCMEC/D3 cells. The internalized cryptococci and extracellular adherent were determined as in Figure 1. As with association, the number of phagocytosed cryptococci increased significantly in a time dependent manner, P = 0.01 and <0.01 for H99 and cap59 respectively. However, there was no difference in internalization of H99 and acapsular cap59 cryptococci, P = 0.5 and 0.8 at 2 hr and 4 hr respectively. Error bars are standard error of the mean, n = 6 repeats.
doi:10.1371/journal.pone.0035455.g003

blood-brain barrier has demonstrated equivalent crossing of the blood-brain barrier by wild type and acapsular cryptococcal yeast cells [32], an observation that implies the dispensability of the capsule for cryptococcal penetration of the blood-brain barrier.

Our finding that neither opsonisation nor active signalling from the cryptococcal cell are required for uptake are in line with recent data suggesting that cryptococcal uptake into brain endothelia is mediated by binding of endothelial CD44 to hyaluronic acid on
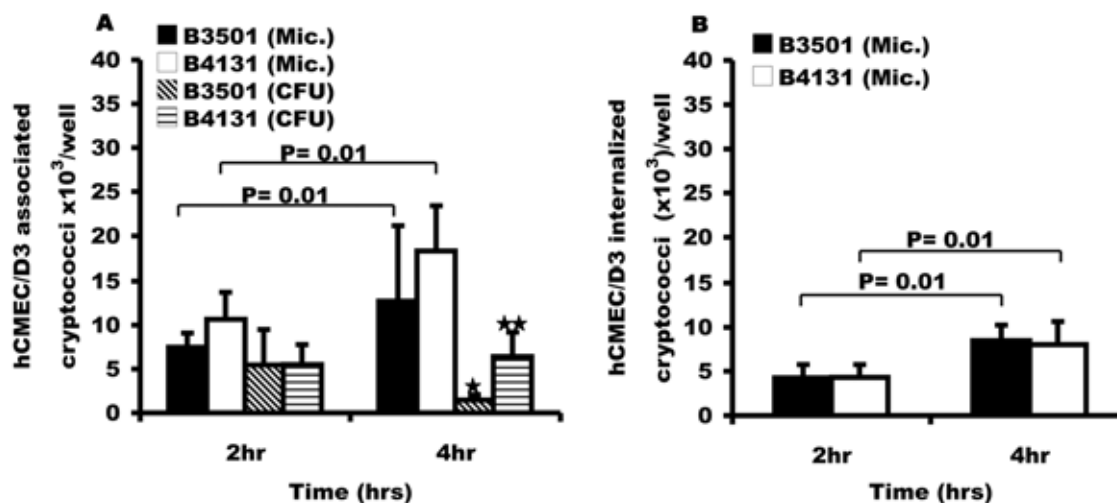

Figure 4. Binding and uptake of B3501 and B-4131 with human brain endothelial cell line, hCMEC/D3. HCMEC/D3 cells were exposed to *C. neoformans* serotype D wild type B3501 and its isogenic acapsular mutant B4131 for 2 hr and 4 hr at 37°C. Microscopic and live CFU counts were performed to determine the association and survival of cryptococci. (A) Association efficiency of B3501 and B4131 cryptococci with hCMEC/D3 cells. Like the H99-cap59 pair, live CFU counts showed a time dependent decrease in the number of associated cryptococci by 4 hr of incubation, ★ = P<0.01, ★★ = P<0.01 for both B3501 and B4131. There was no difference in association by encapsulated B3501 and acapsular B4131, P-value = >0.05 at 2 hr of incubation. However, B4131 was significantly more associated, P = 0.02 (Microscopy) and <0.01 (CFU) by 4 hr of incubation. (B) Internalization of encapsulated B3501 and its acapsular mutant derivative B4131 by hCMEC/D3 cells determined by fluorescence microscopy (Mic). The number of phagocytosed cryptococci increased significantly in a time dependent manner, P = 0.01 for both strains. However, there was no difference in internalization of B3501 and B4131, P = 0.5 and 0.2 at 2 hr and 4 hr respectively. Error bars are standard error of the mean, n = 6 repeats.
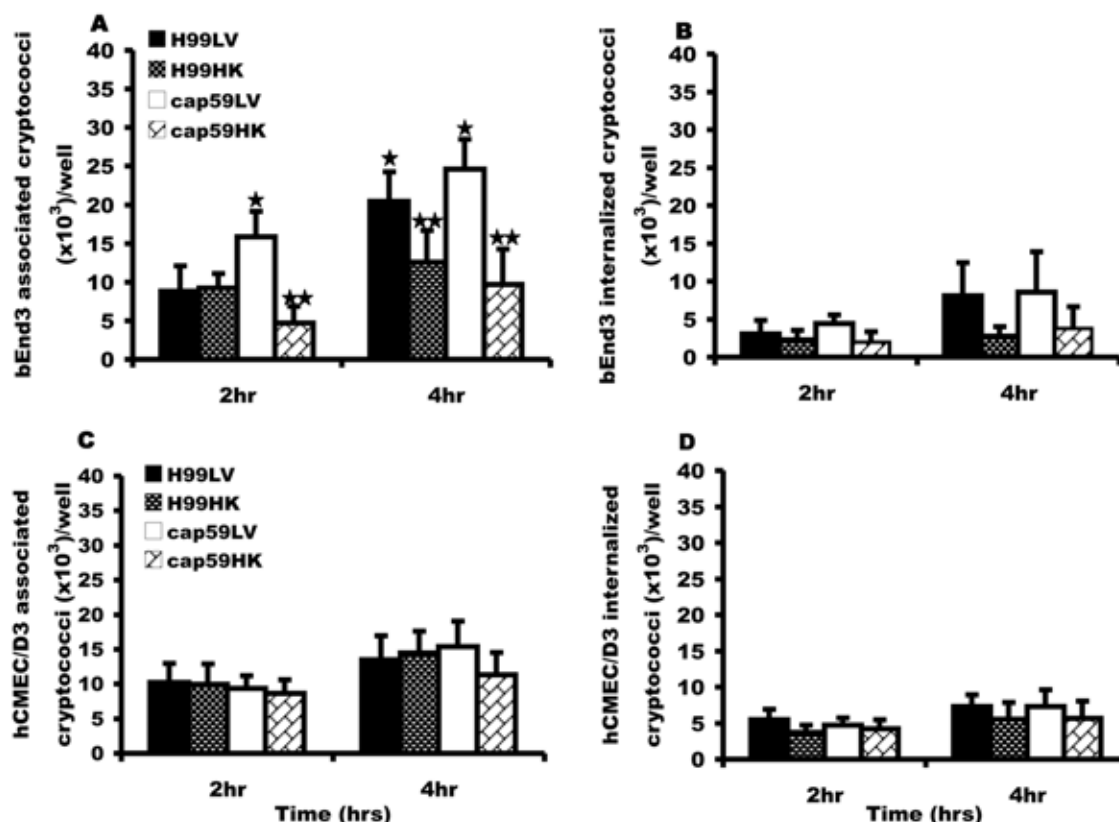doi:10.1371/journal.pone.0035455.g004

Figure 5. Effect of viability on binding and phagocytosis of H99 and cap59 strains by BMEC. Heating for 15 min at 65°C prior to infection killed H99 and cap59 cryptococci. Brain microvascular cells (BMEC), bEnd3 and or hCMEC/D3 cells were exposed in parallel to live (LV) and heat-killed (HK) cryptococci for 2 hr and 4 hr at 37°C and the number of bound and internalized cryptococci was determined by fluorescence microscopy. (A and C) Association efficiency of live and heat-killed H99 or cap59 cryptococci by bEnd3 and hCMEC/D3 cell respectively. There was no difference in association of viable H99 and cap59 cryptococci with hCMEC/D3 cells at either time point, P>0.05. However, viable cryptococci were more associated than non-viable ones by 4 hr of incubation in bEnd3 cells, P<0.01 for both H99 and cap59 respectively. (B and D) Internalization efficiency of LV and HK H99 and cap59 cryptococci by bEnd3 and hCMEC/D3 cells. Both live and heat-killed cryptococci showed a time dependent increase in phagocytosis by both bEnd3 and hCMEC/D3 cells, however the rate of phagocytosis did not vary between the viable and non-viable cryptococci in both cell-lines, P>0.05 at both 2 hr and 4 hr of incubation. Error bars are standard error of the mean, n = 5 repeats.
doi:10.1371/journal.pone.0035455.g005

the yeast surface [25]. Heat killing of the yeast is unlikely to disrupt this interaction. Although viable and non-viable (heat-killed) are equally internalized (this study), the non-viable cryptococci are unlikely to survive lysosomal degradation and hence may not transmigrate across the BBB in vivo [32]. Interestingly, however, our data suggest that human derived endothelia (but not murine bEnd3 cells) may be capable of killing intracellular cryptococci. Presumably crossing the BBB intact thus requires one or more of the virulence factors used by cryptococci to resist phagosomal killing [43], explaining why heat-killed cryptococci can enter endothelial cells but are not seen to transmigrate.

Supporting Information

Figure S1 Binding to fixed endothelial cell monolayers (negative control). To verify that the observed binding occurred in association with endothelial cells, and not due to indirect sequestration of yeast cells, bEnd3 and hCMEC/D3

monolayers were killed by paraformaldehyde fixation prior to cryptococci inoculation. For all conditions, cryptococcal binding was reduced by between one and two log orders, indicating that that viable endothelial cells were responsible for the observed cryptococcal association.
(TIF)

References

1. Lin X (2009) *Cryptococcus neoformans*: Morphogenesis, infection, and evolution. Infect Genet Evol 9(4): 401–416.

2. Park BJ, Wannemuehler KA, Marston BJ, Govender N, Pappas PG, et al. (2009) Estimation of the current global burden of cryptococcal meningitis among persons living with HIV/AIDS. AIDS 23(4): 525–530.

3. Kidd SE, Hagen F, Tscharke RL, Huynh M, Bartlett KH, et al. (2004) A rare genotype of *Cryptococcus gattii* caused the cryptococcosis outbreak on vancouver island (british columbia, canada). Proc Natl Acad Sci U S A 101(49): 17258–17263.

4. Byrnes EJ 3rd, Bildfell RJ, Frank SA, Mitchell TG, Marr KA, et al. (2009) Molecular evidence that the range of the Vancouver island outbreak of cryptococcus gattii infection has expanded into the pacific northwest in the united states. J Infect Dis 199(7): 1081–1086.

5. Byrnes EJ 3rd, Li W, Lewit Y, Ma H, Voelz K, et al. (2010) Emergence and pathogenicity of highly virulent *Cryptococcus gattii* genotypes in the northwest united states. PLoS Pathog 6(4): e1000850.

6. Byrnes EJ, Heitman J (2009) *Cryptococcus gattii* outbreak expands into the northwestern united states with fatal consequences. F1000 Biol Rep 1: 62.

7. Datta K, Bartlett KH, Baer R, Byrnes E, Galanis E, et al. (2009) Spread of *Cryptococcus gattii* into pacific northwest region of the united states. Emerging Infect Dis 15(8): 1185–1191.

8. Neofytos D, Fishman JA, Horn D, Anaissie E, Chang CH, et al. (2010) Epidemiology and outcome of invasive fungal infections in solid organ transplant recipients. Transpl Infect Dis 12(3): 220–229.

9. Mitchell TG, Perfect JR (1995) Cryptococcosis in the era of AIDS–100 years after the discovery of *Cryptococcus neoformans*. Clin Microbiol Rev 8(4): 515–548.

10. Huffnagle GB, McNeil LK (1999) Dissemination of *C. neoformans* to the central nervous system: Role of chemokines, Th1 immunity and leukocyte recruitment. J Neurovirol 5(1): 76–81.

11. Casadevall A, Perfect JR, eds (1998) *Cryptococcus neoformans*. Washington, DC: American Society for Microbiology. 541 p.

12. Lortholary O (2007) Management of cryptococcal meningitis in AIDS: The need for specific studies in developing countries. Clin Infect Dis 45(1): 81–83.

13. Boulware DR, Bonham SC, Meya DB, Wiesner DL, Park GS, et al. (2010) Paucity of initial cerebrospinal fluid inflammation in cryptococcal meningitis is associated with subsequent immune reconstitution inflammatory syndrome. J Infect Dis 202(6): 962–970.

14. Nussbaum JC, Jackson A, Namarika D, Phulusa J, Kenala J, et al. (2010) Combination flucytosine and high-dose fluconazole compared with fluconazole monotherapy for the treatment of cryptococcal meningitis: A randomized trial in malawi. Clin Infect Dis 50(3): 338–344.

15. Kambugu A, Meya DB, Rhein J, O'Brien M, Janoff EN, et al. (2008) Outcomes of cryptococcal meningitis in Uganda before and after the availability of highly active antiretroviral therapy. Clin Infect Dis 46(11): 1694–1701.

16. Bicanic T, Harrison TS (2005) Cryptococcal meningitis. Br Med Bull 72: 99–118.

17. Mwaba P, Mwansa J, Chintu C, Pobee J, Scarborough M, et al. (2001) Clinical presentation, natural history, and cumulative death rates of 230 adults with primary cryptococcal meningitis in zambian AIDS patients treated under local conditions. Postgrad Med J. pp 769–73.

18. Kim KS (2008) Mechanisms of microbial traversal of the blood-brain barrier. Nat Rev Microbiol 6(8): 625–634.

19. Brown RC, Morris AP, O'Neil RG (2007) Tight junction protein expression and barrier properties of immortalized mouse brain microvessel endothelial cells. Brain Res 1130(1): 17–30.

20. Correale J, Villa A (2009) Cellular elements of the blood-brain barrier. Neurochem Res.

21. Charlier C, Nielsen K, Daou S, Brigitte M, Chretien F, et al. (2009) Evidence of a role for monocytes in dissemination and brain invasion by *Cryptococcus neoformans*. Infect Immun 77(1): 120–127.

22. Chang YC, Stins MF, McCaffery MJ, Miller GF, Pare DR, et al. (2004) Cryptococcal yeast cells invade the central nervous system via transcellular penetration of the blood-brain barrier. Infect Immun 72(9): 4985–4995.

23. Chang YC, Stins MF, McCaffery MJ, Miller GF, Pare DR, et al. (2004) Cryptococcal yeast cells invade the central nervous system via transcellular penetration of the blood-brain barrier. Infect Immun 72(9): 4985–4995.

24. Eisenman HC, Casadevall A, McClelland EE (2007) New insights on the pathogenesis of invasive *Cryptococcus neoformans* infection. Curr Infect Dis Rep 9(6): 457–464.

25. Huang SH, Long M, Wu CH, Kwon-Chung KJ, Chang YC, et al. (2011) Invasion of *Cryptococcus neoformans* into human brain microvascular endothelial cells is mediated through the lipid rafts-endocytic pathway via the dual specificity tyrosine phosphorylation-regulated kinase 3 (DYRK3). J Biol Chem 286(40): 34761–34769.

26. Heitman J, Kozel TR, Kwon-Chung KJ, Perfect JR, Casadevall A () *Cryptococcus*: From human pathogen to model yeast. Washington, DC.: ASM Press.

27. Fries BC, Taborda CP, Serfass E, Casadevall A (2001) Phenotypic switching of *Cryptococcus neoformans* occurs in vivo and influences the outcome of infection. J Clin Invest 108(11): 1639–1648.

28. Chen SH, Stins MF, Huang SH, Chen YH, Kwon-Chung K, et al. (2003) *Cryptococcus neoformans* induces alterations in the cytoskeleton of human brain microvascular endothelial cells. J Med Microbiol 52: 961–970.

29. Charlier C, Chretien F, Baudrimont M, Mordelet E, Lortholary O, et al. (2005) Capsule structure changes associated with *Cryptococcus neoformans* crossing of the blood-brain barrier. Am J Pathol 166(2): 421–432.

30. Guerrero A, Jain N, Goldman DL, Fries BC (2006) Phenotypic switching in *Cryptococcus neoformans*. Microbiology 152: 3–9.

31. Jain N, Guerrero A, Fries BC (2006) Phenotypic switching and its implications for the pathogenesis of *Cryptococcus neoformans*. FEMS Yeast Res 6(4): 480–488.

32. Shi M, Li SS, Zheng C, Jones GJ, Kim KS, et al. (2010) Real-time imaging of trapping and urease-dependent transmigration of *Cryptococcus neoformans* in mouse brain. J Clin Invest 120(5): 1683–1693.

33. Jong AY, Stins MF, Huang SH, Chen SH, Kim KS (2001) Traversal of *Candida albicans* across human blood-brain barrier in vitro. Infect Immun 69(7): 4536–4544.

34. Goldman DL, Khine H, Abadi J, Lindenberg DJ, Pirofski L, et al. (2001) Serologic evidence for *Cryptococcus neoformans* infection in early childhood. Pediatrics 107(5): E66.

35. Mukherjee S, Lee SC, Casadevall A (1995) Antibodies to *Cryptococcus neoformans* glucuronoxylomannan enhance antifungal activity of murine macrophages. Infect Immun 63(2): 573–579.

36. Vecchiarelli A, Pietrella D, Bistoni F, Kozel TR, Casadevall A (2002) Antibody to *Cryptococcus neoformans* capsular glucuronoxylomannan promotes expression of interleukin-12Rbeta2 subunit on human T cells in vitro through effects mediated by antigen-presenting cells. Immunology 106(2): 267–272.

37. Bolanos B, Mitchell TG (1989) Phagocytosis and killing of *Cryptococcus neoformans* by rat alveolar macrophages in the absence of serum. J Leukoc Biol 46(6): 521–528.

38. De Jesus M, Chow SK, Cordero RJ, Frases S, Casadevall A (2010) Galactoxylomannans from *Cryptococcus neoformans* varieties *neoformans* and *grubii* are structurally and antigenically variable. Eukaryot Cell 9(7): 1018–1028.

39. Santangelo R, Zoellner H, Sorrell T, Wilson C, Donald C, et al. (2004) Role of extracellular phospholipases and mononuclear phagocytes in dissemination of cryptococcosis in a murine model. Infect Immun 72(4): 2229–2239.

40. Syme RM, Bruno TF, Kozel TR, Mody CH (1999) The capsule of *Cryptococcus neoformans* reduces T-lymphocyte proliferation by reducing phagocytosis, which can be restored with anticapsular antibody. Infect Immun 67(9): 4620–4627.

41. Zaragoza O, Chrisman CJ, Castelli MV, Frases S, Cuenca-Estrella M, et al. (2008) Capsule enlargement in *Cryptococcus neoformans* confers resistance to oxidative stress suggesting a mechanism for intracellular survival. Cell Microbiol 10(10): 2043–2057.

42. Ibrahim AS, Filler SG, Alcouloumre MS, Kozel TR, Edwards JE, et al. (1995) Adherence to and damage of endothelial cells by *Cryptococcus neoformans* in vitro: Role of the capsule. Infect Immun 63(11): 4368–4374.

43. Ma H, May RC (2009) Virulence in *Cryptococcus species*. Adv Appl Microbiol 67: 131–190.